

Copyright
by
Coleman Kent Baker
2020

**The Dissertation Committee for Coleman Kent Baker Certifies that this is the
approved version of the following dissertation:**

**Methods for the Genetic Stabilization of Reporter Flaviviruses and their
Applications**

Committee:

Pei-Yong Shi, PhD, Supervisor or
Mentor

Scott Weaver, PhD, or Co-Supervisor,
Chair

David Beasley, PhD

Andrew Routh, PhD

Sanjay Singh, PhD

**Methods for the Genetic Stabilization of Reporter Flaviviruses and their
Applications**

by

Coleman Kent Baker, B.S.

Dissertation

Presented to the Faculty of the Graduate School of
The University of Texas Medical Branch
in Partial Fulfillment
of the Requirements
for the Degree of

Doctor of Philosophy

**The University of Texas Medical Branch
December 2020**

Methods for the Genetic Stabilization of Reporter Flaviviruses and their Applications

Publication No. _____

Coleman Kent Baker, PhD

The University of Texas Medical Branch, 2020

Supervisor: Pei-Yong Shi

Infectious reporter flaviviruses have been reported since 2003, and they have the potential to be utilized in diverse scientific areas such as investigating viral pathology, conducting high-throughput drug screens, running rapid serum neutralization tests, and diagnosing disease. Despite the value of these applications, their utility has been limited due to genetic instability after continued growth in cell culture. Previous studies have hypothesized this partial or complete loss of reporter gene is the result of recombination. This work describes two methods that can be used to stabilize luciferase-carrying flaviviruses: recombination-dependent lethal mutations and optimizing the capsid duplication length. The first of these methods was shown effective for stabilizing Zika and yellow fever viruses to ten passages in cell culture. The effectiveness of the second method to likewise stabilize reporter flaviviruses was demonstrated with Zika, yellow fever, dengue serotypes 1-4, Japanese encephalitis, and West Nile viruses. Notably, these viruses can be used to determine serum neutralization titers in less than twenty-four hours, whereas the traditional assay takes up to a week. The stabilization of flaviviruses bearing reporter

or other trans-genes opens doors for their application in vaccine efficacy evaluation, disease diagnosis, pathogenesis studies, and treatment of diverse afflictions.

TABLE OF CONTENTS

List of Tables	ix
List of Figures	x
List of Abbreviations	xii
INTRODUCTION.....	15
Chapter 1-Introduction.....	15
Flaviviruses	16
Genome Structure and Organization.....	16
Structural Proteins.....	16
Capsid	16
Pre-membrane and Envelope	17
Non-structural Proteins	17
NS1	17
NS2A	18
NS2B-NS3	18
NS4A-NS4B	19
NS5	19
Flavivirus UTRs.....	19
5' UTR	20
3' UTR	20
Flavivirus Life Cycle	21
Flavivirus Diagnosis	22
NAAT	22
Serology	22
Reporter Viruses	22
Timeline of Reporter Flavivirus Design	23
Methods for Further Stabilization of Reporter Flaviviruses	27
Applications of Reporter Flaviviruses	28
Conclusions.....	30

LONG TERM STABILIZATION OF REPORTER FLAVIVIRUSES	37
Chapter 2- Recombination Dependent Lethal Mutations	37
Introduction.....	37
Materials and Methods.....	38
Viruses and Cells	38
Capsid Mutation Screens	39
Immunofluorescence Assay	39
Focus Forming Assay	40
Growth Curve.....	40
Luciferase Assay	41
Reporter Virus Passaging and Stability	41
Reporter PRNT Assays	41
Plaque Reduction Neutralization Tests	42
Antiviral Assays.....	42
IVIS	43
Statistical Analysis.....	43
Illustrations	43
Results.....	43
Recombination-Dependent Fatal Mutations	43
Stable NanoLuc ZIKV	44
Stable NanoLuc YFV	45
Reporter Virus Applications	46
Discussion.....	48
Chapter 3: Reporter Stabilization by Optimization of Capsid Duplication Length ...	63
Introduction.....	63
Materials and methods	65
Viruses and cells	65
Immunofluorescence assay	66
Focus forming assay	67
Reporter virus passaging and stability	67
Growth kinetics by focus forming assay.....	68

Reporter neutralization assays	68
Antiviral assays	68
Luciferase Expression	69
Mosquito infections	69
Statistical analysis	70
Illustrations	70
Results.....	70
Panel of reporter flaviviruses	70
Extended capsid duplication	71
Effect of extended capsid duplication on viral growth	72
Rapid neutralization tests and antiviral discovery	73
ZIKV C38 in mosquitoes	73
Discussion.....	74
Conclusion	76
DISCUSSION.....	88
Chapter 4: Development of Stable Transgene-bearing Flaviviruses	88
Introduction.....	88
Recombination-Dependent Lethal Mutations in Other Flaviviruses	88
Combination of Methods	89
Further Optimization.....	90
Future Directions	91
Flavivirus Diagnostics	91
Glioblastoma	92
Bioluminescent Imaging	94
Vaccine Platform	96
Conclusion	96
References.....	101
Vita	117

List of Tables

Table 1.1 Summary of published reporter flaviviruses.....	36
Table 2.1 Virus strains used to raise MIAF	62

List of Figures

Figure 1.1 Flavivirus Genome.	32
Figure 1.2 Flavivirus Life Cycle	33
Figure 1.3 Flavivirus Reporter Schemes-Less Stable	34
Figure 1.4 Flavivirus Reporter Schemes-Stable.	35
Figure 2.1 Identification of Recombination-Dependent Fatal Mutations.	51
Figure 2.2 A Stable NanoLuc ZIKV	53
Figure 2.3 Additional Viral Characterization	55
Figure 2.4 A Stable NanoLuc YFV.	57
Figure 2.5 Applications of Stable Reporter Viruses.	58
Figure 2.6 Neutralization Curves	60
Figure 2.7 DK Nano and DK23 Nano in A129 Mice	61
Figure 3.1 Panel of Reporter Flaviviruses.	77
Figure 3.2 DENV3 and DENV4 In vitro ligation cloning scheme	78
Figure 3.3 WNV IFA and Genetic Stability	79
Figure 3.4 Passaging Scheme	80
Figure 3.5 Extended Capsid Duplication.	81

Figure 3.6 Effect of Capsid Duplication Length on Viral Growth.	82
Figure 3.7 ZIKV and ZIKV WT Growth Comparison	83
Figure 3.8 Neutralization and Antiviral Assays.....	84
Figure 3.9 Kinetics of luciferase expression on C6/36 cells.....	86
Figure 3.10 ZIKV C38 Nano in Mosquitoes.	87
Figure 4.1 Increasing number of capsid mutations in JEV Nano.	98
Figure 4.2 Stability of DK23 mScarlet and DK23 iRFP670	99
Figure 4.3 C38a Recombination.	100

List of Abbreviations

ATCC	American Type Culture Collection
BHK	baby hamster kidney
BLI	bioluminescent imaging
bp	base pair
C	capsid protein
C25	first 25 amino acids of capsid protein
cHP	conserved hairpin
CPE	cytopathic effects
CS	cyclization sequence
CTLA4	cytotoxic T-lymphocyte-associated protein 4
DAR	downstream of AUG region
DB	dumbbell
DCS-PK	downstream of cyclization sequence pseudoknot
DENV1	dengue virus serotype 1
DENV2	dengue virus serotype 2
DENV3	dengue virus serotype 3
DENV4	dengue virus serotype 4
DMEM	Dulbecco's Modified Eagle Medium
DMEM	Dulbecco's modified Eagle medium
DPBS	Dulbecco's phosphate buffered saline
E	envelope protein
ER	endoplasmic reticulum
F2A	foot and mouth disease virus 2A
FBS	fetal bovine serum

FFU	foci forming units
GFP	green fluorescent protein
GSC	glioblastoma stem-like cell
HCV	hepatitis C virus
hpi	hours post infection
IFA	immunofluorescence assay
JEV	Japanese encephalitis virus
kb	kilobase
LGTV	Langat virus
LOD	limit of detection
MIAF	mouse immune ascites fluid
MOI	multiplicity of infection
MVEV	Murray Valley encephalitis virus
NAAT	nucleic acid amplification testing
Nano	Nanoluciferase
NanoLuc	Nanoluciferase
NPC	neural progenitor cells
NSC	neural stem cells
P2A	porcine teschovirus 2A
PBS	phosphate buffered saline
PBS	phosphate buffered saline
PCR	polymerase chain reaction
PD1	programmed cell death protein 1
PD-L1	programmed cell death protein 1 ligand
POWV	Powassan virus
prM	pre-membrane protein
PRNT	plaque reduction neutralization test

RLuc	Renilla luciferase
RRID	Research Resource Identifiers
RT-PCR	reverse transcription-polymerase chain reaction
sfRNA	subgenomic flavivirus RNA
sHP	small hairpin
SL	stem loop
T2A	thosea asigna virus 2A
TBEV	tick-borne encephalitis virus
UAR	upstream of AUG region
UTR	untranslated region
WNV	West Nile virus
WT	wild type
YFV	yellow fever virus
YFV17D	yellow fever virus vaccine strain 17D
ZIKV	Zika virus

INTRODUCTION

Chapter 1-Introduction¹

The past two decades have been a lesson in the potential of unknown or unrecognized RNA viruses to emerge from animal reservoirs in new locations to cause local epidemics or widespread pandemics. In 1999, the United States saw the introduction of West Nile virus, which has caused tens of thousands of cases of neurological disease [1]. Subsequently, 2002 saw the first outbreak caused by a new coronavirus, Severe Acute Respiratory Syndrome Coronavirus (SARS CoV), which infected thousands of people before control measures ended the spread [2]. The yearly influenza turned particularly worrisome in 2009 with the emergence of an especially deadly strain of influenza A with swine origins that killed an estimated 284,000 people worldwide [3]. Notably, the second novel coronavirus outbreak happened in 2012, with the causative agent, Middle Eastern Respiratory Syndrome Coronavirus (MERS CoV), causing over six hundred deaths in 27 countries [2]. The largest Ebola virus outbreak ravaged West Africa for four years starting in 2013, which outbreak led to transmission nosocomial and other transmission on multiple continents [4]. Shortly thereafter, the little-known mosquito borne Zika virus shocked scientists after its introduction to the Americas demonstrated its non-vectorized transmission and ability to cause fetal malformations [5]. Finally, the current pandemic of coronavirus infectious disease 2019 (COVID-19), caused by yet another novel coronavirus, continues to spread worldwide, with cases currently over 19 million and 718,518 deaths globally [6]. Each of these instances has demonstrated the progress still to be made in studying and counteracting these and future diseases.

¹ Content of this chapter has been previously published: Baker, C.; Shi, P.-Y. Construction of Stable Reporter Flaviviruses and Their Applications. *Viruses* 2020, 12, 1082, doi:10.3390/v12101082.

FLAVIVIRUSES

Two of the above examples from the past twenty years, West Nile (WNV) and Zika (ZIKV) viruses, are part of the insect vectored pathogens from the Flavivirus family. This family also includes the mosquito-transmitted dengue virus (DENV), Japanese encephalitis virus (JEV), and yellow fever virus (YFV) as well as the tick-transmitted tick-borne encephalitis virus (TBEV), Langat virus (LGTV) and Powassan virus (POWV). Collectively, these viruses cause greater than 390 million infections yearly, with the majority of those being from the four serotypes of dengue virus[7]. Along with the more well-known and studied of the Flaviviruses, come a number of lesser known but emerging family members with outbreak potential [1]. Discouragingly, current medical countermeasures are restricted to vaccines with limited availability or efficacy and no direct-acting antivirals available [8].

GENOME STRUCTURE AND ORGANIZATION

The Flavivirus family consists of positive sense, single-stranded RNA viruses. Their ~11 kb genome is translated as one large polyprotein that is co- and post-translationally cleaved into three structural proteins (capsid [C], pre-membrane [prM], and envelope [E]) and seven non-structural proteins (NS1, NS2A, NS2B, NS3, NS4A, NS4B, and NS5) by cellular and viral proteases (Fig. 1.1A). A brief overview of each of these proteins, as well as the structures and sequences found in the untranslated regions of the genome, follows.

Structural Proteins

CAPSID

The capsid protein, which is primarily responsible for the encapsulation of the viral RNA, is made up of 5 alpha helices, the last of which acts as a signal peptide for ER translocation and is cleaved on both sides to give soluble protein. Soluble capsid proteins

form dimers in solution and crystal structures, with one side being predominantly hydrophobic and the other highly charged, giving rise to theorized models of RNA binding [9]. Notably, the extreme N and C termini of the protein have not been solved in published capsid structures due in part to their hypothesized flexibility [10–13]. There is also poor understanding of the mechanism of viral RNA encapsidation, though one recent study has shed some light on C-prME interactions in the immature ZIKV particle [14].

PRE-MEMBRANE AND ENVELOPE

Pre-membrane and envelope proteins each have two transmembrane domains and form the outermost shell of the virus particle [9]. prM functions as an E protein chaperone, specifically shielding the E protein fusion loop as the immature viral particle transits from the ER to the Golgi apparatus and is exocytosed. A significant structural reorganization takes place during transit, in which pH and proteolytic triggers cause E trimers to lie flat and transition to dimers. A 91-residue portion of prM, referred to as pr, is then cleaved by furin, leaving mature virus to be released [15].

Flavivirus E protein is responsible for binding cellular receptors, triggering endocytosis and entry of the virus. Notable receptors and attachment factors include DC-SIGN, TIM/TAM receptors, integrins like $\alpha_v\beta_3$ and $\alpha_v\beta_5$ [16,17], and chaperoning heat shock proteins like HSC70 [18]. The M and E proteins are also among the most immunogenic flavivirus proteins and constitute the majority of the targets of the humoral immune response, including neutralizing epitopes [19].

Non-structural Proteins

NSI

The first non-structural flavivirus protein plays a number of roles in the virus life cycle. It functions intracellularly as a dimer to assist in viral replication, in which it interacts

with NS4A and NS4B to aid in membrane rearrangement [20]. NS1 is also the only secreted protein in the flavivirus genome, where it has been shown to increase vascular leakage, contributing to shock and hemorrhage in cases of severe dengue infection [21]. As a secreted marker of infection, NS1 can be detected in the blood by ELISA and this method is regarded as a specific and early method of disease diagnosis [22].

NS2A

NS2A is a small, membrane associated protein with varied roles. While it has been known to play a role in membrane rearrangement, viral genome replication, and virion formation, recent advances have furthered understanding of this crucial protein. It has been shown for both ZIKV and DENV2, that NS2A recruits both the prM-E and NS2B-NS3 complexes, as well as binds viral RNA associated with C [23,24]. This implicates NS2A as the chief chaperone for virion assembly, bringing structural and non-structural proteins together for proper processing and interactions to form immature virus particles.

NS2B-NS3

NS2B functions primarily to recruit NS3 to the ER membrane and is a critical cofactor for NS3 protease activity. NS3 is the sole viral protease and is responsible for six of the twelve proteolytic cleavage events across the flavivirus polyprotein. Along with N-terminal protease activity, the C-terminus of NS3 also has NTPase/helicase activity. This function is essential in the replication of the viral genome for relieving RNA structural constraints and unwinding double-stranded intermediates [25]. As a multi-functional, enzymatic viral protein, NS3 has also been a major target of antiviral drug development, though no drugs are yet approved [26].

NS4A-NS4B

These two small, transmembrane proteins interact with each other and recruit other viral proteins, including NS1 [27], to reorganize the ER membrane and facilitate viral genome replication [28]. They also function to modulate cellular function by inducing autophagy [29] or blocking induction of the interferon response [30].

NS5

NS5 is the largest flavivirus protein and contains both an N-terminal methyltransferase domain and a C-terminal RNA dependent RNA polymerase domain [31]. The methyltransferase domain is responsible for capping the genomic RNA and adding an N7 methyl group to the guanine cap. The RNA strand is then also methylated at the 2' O position [32]. Along with genome replication, NS5 is also a potent interferon antagonist, primarily targeting STAT2 and causing its degradation. STAT2, when uninhibited, serves as a transcription factor for interferon stimulated genes[33].

Flavivirus UTRs

The genome's single open reading frame is flanked on both 5' and 3' ends by an untranslated region (UTR) that, among other functions, contains functional/structural motifs, such as the cyclization sequence, that are critical for RNA replication (Fig. 1.1B). These highly ordered structures and sequences participate in long range RNA interactions that cyclize the genome allowing for replication by NS5. Although these regions can vary between different flaviviruses, the following is a general review of known sequences and structures found in the UTRs and coding regions that facilitate replication and/or translation.

5' UTR

The capped 5' end of the genome contains two large stem loops (SL), termed SLA and SLB. SLA is a recruitment factor for NS5, which then allows for negative strand synthesis once the genome is cyclized [34]. SLB contains one of the identified regions that plays a role in genome cyclization, the 5' upstream of AUG region or 5' UAR. This region, located just upstream of the start codon, pairs with the 3' UAR located in the 3' UTR and helps stabilize genome cyclization and replication [35].

Beyond the 5' UTR and into the coding region of the capsid gene, lay a number of other important RNA motifs for genome cyclization, replication, and translation. The 5' downstream of AUG region (5' DAR) participates by binding its complement found in the 3' UTR (3' DAR) and so participates in genome cyclization. Following the 5' DAR there is a predicted and confirmed conserved hairpin structure (cHP) that functions to stall the ribosomal scanning of the positive sense viral RNA so that translation can be correctly initiated. This structure also has a role in proper replication of the viral genome [36,37]. Immediately following the cHP is the RNA sequence that was first suggested to be involved in genome cyclization, the 5' cyclization sequence (5' CS), which binds the complementary CS found in the 3' UTR (3' CS) [38]. Multiple reports also point to the sequence immediately following the 5' CS as being involved in either genome replication or encapsidation or both [39–41]. This region has been given different terminology, though this work will refer to it as the downstream of cyclization sequence pseudo-knot, or DCS-PK [40].

3' UTR

The 3' UTR has a number of structures and sequences that play essential roles during the viral life cycle. The sequences important for genome cyclization have been mentioned above with their 5' binding partner. Additional structural features are abundant

in the 3' UTR and their functions have been probed and studied using *in silico* modeling techniques, biochemical assays, and reverse genetic approaches. The beginning of the 3' UTR contains a region that varies between different members of the Flavivirus genus, though the presence of stem loops and pseudoknot interactions are a common theme. This variable region is preceded by two dumbbell structures that in the case of some viruses also contain pseudoknots. Finally, there is a small hairpin (sHP) and highly structured 3' stem loop (3' SL) [42]. The variable region stem loops and pseudoknot, as well as the dumbbells that follow, have been shown to stall cellular RNA exonucleases, leaving different lengths of 3' UTR RNAs termed subgenomic flavivirus RNAs (sfRNA) [43–45]. These short RNAs play a number of different roles in increasing the virus's ability to productively infect a host cell, such as block the interferon response [46,47] and RNA interference pathways [48].

FLAVIVIRUS LIFE CYCLE

Figure 1.2 gives an overview of the viral life cycle undergone by flaviviruses. Virions bind a number of cellular receptors and are internalized by receptor-mediated endocytosis. As the endosome progresses through the cytoplasm, pH drop triggers a conformational change in E protein, initiating membrane fusion and release of viral RNA [1]. The RNA is directly used to translate viral proteins on the ER membrane, where genome replication and formation of the immature viral particle occur [49]. Subsequently, viral particles bud and traffic to the trans Golgi network, where glycosylation occurs on the E protein [50,51]. As the viral particle moves through the trans Golgi network, pH changes induce a conformational change in prM and E, as well as furin-mediated cleavage of pr from M. This last step leaves a mature and infectious flavivirus virion [9].

FLAVIVIRUS DIAGNOSIS

NAAT

Diagnosis of flavivirus infection is preferentially done by nucleic acid amplification testing (NAAT), traditionally RT-PCR based techniques. This method is highly specific and, once reagents have been generated, relatively straightforward and fast. If an acute serum sample is available and tests positive, it is enough for diagnosis [52]. The downfall with NAAT is that transient and often low viremia associated with flavivirus infection mean negative results from NAAT do not mean no infection, and even positive results do not necessarily indicate the presence of infectious virus [53]. The next step of the testing paradigm is serology.

Serology

The presence of IgM, the first antibody type generated against a new infection, is typically indicative of a recent infection. Flavivirus serology assays focus heavily on IgM capture immunoassays or ELISAs. These benefit from being relatively fast and easy to carry out so many more laboratories have this capability [54]. Negative ELISA results are generally conclusive, however positive results must be sent for additional confirmation by plaque reduction neutralization testing due to flavivirus cross-reactivity [55]. The plaque reduction neutralization test measures levels of neutralizing antibodies against a specific virus, allowing the previous infectious agent to be determined [52]. These tests are very specific and powerful for diagnosis but suffer from long assay time and low throughput [52], the need for highly trained technicians [53], and do not differentiate between recent and past infections [54]. Novel solutions are needed to address these issues.

REPORTER VIRUSES

The cloning and subsequent manipulation and experimentation of flavivirus genomes with reverse genetic tools has resulted in a greater understanding of the viral and

host determinants of infection in both mammalian and insect hosts [56] as well as paved the way for designed vaccines [57,58] and tools such as replicons [59] and reporter viruses. Reporter viruses enable simple, rapid, and high-throughput quantification of virus in a variety of settings and applications, making them powerful tools for research, diagnosis, and medicine. The following is a summary and discussion of the development and shortcomings of reporter flaviviruses, covering different methods of construction and their influence on the long-standing problem of genetic instability. Recent work by other groups towards this end are also considered. A discussion of the current applications of reporter flaviviruses is included, as well as how current and future applications can be benefited by the increased genetic stability afforded by recent advances.

Timeline of Reporter Flavivirus Design

The first reporter flavivirus constructs were made with replicon RNAs, which are autonomously replicating viral RNAs that lack structural proteins necessary for viral particle formation. Replicons for Kunjin virus (KUNV) were first engineered with a chloramphenicol acetyltransferase (CAT) gene [60] followed by a green fluorescent protein (GFP) gene [61] in a permissible location in the 3' UTR immediately following an internal ribosome entry site (IRES). Similar work was also done with WNV [62]. Replicons are powerful tools for viral replication experiments and testing drugs that affect viral replication, especially as they require less strict containment measures, but they lack viral structural proteins and do not complete a full viral life cycle. The KUNV replicon approach was later applied for the establishment of a hepatitis C virus (HCV) replicon system [63,64] that was essential for the development of successful HCV therapeutics.

Full-length, infectious viruses can be more difficult to clone due to instability in bacterial plasmids, but they do not have the shortcomings of replicons which do not cover virus entry/fusion and virion assembly/release. The bacterial instability challenge was first

overcome by *in vitro* ligation of cDNA fragments that cover the complete YFV genomic RNA sequence [65]. Similar approaches were used to develop infectious clones for JEV [66], DENV2 [67], and TBEV strain Hypr [68]. For other flaviviruses, stable full-length infectious clones were established for DENV-4 [69], KUNV [70], TBEV strain Neudoerfl [68], Murray Valley encephalitis virus (MVEV) [71], TBEV strain Langat [72], and WNV epidemic strain [73]. The key solution to overcome the stability issue when amplifying cDNA clones in *E. coli* is to use low copy number plasmid vectors.

The first report of a full-length reporter flavivirus came in 2003 using JEV [74] which was engineered with GFP and luciferase in the 3' UTR, similar to the previously published KUNV replicons (Fig. 1.3A).

Successively, two reports of infectious reporter WNV were published in 2005, one with green fluorescent protein (GFP) [75], and one with Renilla luciferase (RLuc) [76], both reporter genes, under control of an IRES, placed in the 3' UTR. These reports both document the genetic instability problem that plagued reporter flaviviruses for the next 15 years. In the first report, genetic stability was assayed by serial passage in HEK293T cells then analyzing cells by flow cytometry for E protein and GFP signals after 48 hours of infection. Greater than 90% of cells stained positive for E protein, while <60% were GFP positive at 48 and 96 hours and GFP positive cells dropped to <10% by 144 hours. Viral RNA was also harvested at different times post infection on BHK-21 cells and used as a template for RT-PCR. Band size of the products was resolved on an agarose gel using electrophoresis, showing a decrease in the size of the amplicon containing GFP as time passed. Cloning and sequencing of these amplicons indicated that deletions across the IRES/GFP sequences were occurring, implicating recombination as the source of genetic instability [75]. This report also showed that placement of a reporter gene attenuated viral growth when compared to the parental virus. The second report, using WNV-RLuc,

passed the virus seven times on BHK cells, followed by RT-PCR on viral RNA. The RT-PCR product of the 3' UTR matched the size of the product from WT WNV and not reporter WNV. These results corroborated those from WNV-GFP and established RT-PCR on passaged viral RNA as the traditional assay to assess genetic stability. Similar versions of other reporter flaviviruses, DENV [50,77] and ZIKV [78], using an IRES in the 3' UTR have been made though not every report details the instability of the reporter gene.

Another, less used, strategy for constructing reporter flaviviruses was first published in 2007 [79]. In short, EGFP was engineered in the 17D vaccine strain of YFV at the junction between viral envelope protein (E) and nonstructural protein 1 (NS1), with the stem-anchor domain of E and amino-terminus of NS1 duplicated to maintain correct proteolytic processing and membrane orientation (Fig. 1.3B). Notably, duplicated regions of the genome can lead to increased levels of homology-directed recombination [80], which had already been associated with reporter virus instability. Despite this, the authors did not report codon scrambling of the duplicated sequences to decrease homologous recombination. Stability results from this construct were mixed, with two of five plaque purified viral populations showing loss of reporter signal between passage five and ten in Vero cells by flow cytometry. This method has been used to design EGFP reporter LGTV [81], a tick-borne flavivirus, and Nanoluciferase (NanoLuc) and EGFP ZIKV constructs [82]. The E/NS1 NanoLuc ZIKV showed stability to ten passages but grew to lower titers than other reporter schemes. However, EGFP ZIKV did not have detectable fluorescence after transfection, leading the authors to conclude that this region is more restrictive in the sequences that can be engineered there. Our own experience (unpublished data) affirms that this method is less robust than those described hereafter. Of note, this strategy was used to create YFV expressing simian immunodeficiency virus (SIV) gag protein and, after modifying the gag sequence, it was reported stable up to twenty passages [83].

The most robust scheme for reporter flavivirus construction to date was published in 2007 using YFV [84]. In this method, EGFP was placed between the 5' UTR and the capsid gene. Importantly, RNA signals for replication can be found in both the 5' UTR and the capsid gene so, a portion of the capsid was necessarily duplicated upstream of the reporter gene. The reporter gene was then followed by the 2A sequence from foot and mouth disease virus (FMDV, F2A) to ensure EGFP separation from the polyprotein. To reduce homology and usage of the downstream 5' cyclization sequence, the codon sequence of the complete capsid gene was optimized (Fig. 1.3C). To assess genetic stability, virus was passaged five times in BHK-21 cells. Cells were then stained for viral antigen and analyzed by flow cytometry for both viral antigen and GFP. Results indicated 11 % of the viruses had lost GFP signal, indicating this strategy to be more stable than IRES driven cassettes in the 3' UTR.

The capsid duplication strategy has been successfully applied to many other flaviviruses, with slight variations giving different results in stability and utility, though addition of a reporter gene causes general attenuation in all cases [82,85–95]. As a rule, reporter viruses made without reducing the homology between duplicated capsids show marked instability, similar to the 3' UTR reporter viruses [86,91,93–95]. On the other hand, reducing the homology increases stability, reported usually out to five passages in cell culture [87,88,90,94]. Reporter WNV and JEV with no homology reduction were initially shown to be unstable. Then, multiple rounds of plaque purification led to selection of stable variants that all contained a mutation in the downstream copy of the 5' cyclization sequence [91,93], lending evidence that decreasing homology, perhaps especially in the cyclization sequence, can increase stability. Engineering of similar mutations in other flaviviruses though, has not led to similar levels of stability [90]. Lastly, a report using DENV indicated that doubling the 2A sequence immediately downstream of the reporter gene could increase genetic stability by up to two or three passages [94].

Methods for Further Stabilization of Reporter Flaviviruses

As seen through the decade following the first reporter flavivirus, better design methods have resulted in more stable, and more robust, reporter viruses. Despite these improvements, interest still remains in engineering increased stability. Viruses carrying reporter genes with long-standing stability can be used in long-term pathology experiments, such as experiments involving transmission among multiple hosts, in diagnostic applications where reliability of the reporter signal is crucial, and in industrial applications where large viral batches are needed from small seed stocks. Therefore, recent work has shown multiple strategies that can be applied to ensure engineered reporter genes are maintained.

Interest recently in split reporter proteins, where the large subunit of the protein becomes active after addition of a smaller, critical subunit, has increased because of their minimal genome perturbation and ability to be introduced by CRISPR technology [96]. Such a system has been developed for NanoLuc [97] and was applied to JEV and DENV4 by Tamura, *et al* [98]. The small size of the insert, 57 nucleotides, was initially engineered after the E protein and includes a linker sequence, the small NanoLuc subunit (HiBit), and a small NS1 duplication to ensure proper polyprotein processing. Stability was initially shown out to five passages and, notably, reporter viruses replicated similarly to parental viruses *in vitro*. Later, this work was further expanded on with experiments in mice infected with JEV-HiBit [99]. Reporter virus-infected mice showed less mortality than those infected by WT JEV, highlighting the attenuation even a small insert can cause. Further optimization of the insertion site after protein modeling, *in vitro* screening, and *in vivo* experiments led to a JEV-HiBit virus with an insert at NS1₃₄₉, with no duplication of NS1 (Fig. 1.4A).

This improved reporter virus was stable to ten passages in Huh7 cells and, remarkably, had similar mortality to WT JEV in immunocompetent mice. This leads to a potent tool for assessing viral titers in *in vitro* and *in vivo* experiments, with the drawback of being unable to do live animal imaging because of the challenges of supplying the large NanoLuc subunit and the secretory nature of NS1.

Volkova, *et al* developed a separate, elegant technique using ZIKV bearing NanoLuc as a model [82]. They built on the capsid duplication method, noting that, for ZIKV, the reported sizes used for the duplication range from 25 amino acids [89], to 33 amino acids [95], to duplication of the full capsid [88]. They methodically tested duplication lengths, concluding that a duplication of 50 amino acids (C50) is the shortest length that replicates similarly to WT ZIKV. To further ensure stability, a +1-frameshift mutation was introduced at the beginning of the C50 and restored at the end of C50 (Fig. 1.4B). This strategy preserves the RNA elements in the C50 but changes the amino acids that are translated. If recombination deletes the engineered NanoLuc, the +1 frameshift mutation, and not the -1 restorative mutation, is introduced into the polyprotein resulting in mistranslation. This method secured the NanoLuc gene for ten passages.

Applications of Reporter Flaviviruses

Reporter genes, including fluorescent and bioluminescent genes, allow for easier quantification of virus levels. This simple concept has seen many applications that advance virus and disease understanding as well as countermeasure development. One of the earliest reports of reporter flaviviruses was in conjunction with antiviral compound testing. Traditionally, these tests are done by adding virus and putative antiviral compounds to relevant cells. Following multiple rounds of viral replication, supernatant samples are assayed by plaque or focus-forming assay, which take up to five days or more to obtain results and are not amenable to high-throughput. Using reporter viruses, results can be

obtained using reporter output in place of infectious virus, increasing throughput, turnaround, and ease of quantification [76,77,87,89,91,100,101]. This technology has enabled high-throughput compound library screens, in which hundreds to thousands of potential antiviral compounds can be tested.

Similar to antiviral testing, conventional testing for neutralizing antibodies by plaque reduction neutralization tests (PRNT) is a long and labor-intensive process. Several methods for using reporter gene output, instead of viral titers, have been described to shorten this assay from a week to as little as 4 hours and increase throughput by using either a flow cytometer or plate reader [101–104]. In addition, the ability to make chimeric reporter flaviviruses, or viruses with heterologous prM-E genes, has the potential to quickly expand this method to many other flaviviruses [105–107]. However, it remains to be determined if a chimeric virus containing a heterologous viral prM-E could be equally neutralized by positive serum specimens as an authentic virus without chimeric prM-E. Neutralization assays play an important role in both vaccine efficacy trials and flavivirus diagnostics, and as such, stable reporter constructs have great potential to hasten both of these pursuits. In both cases, these laboratories are not routinely equipped with necessary equipment, such as an electroporation apparatus, nor the technical expertise to rescue stock reporter viruses when more is required. Stable reporter viruses allow these crucial laboratories to amplify viral stocks many times over and maintain confidence in the reporter signal output. Thus, recent advances could allow this technology to be used more easily and routinely, increasing the pace of disease diagnosis and vaccine trials.

Another powerful application of reporter flaviviruses comes in the use of luciferase carrying viruses to be quantified in living animals. Powerful cameras can detect luciferase signals in infected mice, allowing for temporal quantification and tracking of infection in the same mice. This real-time view of infection, also known as bioluminescent imaging

(BLI), also reduces the number of mice needed and can represent viable models for both antiviral and vaccine studies. Such studies have already been done with DENV2 [90] and JEV [93]. More stable reporter viruses could be used in a similar fashion to model not only pathology or medical countermeasures, but also host-host transmission over an extended time. As the flavivirus life cycle involves both insect and mammalian hosts, this type of proposed model could benefit our understanding of this complex progression.

The possibility of approved flavivirus vaccine strains, specifically the 17D strain of YFV, being used to deliver heterologous antigens as a vaccine has long been considered and studied. It was initially restricted to small T and B cell epitopes engineered either in a space in the envelope protein [108,109] or between NS2B and NS3 [110–112] and was thus limited in scope and efficacy. Longer antigens have been developed in the E/NS1 junction (see Fig. 1.2B) with mixed results [83,113]. The newly developed gene stabilization methods for flaviviruses open the door to reliable delivery of larger heterologous antigens that can be used as experimental vaccines. As YFV17D is one of the oldest and best performing vaccines available, this method represents a promising pathway for rapid vaccine development against new and emerging pathogens.

CONCLUSIONS

Since first creation, reporter flaviviruses have found uses in molecular virology [85,86], antiviral drug studies [76,77,87], pathology studies (including live animal imaging) [90,93,99], and neutralizing antibody quantification [101–103]. Initial methods of reporter virus construction, placing an IRES driven gene in the 3' UTR, were found to be genetically unstable due to recombination. Subsequent methods, using the 5' UTR-capsid junction, proved more robust and stable if homology was reduced in duplicated capsid regions. Further improvements to achieve long-term stability, usually regarded as stable for ten passages in cell culture, was the goal of this project. The greater stability of

these viruses would enable more widespread and diverse use of these virological tools. ZIKV was used as an initial model and it was hypothesized that a ZIKV construct with long-term stability will be beneficial as both a diagnostic tool and an effective therapeutic. The following dissertation will describe two different methods for stabilizing reporter flaviviruses as well as their application in drug screening and serum neutralization tests.

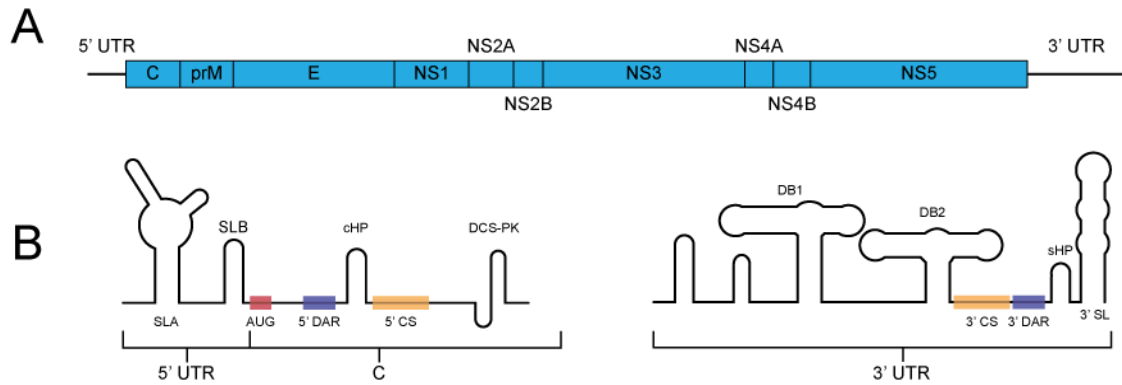


Figure 1.1 Flavivirus Genome.

A. General flavivirus genome organization. C-capsid, prM-pre-membrane, E-envelope, NS-nonstructural. B. Depiction of some of the important RNA structures and sequences at the 5' and 3' ends of the flavivirus genome. SLA-Stem Loop A, SLB-Stem Loop B, AUG-Start codon, 5' DAR- 5' downstream of AUG region, cHP-conserved hairpin, 5' CS- 5' cyclization sequence, DCS-PK- downstream of cyclization sequence pseudoknot, DB1-dumbbell 1, DB2-dumbbell 2, 3' CS- 3' cyclization sequence, 3' DAR- 3' downstream of AUG sequence. Note that some of the structures and sequences at the 5' end are within the coding region of the capsid gene.

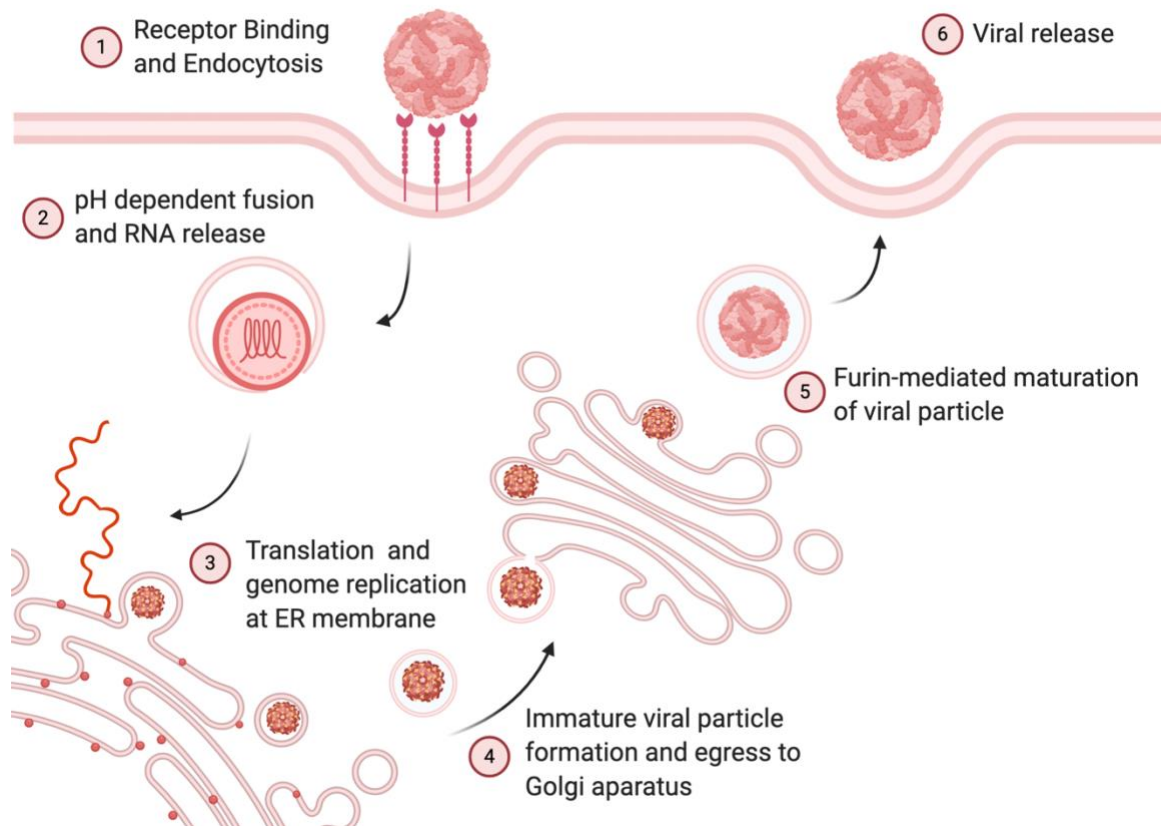


Figure 1.2 Flavivirus Life Cycle

General scheme of the major steps of the flavivirus life cycle.

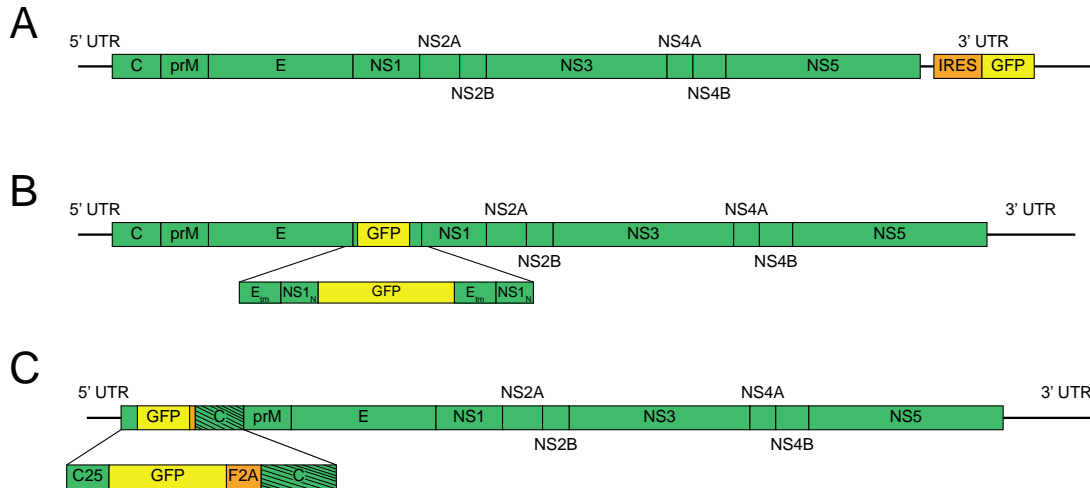


Figure 1.3 Flavivirus Reporter Schemes-Less Stable

A. 3' UTR reporter insertion. The reporter gene is inserted into a permissive site in the 3' UTR under control of an internal ribosomal entry site (IRES). B. E/NS1 reporter insertion. The reporter gene is placed at the junction between E and NS1, with a duplication of the N-terminus (N) of NS1 and the transmembrane (tm) domains of E. C. 5' reporter insertion. The reporter gene is placed at the junction of the 5' UTR and the capsid protein. The first 25 amino acids of the capsid are duplicated (C25) and the reporter gene is followed by the foot and mouth disease virus 2A sequence (F2A) and codon scrambled capsid gene (represented by the slanted lines).

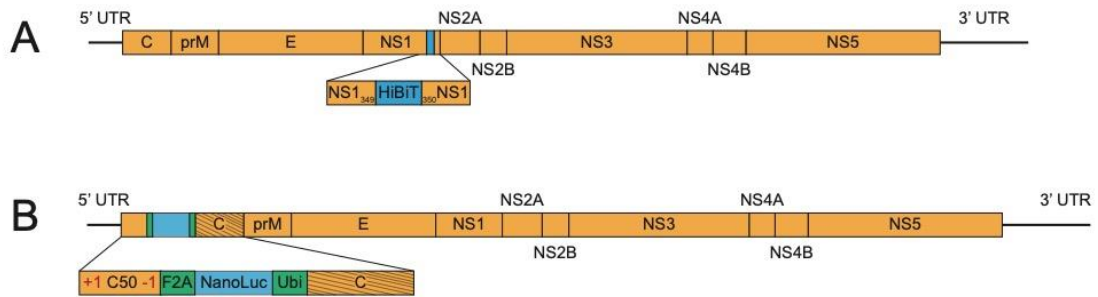


Figure 1.4 Flavivirus Reporter Schemes-Stable.

A. NS1 insertion of split luciferase. The small subunit of split NanoLuc (HiBit) was inserted in NS1 at amino acid 349. B. C50 with frameshift mutation. The reporter gene is engineered after a duplication of 50 capsid amino acids (C50) and flanked by F2A and the ubiquitin sequence (Ubi). C50 contains a +1-frameshift mutation after the fourth codon, which is restored at the end of C50. Slanted lines indicate codon scrambling.

Table 1.1 Summary of published reporter flaviviruses.

Year of publication	Reporter gene and flavivirus	Reference
1997	CAT KUNV replicons	[60]
1999	GFP KUNV replicon	[61]
2003	IRES-GFP/Luc JEV	[74]
2005	IRES-GFP WNV	[75]
2005	IRES-RLuc WNV	[76]
2007	IRES-RLuc DENV2	[50]
2007	E/NS1-GFP YFV	[79]
2007	5'-GFP YFV	[84]
2009	5'-RLuc DENV2	[85,86]
2010	IRES-RLuc DENV2	[77]
2011	5'-RLuc DENV2	[87]
2012	5'-GFP/FLuc DENV2	[90]
2014	E/NS1-gag YFV	[83]
2016	5'-RLuc ZIKV	[89]
2016	5'-GLuc WNV	[91]
2016	5'-GFP ZIKV	[95]
2017	E/NS1-GFP LGTV	[81]
2017	5'-GFP/mCherry/NanoLuc ZIKV	[88]
2017	5'-RLuc JEV	[93]
2017	NS1-HiBiT JEV/DENV4	[98]
2018	5'-GFP/Clover2/bfloGFP DENV2	[94]
2019	5' NanoLuc DTMUV	[92]
2019	NS1-HiBiT JEV	[99]
2020	IRES-NanoLuc/GFP ZIKV	[78]
2020	E/NS1-NanoLuc/GFP ZIKV	[82]
2020	5'-GFP/NanoLuc ZIKV	[82]
2020	5' w/+1C-1 NanoLuc/GFP ZIKV	[82]

LONG TERM STABILIZATION OF REPORTER FLAVIVIRUSES

Chapter 2- Recombination Dependent Lethal Mutations²

INTRODUCTION

The preceding summary of reporter flavivirus work done since the first reverse genetics system was developed [65] shows the considerable advances that have been made in the construction and application of these tools. It also highlights the shortcomings and hurdles that still need to be overcome. The largest hurdle is that of recombination-mediated genetic instability, which limits widespread reporter flavivirus use.

Reporter virus stability (defined by how long it can be grown on cells and maintain an intact, functional reporter gene) is vital for long-term pathogenesis studies that rely on reporter gene output. As arboviruses, flaviviruses cycle between mammalian and insect hosts. Experiments that capture this complicated life cycle could be simplified by the use of reporter viruses, though the long-term nature of these investigations would require these viruses to be exceptionally stable and retain near-WT levels of virulence. Reporter DENV and JEV have been analyzed *in vivo* using BLI, though not in the context of multi-host transmission [90,93]. Additionally, diagnostic and industrial use of reporter flaviviruses for large-scale drug screens and serology assays will require stiff confidence in the reporter output and how it relates to viral titers. To answer these unmet needs, we developed a method of stabilizing reporter flaviviruses to greater than ten passages, using Zika virus as a model.

² Contents of this chapter have been previously published: Baker C, Xie X, Zou J, Muruato A, Fink K, Shi P-Y. Using recombination-dependent lethal mutations to stabilize reporter flaviviruses for rapid serodiagnosis and drug discovery. *Ebiomedicine* 2020; **57**: 102838.

The first Zika reporter virus was published alongside the first cDNA clone of that virus [89]. While its stability was not reported, other ZIKV constructs have been made and their stability after passaging reported [78,88,95,114]. None have been reported as stable beyond four or five passages in cell culture, with the exception of a recently published Zika reporter virus that uses a similar method as that developed here [82]. Their work compares different lengths of duplicated capsid and the effect thereof on viral replication. This testing, coupled with a frameshift mutation in the duplicated portion, was sufficient to stabilize their reporter virus, with the frameshift mutation disrupting correct protein translation if recombination occurs.

Our initial efforts to stabilize a reporter gene focused on codon optimization of the reporter gene sequence. The capsid duplication method of reporter flavivirus construction was chosen due to its robustness. Two strategies were tested: codon matching to the ZIKV genome and reduction of AU rich regions. It is well known that cell types have a preference for certain codons and that this can affect protein production and transcript stability [115]. These methods were tested by serial passaging experiments but had little effect on stability (data not shown). A new technique was needed.

Here, we have developed a strategy to stabilize reporter flaviviruses, using recombination-dependent lethal mutations in the duplicated capsid portion to block virion formation upon recombination. We showed this strategy to be effective for stabilizing both a NanoLuc ZIKV and YFV to greater than ten passages and demonstrated these stabilized viruses' effectiveness in serology and antiviral assays.

MATERIALS AND METHODS

Viruses and Cells

Zika virus strain Dakar 41525 and YF17D strain YFS11 were cloned into full-length plasmids using the low copy pCC1 vector as has been previously described [89,116]. The NanoLuc gene and capsid mutations for ZIKV were inserted using an overlap PCR,

restriction digest, and ligation strategy. Gene insertions and mutations were cloned in YFV using NEBuilder HiFi DNA Assembly mix (NEB E2621). Viruses were recovered after electroporation (Biorad GenePulser Xcell) of *in vitro* transcribed RNAs in Vero (ATCC Cat# CCL-81, RRID: CVCL 0059) cells as previously described [89]. All Vero cells were grown in Dulbecco's Modified Eagle Medium (DMEM, Gibco 11965) supplemented with 10% fetal bovine serum (FBS, Hyclone SH30071) and 1% penicillin/streptomycin (Gibco 15140). Huh7 cells (RRID: CVCL 0336) were grown in DMEM with Glutamax (Gibco 10566) supplemented with 10% FBS, 1% penicillin/streptomycin, and 1% non-essential amino acids (Gibco 11140). Infections were carried out in the same media excepting supplementation with 2% fetal bovine serum instead of 10%. Cells were grown at 37°C in a humidified incubator with 5% CO₂.

Capsid Mutation Screens

This experiment was carried out as detailed in [86]. Briefly, *in vitro* transcribed RNAs were electroporated into Vero cells and plated in 24-well plates. Cells electroporated with no RNAs were used as a negative control (mock). At 4, 24, 48, 72, and 96 h, the supernatants were harvested, and the cells were washed with phosphate buffered saline (PBS, Gibco 10010023), lysed with Cell Culture Lysis Reagent (Promega E153A), and frozen at -80°C. The supernatants were used to infect fresh Vero cells, which were washed and lysed at 24 h. Lysed cells were moved to a 96 well plate and read for luciferase activity after addition of NanoGlo substrate (Promega N1150) using a Biotek Cytation 5 plate reader according to the manufacturer's recommendation.

Immunofluorescence Assay

Vero cells were aliquoted into chamber slides post-electroporation. At the indicated time points, cells were washed with PBS and fixed with cold methanol, covered, and placed at -30°C for >30 minutes. Slides were then washed with PBS and blocked with PBS+1%

FBS overnight at 4°C. The pan-flavivirus envelope antibody 4G2 (ATCC Cat# HB-112, RRID: CVCL J890) was used to probe for infected cells. A secondary goat anti-mouse IgG antibody conjugated with Alexa Fluor 488 (Thermo Fisher Scientific Cat# A-11001, RRID: AB 2534069) was then used to probe for 4G2. Slides were stained with DAPI (Vector Laboratories, H-1200) and then imaged on a Nikon Eclipse Ti2 microscope. ImageJ (NIH) was used to process these images.

Focus Forming Assay

All viruses were titered using a focus-forming assay. Viruses were serially diluted ten-fold and used to infect Vero cells that had been seeded the day previously at 2×10^5 cells per well in a 24-well plate. After a 1-h infection, the inoculum was removed and methylcellulose (Sigma C5013) and DMEM was overlaid. At four days post infection, the overlay was removed, and cells were fixed with a 1:1 solution of methanol/acetone for >15 minutes. Plates were washed with PBS 3X, blocked with PBS+3% FBS, and then incubated with virus-specific mouse immune ascites fluid (MIAF, World Reference Center for Emerging Viruses and Arboviruses, UTMB). After >1-h incubation with MIAF, plates were washed and incubated with a horseradish peroxidase-conjugated anti-mouse IgG antibody (SeraCare KPL Cat# 474-1806, RRID: AB 2307348). After a 3X PBS wash, foci were developed using an AEC peroxidase substrate kit (Enzo 43825) according to the manufacturer's protocol. Images were acquired with a BioRad ChemiDoc Imaging System.

Growth Curve

Vero cells were seeded at 8×10^5 cells per well in a six well plate the day before infection. Cells were infected at a MOI of 0.01 for 1 h followed by a 3X PBS wash and addition of media supplemented with 2% FBS. Cell supernatant samples were taken at 24, 48, 72, 96, and 120 h and titered by focus-forming assay. Samples at 24 hours were directly

used for focus-forming assay, while samples taken at 48-120 hours were first diluted 10-fold, thus giving a ten-fold difference in the limit of detection.

Luciferase Assay

Vero cells were seeded in an opaque, white 96 well plate at 1.5×10^4 cells per well the day before infection. Viruses were diluted to a MOI of 0.5 and added to plates after removal of media. At the indicated time points, the media was removed, and cells were washed 2X with PBS. NanoGlo substrate, diluted 1:50 in NanoGlo Assay Buffer, was then directly added to cells and plates were read on a BioTek Cytation 5 instrument after 3 minutes.

Reporter Virus Passaging and Stability

Virus recovered after electroporation formed the P0 stock. 500 μ L of this was added to a T75 flask seeded the day before with Vero cells. The infection continued until cell death was observed (3-day average for DK Nano and YF Nano, 4-day average for DK23 Nano and YF4 Nano) after which media was harvested, clarified by centrifugation, and aliquoted. 500 μ L of an aliquot was then used to infect a fresh T75 flask for a new passage. This was carried out in duplicate series for each virus. Stability was assessed by isolating viral RNA (Qiagen 52904) and using this for an RT-PCR reaction (Invitrogen 12574) with primers encompassing the 5' UTR through the capsid. The products were then run on a 0.6% agarose gel to observe size.

Reporter PRNT Assays

Reporter neutralization tests were done by serially diluting sera two-fold, starting at 1:50 in DMEM. Serum samples against ZIKV and DENV1-4 were pooled from mice infected with the respective virus. YFV and JEV serum samples were from mice vaccinated against the virus. Normal serum was pooled from mice that were naïve for flavivirus

infection. Serially diluted serum samples were mixed 1:1 with the respective reporter virus and incubated at 37°C for 1 h. The virus/sera mixture was then plated on Vero cells in a white 96 well plate that was seeded at 1.5×10^4 cells per well the day before. After a 4-h infection at 37°C, the wells were washed 2X with PBS and 50 μ L of NanoGlo substrate diluted 1:50 in NanoGlo Assay Buffer was added to each well. Plates were read in a BioTek Cytation 5 plate reader after 3 minutes. Positive controls consisted of virus infection with no sera. Negative controls comprised virus plated in wells with no cells. This negative control allows for subtraction of background luciferase signals from the virus media. Results were graphed as a percent of positive control, with the negative control set as zero. The data were analyzed by four parameter nonlinear regression, with the top and bottom constrained to 100 and zero, respectively.

Plaque Reduction Neutralization Tests

PRNT assays were done as previously published [103]. Briefly, 2-fold serially diluted serum samples were mixed 1:1 with virus equal to 200 plaque-forming units. After 1-h incubation at 37°C, the mixture was placed on a confluent monolayer of Vero cells in a 6-well plate for 1 h. Afterwards, the inoculum was replaced with a methylcellulose overlay and the plates were further incubated until plaques became clear under a microscope. The wells were then stained with crystal violet and plaques were counted.

Antiviral Assays

The panflavivirus inhibitor NITD008 was two-fold serially diluted in 90% DMSO to a concentration starting at 10 μ M. These were mixed with virus (MOI 0.01) and plated on Huh7 cells that were seeded at 1.5×10^4 cells per well the previous day. Cells were washed 48 h post infection three times with PBS followed by addition of NanoGlo substrate diluted 1:100 in NanoGlo Assay Buffer. Plates were read by a BioTek Cytation 5 plate reader after 3 minutes.

IVIS

An equal mix of male and female mice (5 M, 6 F) were infected at three-weeks old by subcutaneous route with both DK Nano and DK23 Nano. They were weighed daily and monitored for signs of distress such as hunched posture and ruffled fur. The mice were bled on days 3-6 and imaged with an IVIS apparatus daily on days 0-7 and then every other day on days 8-14. For imaging, mice were subcutaneously given 100 μ L of NanoGlo substrate diluted 1:50 in PBS. Mice were then anesthetized by isoflurane and transferred inside the apparatus, which allowed for continual delivery of anesthetic. The program was initialized, and images were captured.

Statistical Analysis

Graphpad Prism 8 was used for graphing and statistical analysis. Statistical tests used, as well as significance levels, are denoted in the figure legends. Instead of standard deviation, all replicated values are shown on each graph.

Illustrations

Figures were created using Biorender and Adobe Illustrator.

RESULTS

Recombination-Dependent Fatal Mutations

Flavivirus reporter genes are commonly engineered at the beginning of the genome, after the 5' UTR [84,85,87,89] (Fig. 2.1a). RNA regulatory elements are present in both the 5' UTR and the capsid gene, [reviewed in [117,118]], thus the beginning of the capsid gene (25 amino acids) must be duplicated before the reporter gene in order to preserve viral translation and replication (see Fig. 2.1a). Duplicating this portion of the capsid greatly increases the chance of homology-mediated recombination, leading to elimination of the

reporter gene. Reducing the homology by codon optimization of the full capsid gene improves stability but does not stop recombination (see Fig. 2.2E, DK Nano, top panels). We explored a further way of stabilizing a reporter ZIKV (Dakar strain, DK). It is known that DENV requires a threshold of positive charges at the beginning of the capsid protein in order to form infectious viral particles [86]. We hypothesized that this information could provide a way to stabilize a reporter ZIKV. Charge reversing mutations, from positively to negatively charged amino acids, were designed in the C25 region that upon recombination would become part of the full capsid gene and lead to non-infectious viral particle formation (Fig. 1b). In this way, only non-recombined reporter viruses are passed on.

To test this strategy, we first engineered an increasing number of positive to negative charge mutations in the full capsid gene of a NanoLuc reporter ZIKV to find what was sufficient to stop viral particle formation (Fig. 2.1c). Fig. 2.1d details the experimental scheme. Luciferase levels assayed at 4, 24, 48, 72, and 96 h following transfection of *in vitro* transcribed RNAs indicate robust translation and replication for all viruses (Fig. 2.1e). The supernatants for each of these time points was used to infect fresh Vero cells which were assayed for luciferase levels as a surrogate for infectious virus. The very low luciferase levels for DK Nano C567,23 (numbers represent the amino acid position in capsid protein) indicate that four capsid mutations are necessary to abrogate production of infectious virus (Fig. 2.1f).

Stable NanoLuc ZIKV

The four-amino acid capsid mutations (found to be necessary to stop virus formation) were engineered in the C25 region of a reporter ZIKV (designated DK23 Nano) and compared against a reporter ZIKV without capsid mutations (DK Nano) (Fig. 2.2a). Both reporter viruses show delayed growth and spread post-electroporation compared to DK WT (non-reporter) virus by immunofluorescence assay (IFA). The replication of DK23

Nano was further delayed compared to DK Nano; nevertheless, by day 3, 100% of cells were E protein positive (Fig. 2.2b). Growth kinetics were assayed by both focus-forming (Fig. 2.2c, top panel) and luciferase assay (bottom panel). Jointly, these experiments show that DK23 Nano was attenuated in replication when compared to DK Nano, but appreciable titers ($>10^6$ FFU/ml) and luciferase levels ($>10^5$ light units) were still attained. Both viruses were serially passaged ten times in duplicate as detailed in Fig. 2.2d. Stability was assessed by observation of the size of the RT-PCR product from the 5' UTR to the capsid. The RT-PCR product of DK Nano decreases in size at P6 or P7 (Fig. 2.2e, top panels), while the DK23 Nano product is consistent through P10 (bottom panels). P10 RT-PCR products were sequenced, and results confirmed that DK23 Nano was unchanged while DK Nano had reverted to WT. Comparison of foci size between P0 and P10 showed consistent results from DK23 Nano, while DK Nano P10 foci resembled DK WT plaques in that they were large and formed distinct plaques—indicating that the virus had reverted to WT levels of virulence (Compare Figs. 2.2f and 2.3a). Finally, luciferase assay carried out at multiple MOIs comparing P0 and P10 viruses showed that DK23 Nano P10 virus performed robustly, even significantly more robustly than the original P0 virus (Fig. 2.2g, right panel). Sequencing the DK Nano and DK23 Nano P10-1 and P10-2 viruses showed minimal consensus level amino acid changes (Fig. 2.3b). In contrast, DK Nano showed considerably decreased luciferase activity (Fig. 2.2g, left panel). Collectively, these data demonstrate that recombination-dependent lethal mutations were successful in stabilizing a NanoLuc reporter ZIKV to at least ten passages in cell culture.

Stable NanoLuc YFV

We next hypothesized that this strategy for stabilizing reporter ZIKV could be successful with another flavivirus, YFV. We followed a similar workflow with YFV as with ZIKV and first screened charge-reversing mutations in the full capsid gene of a YF17D NanoLuc virus (Fig. 2.4a). These mutations did not affect viral translation and

replication after the genome-length RNAs were electroporated into cells (Fig. 2.4b, left panel). Infection outcomes indicated that, similar to ZIKV, four capsid mutations were necessary and sufficient to block viral particle formation (Fig. 2.4b, right panel). The YF4 Nano virus was created carrying four capsid mutations in the C25 (Fig. 2.4c). Viral growth characteristics were assayed by IFA post-electroporation (Fig. 2.4c), replication curve (Fig. 2.4d), luciferase kinetics (Fig. 2.4e), and focus-forming assay (Fig. 2.4d). These data together show that YF4 Nano, similar to DK23 Nano, was attenuated when compared to YF Nano, but that high titers (8×10^5 FFU/ml) and robust luciferase ($>10^5$ light units) levels could still be attained. YF Nano and YF4 Nano were passaged for ten rounds on Vero cells and their stabilities were evaluated by RT-PCR band size (Fig. 2.4f). The P10 bands were sequenced and P0 and P10 viruses were compared in a luciferase assay. The YF Nano without the four mutations rapidly lost its luciferase expression (Fig. 2.4g, top panels), whereas the P10 of YF4 Nano with the designed mutations consistently retained luciferase activities (bottom panels). Together, these results validate that recombination-dependent lethal mutations are not only effective for stabilizing a reporter ZIKV but can be effectively applied to another flavivirus.

Reporter Virus Applications

To establish the utility of these novel reporter viruses, we used both DK23 Nano and YF4 Nano viruses in plaque reduction neutralization tests (PRNT). Reporter viruses have been proposed and used in these assays previously, as a way to increase throughput and decrease assay turnaround time [102,103]. However, due to the bright nature of NanoLuc, we found that these assays can be read as early as 2-4 h post infection (Fig. 2.2c for reporter ZIKV and Fig. 4e for reporter YFV, Fig. 2.6a), which is a significant improvement over the traditional three to five days of a standard PRNT and the 24-48 h of other reporter PRNT assays. The luciferase signals at 2-4 h post infection represent initial translation of input genomic RNA after virus entry [100].

Fig. 2.5a shows a scheme for the reporter neutralization tests. DK23 Nano and YF4 Nano were used to evaluate the neutralizing activity of a panel of sera from mice previously vaccinated/infected with relevant flaviviruses, including ZIKV, YFV, JEV, WNV, and DENV1 to DENV4. Fig 2.5b summarizes the cross-neutralizing titers, whereas Figs. 2.6b-c present the raw neutralizing curves. When tested against ZIKV DK23 Nano, ZIKV-sera consistently neutralized the virus; only one DENV3-serum weakly neutralized ZIKV; all other flavivirus-sera had NT₅₀ values below the initial dilution of 1:50 (Fig. 2.5b). Likewise, when tested against YF4 Nano, only YFV-sera fully neutralized the virus, whereas other sera NT₅₀ values were either below or just above the first 1/50 dilution (Fig. 2.5b). Compared with ZIKV, YFV seemed to be weakly cross neutralized by other flavivirus sera. As negative controls, uninfected mouse sera did not neutralize ZIKV though some neutralization was seen with YFV (titer of 1/51). The latter result indicates that the neutralizing titers in the range of 1/50 and 1/64 against YFV should be considered negative (Fig. 2.5b).

Furthermore, a panel of ZIKV-positive human sera were analyzed by both reporter and plaque reduction neutralization tests (Fig. 2.5c) and the results from both were graphed on separate axes for comparison (Fig. 2.5d). The R² value of 0.93 affirms that the reporter neutralization results are strikingly similar to those from a traditional neutralization test. Together, these outcomes support the conclusions that (i) reporter viruses could be used for measuring neutralizing antibody titers, (ii) the relative neutralizing levels among different flaviviruses may indicate the type of viral infection, (iii) flavivirus antibodies cross neutralize, (iv) reporter viruses can be used in place of traditional PRNT assays for improved turnaround time.

Finally, we tested the utility of reporter viruses for antiviral testing. Huh7 cells were treated with a known flavivirus inhibitor NITD008 (an adenosine analog [119]) upon infection with the two viruses (Fig. 2.5e). At 48 h post infection, the luciferase signal was inhibited by NITD008 in a dose-responsive manner, leading to EC₅₀ of 0.47 μ M for ZIKV (Fig. 2.5f) and 0.46 μ M for YFV (Fig. 2.5g). These EC₅₀ values are equivalent to the previously reported values using plaque reduction assay [119,120], demonstrating the utility of reporter viruses for antiviral testing.

DISCUSSION

Reporter flaviviruses, useful tools though they are, have been stymied by instability since they were first described. Efforts to rectify this shortcoming, until recently, have been inadequate. We have developed a method for stabilizing reporter flaviviruses, using recombination-dependent lethal mutations, and shown it to be successful for two flaviviruses, ZIKV and YFV. This strategy relies on two functions that the capsid gene plays in the viral life cycle. The capsid gene codes for the capsid protein, which requires positive charges in the N-terminus, though their role is still unclear. It has been proposed that they assist in binding viral RNA [86], though models of capsid-RNA binding have been suggested that do not include the N-terminus [12,121]. The N-terminus is flexible and unstructured and accordingly this region has yet to be incorporated in solved crystal structures. Though its function remains obscure, our results show that multiple flaviviruses, not just DENV, require a threshold of positive charges in this region for virion assembly.

The capsid gene also provides RNA replication elements essential for viral replication. The flavivirus 5' UTR is highly structured, with two well defined stem loops, A and B. The start codon (the beginning of the capsid gene) is present on the descending side of stem loop B. Other required RNA signals in the capsid gene include the well-defined 5'CS [34], the cHP [36], 5' DAR [122], and DCS-PK [40]. Ideally, the engineered capsid

mutations that stabilize the reporter flaviviruses would change the protein charge, but not perturb these cis-acting RNA elements. The attenuation of replication seen when comparing DK Nano and DK23 Nano or YF Nano and YF4 Nano indicates we have not wholly achieved this ideal condition. Exhaustive screening of mutations in this region may yield a mutant that is more replication robust compared to what has been published here, though it is unlikely to be completely unattenuated. It is possible that simply increasing the length of the genome perturbs genome cyclization or viral RNA packaging and thus agitates the viral life cycle. As demonstrated, the attenuation inherited with the stability does not inhibit the virus' capacity for robust growth in cell culture, nor its utility as a screening and serological tool. We have shown this system is valuable for rapidly testing sera for neutralizing antibodies and compounds for antiviral activity, though the number of serum samples and compounds tested was relatively small. Further validation with more serum samples, including those with a broad range of neutralizing activity, and antiviral compounds is warranted.

Recently, Volkova, *et al.* published a paper describing a stable Zika NanoLuc and EGFP virus. Their strategy, analogous to ours in that it stops viruses that have recombined, involves adding a frameshift mutation at the beginning of the duplicated capsid. This elegant approach involves very little perturbation of RNA elements and still results in a stable virus [82]. It should be noted that the C25 NanoLuc ZIKV here reported is significantly more robust than their described C25 ZIKV, as seen by comparison of viral titers from growth kinetics on Vero cells. Another elegant and successful approach in flavivirus reporter constructs was first reported in [98] and further improved on in [99]. A split NanoLuc construct was utilized and engineered in a permissive site in JEV NS1. Such a small insertion (11 amino acids) lends itself to great stability and Tamura, *et al.* modeled and tested insertion sites until the reporter virus and WT JEV had no statistical difference in mortality in mice. Despite stability and lack of attenuation, this system sacrifices the

flexibility present when the virus codes the full protein, most notably being unable to perform *in vivo* imaging.

The long-term stability of reporter flaviviruses could be used to further probe the complicated, multi-host life cycle of these human pathogens. *In vivo* imaging of ZIKV transmission between live mice and mosquitoes was the original goal of this research project. Unfortunately, neither the DK Nano nor the DK23 Nano virus succeeded in causing disease in A129 mice or showing robust luciferase signal in an IVIS setup (Fig 2.7). Mice did become briefly viremic but did not lose weight or show outward signs of disease. Rectifying these shortcomings are ongoing research aims.

In conclusion, we have achieved a stable NanoLuc ZIKV and YFV by incorporating recombination-dependent lethal mutations that abolish formation of viral particles if they have recombined. These viruses have potential to be used in enhanced, rapid-turnaround, PRNT assays and drug screenings. They can also be used as a platform for stable, long-term transgene delivery.

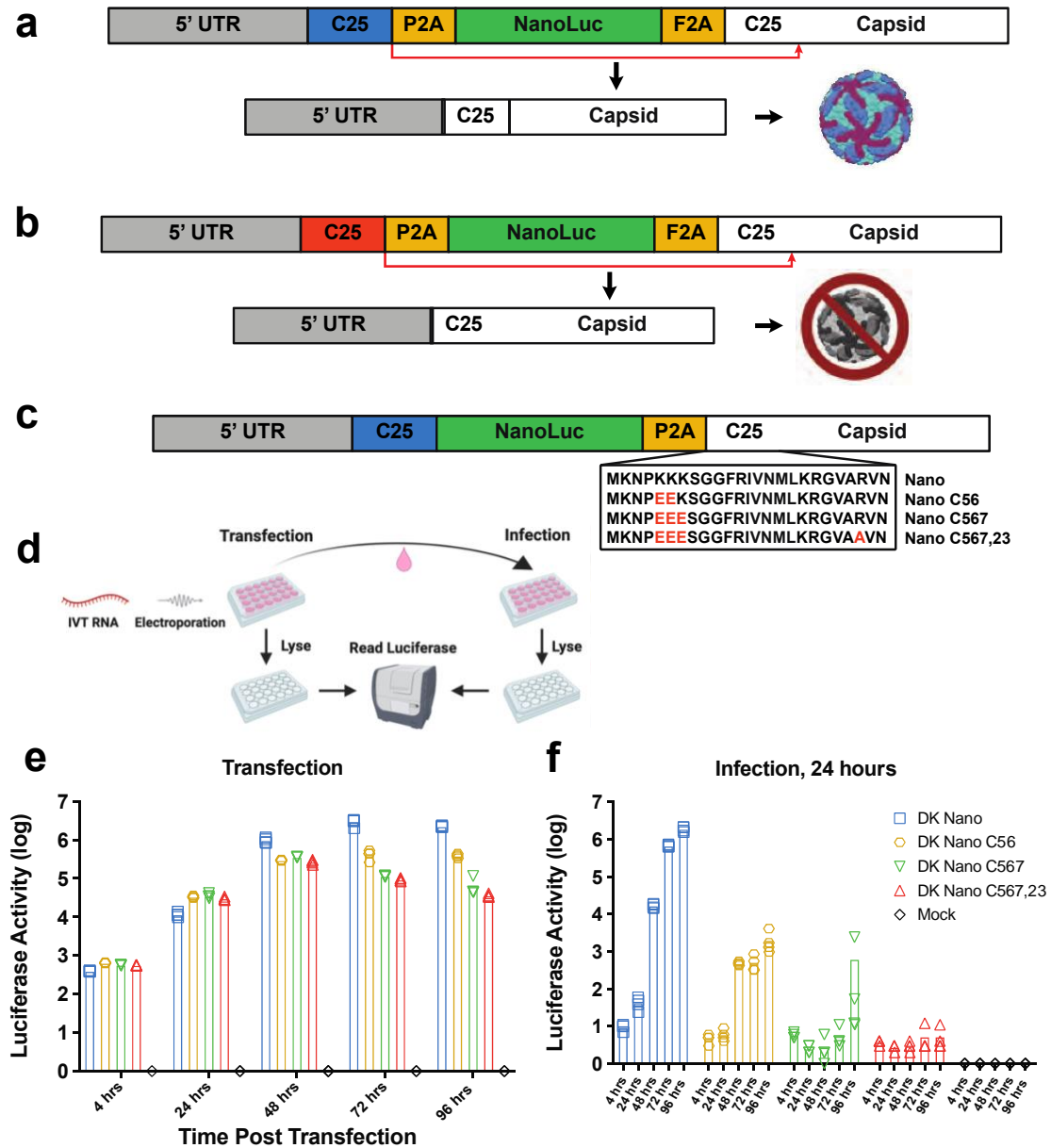


Figure 2.1 Identification of Recombination-Dependent Fatal Mutations.

a. Scheme of reporter ZIKV based on the African lineage Dakar 41525 strain (DK). The nano luciferase gene (Nano) is eliminated by recombination, resulting in WT virus, despite codon optimization (denoted by white C25). **b.** Scheme of reporter virus carrying recombination-dependent lethal mutations in the C25 (indicated in red). These mutations become lethal to viral particle formation upon recombination with the full capsid protein. **c.** Genome scheme for deleterious capsid mutation screen. Basic amino acids in the

beginning of the capsid protein were mutated to negative or neutral amino acids. **d.** Experimental scheme to screen capsid mutations for effect on viral particle formation. *In vitro* transcribed RNAs of full-length reporter ZIKV with-and-without capsid mutations were electroporated on Vero cells and plated on 24 well plates (n=4). At 4, 24, 48, 72, and 96 h post transfection, cell supernatants were collected for subsequent infection and cells were washed and lysed for luciferase measurement (transfection). The cell supernatants were used to infect naive Vero cells, which were all washed and lysed 24 h post infection after which luciferase readings were taken. Each virus was done in quadruplicate. **e.** Luciferase readings from electroporated RNAs at the indicated time points. **f.** Luciferase readings taken at 24 h post infection with supernatants collected at the time points indicated on the X axis from E. High luciferase activity indicates that high titers of infectious virus were made post electroporation, with results indicating charge-reversing mutations in the capsid inhibit viral particle formation.

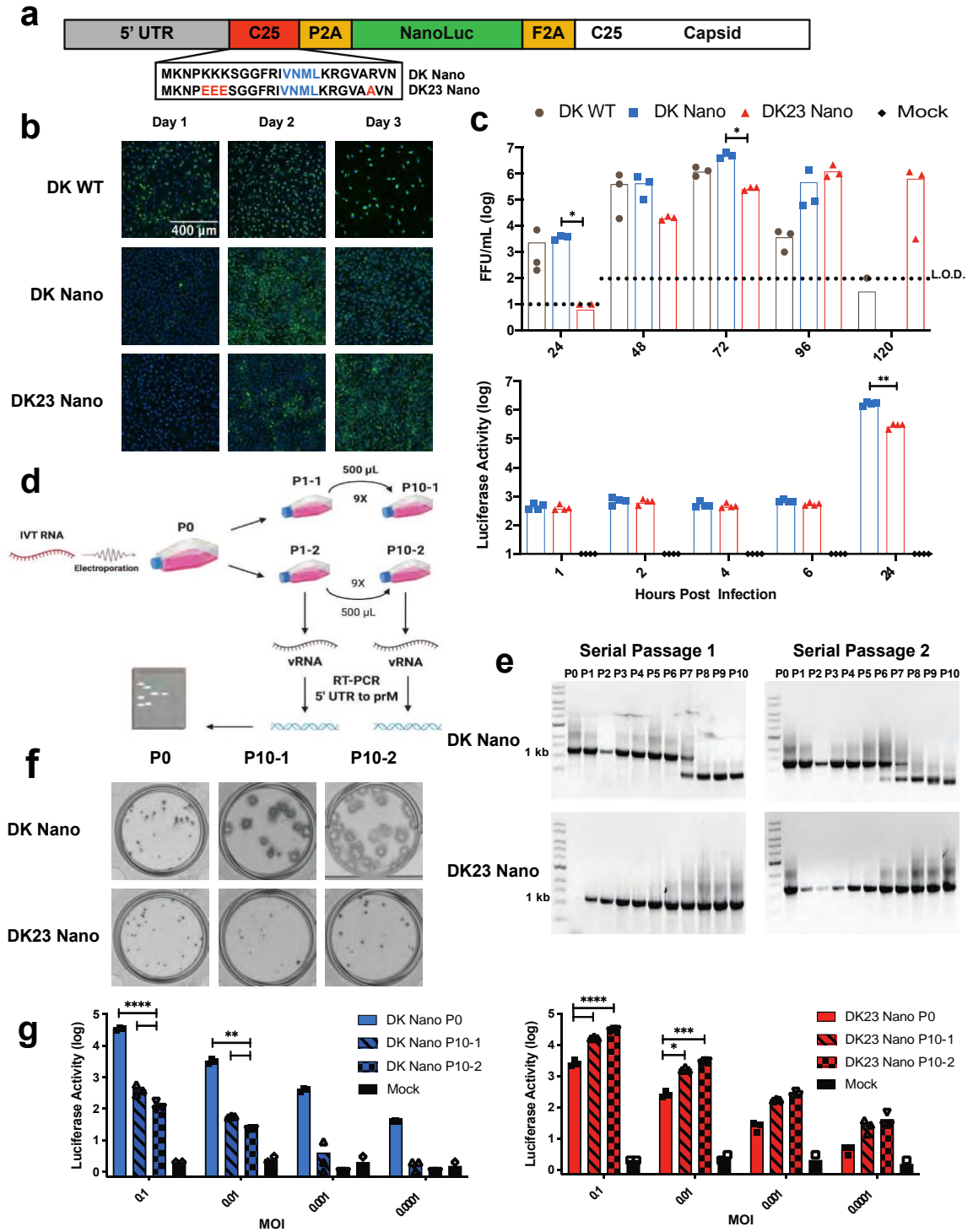


Figure 2.2 A Stable NanoLuc ZIKV.

a. Genome scheme of reporter ZIKV with and without capsid mutations. For reference, the amino acids corresponding to the 5' cyclization sequence are highlighted in blue. **b.**

Comparison of WT Dakar strain ZIKV, DK Nano, and DK23 Nano IFA. Vero cells were seeded post-electroporation and fixed on days 1-3. Viral envelope protein was probed by 4G2 Ab. Scale is the same for all pictures. **c.** Replication kinetics of the different viruses on Vero cells by both focus forming (MOI 0.01, n=3) and luciferase assay (MOI 0.5, n=4). Data comparison was done with 2-way ANOVA, using Tukey's post-hoc test for multiple comparisons (*= $p<0.05$, **= $p<0.01$). **d.** Virus passaging scheme. Virus collected post electroporation was termed P0 and 500 μ L was used to inoculate a T75 flask of naive Vero cells. Infection proceeded until CPE was observed, ~3 days, after which virus was harvested and 500 μ L was passaged onto fresh Vero cells until P10 was reached. This was done in two independent passaging series. Viral RNA was harvested from each passage and RT-PCR performed from the 5' UTR through the end of the capsid gene. Stability was observed by the size of the RT-PCR band compared to P0. **e.** Passage results from two independent series P0 to P10 for DK Nano and DK23 Nano. RT-PCR band for full length reporter virus is 1,225 bp. The WT, non-reporter virus product is 508 bp. DK Nano shows instability at P6 or P7, while DK23 Nano maintains a consistent RT-PCR product size through P10. **f.** Focus sizes for DK Nano and DK23 Nano P0 and P10 after 4 days of infection on Vero cells. The P0 viruses formed tiny foci for both DK Nano and DK23 Nano viruses. However, the P10 DK Nano developed large foci, whereas P10 K23 Nano remained tiny foci. **g.** Luciferase assay of P0 and P10 viruses. Vero cells were infected with indicated viruses at different MOIs. At 24 h post infection, intracellular luciferase activities were measured. Each time point was repeated 3 times, with each replicate shown. 2-way ANOVA with Tukey's post-hoc test was used to assess significance (*= $p<0.05$, **= $p<0.01$, ***= $p<0.001$, ****= $p<0.0001$).

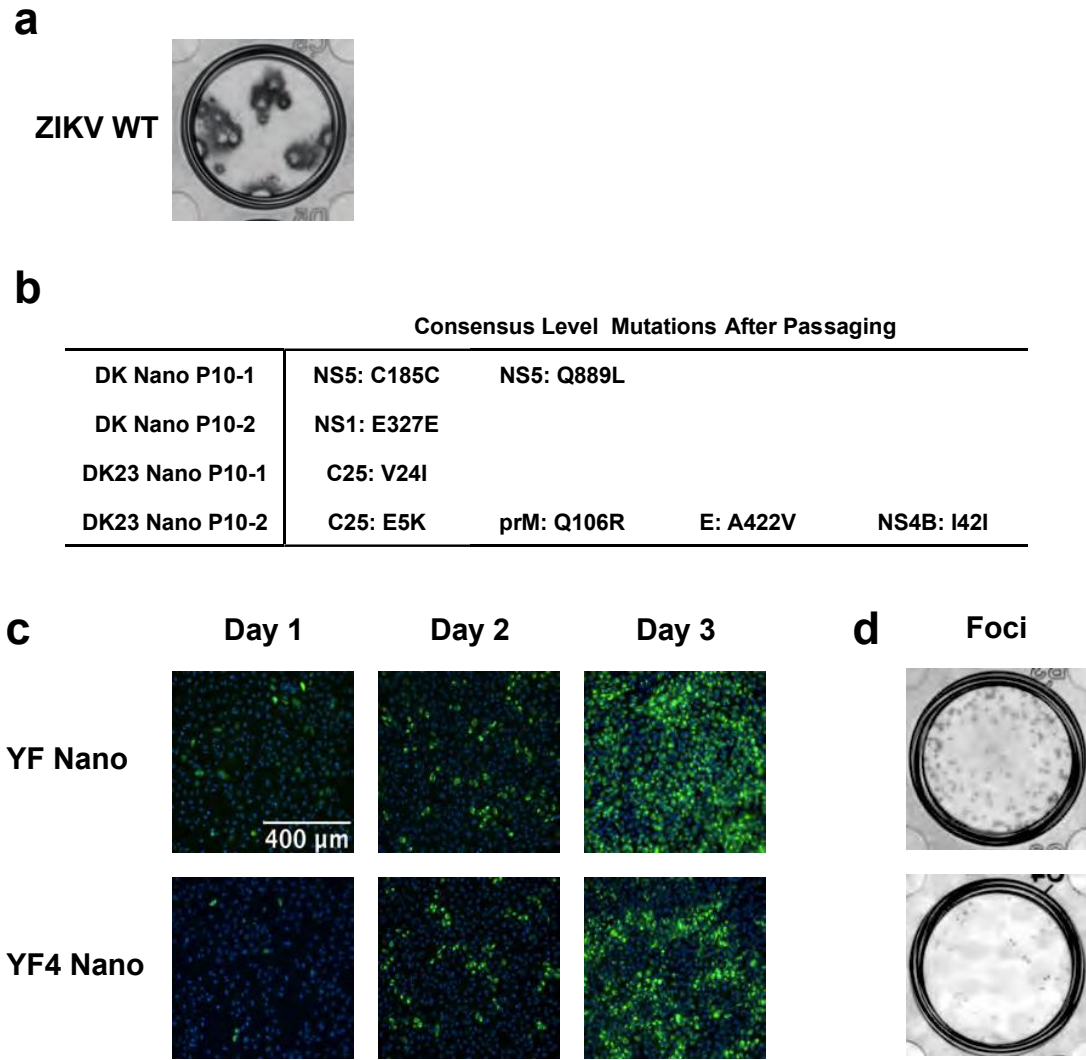


Figure 2.3 Additional Viral Characterization

a. DK WT foci on Vero cells. **b.** Consensus-level mutations found in DK Nano and DK23 Nano viruses after ten passages on Vero cells. **c.** Immunofluorescence assay showing infection of YF and YF4 Nano viruses on Vero cells after electroporation. Viruses were probed by 4G2 antibody while cells were counterstained using DAPI. The scale of all images is the same. **d.** Foci of the respective YF viruses after a four-day infection on Vero cells.

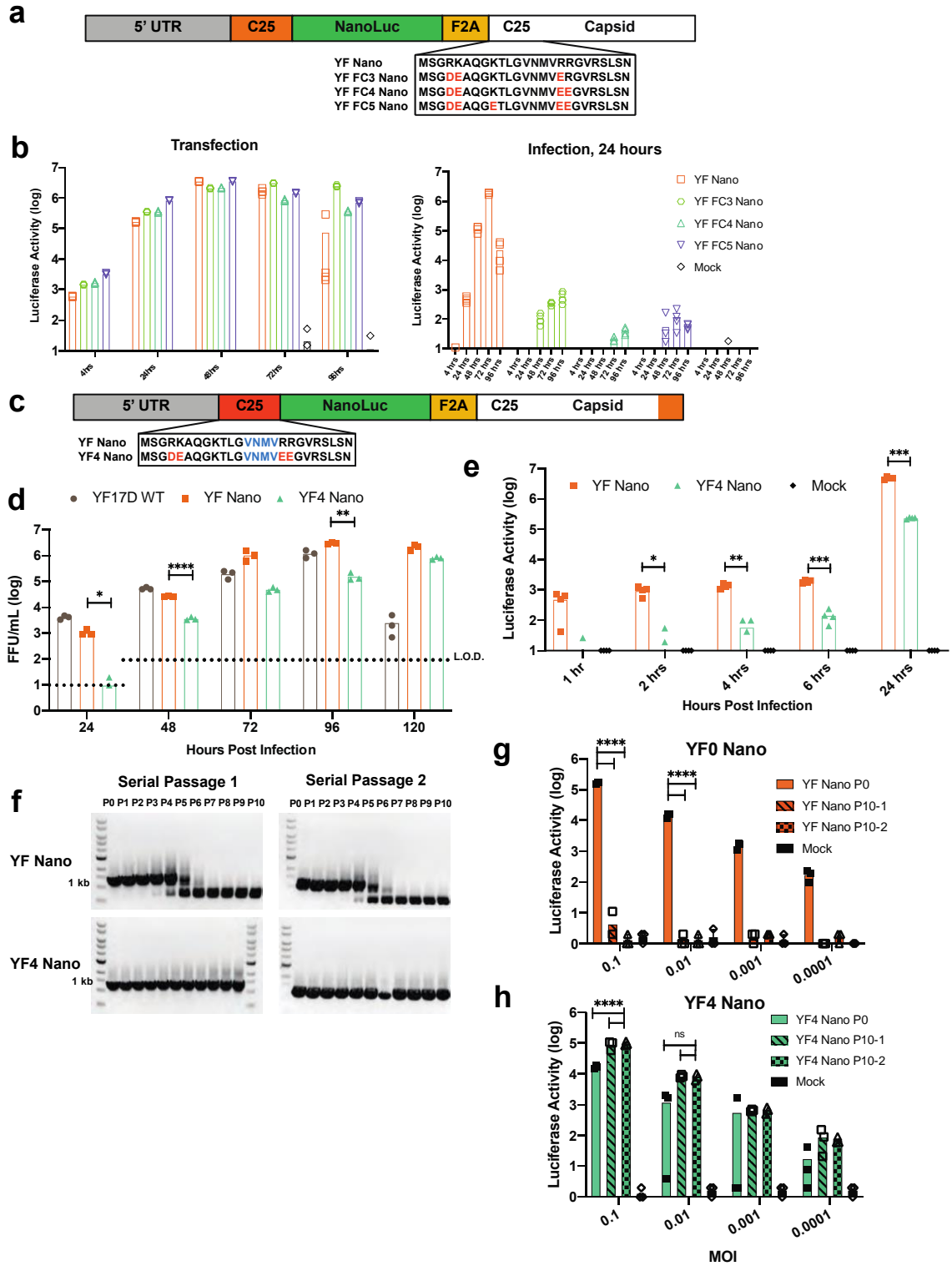


Figure 2.4 A Stable NanoLuc YFV.

a. Genome scheme of YF17D reporter virus carrying different charge-reversing capsid mutations. These viruses were used to screen deleterious capsid mutations in YFV. **b.** YFV capsid mutation screen results. See Fig. 1d for experimental scheme. Transfection results for different YFVs with capsid mutations taken at different time points after electroporation show robust luciferase expression. Subsequent infection using infected cell supernatants taken at the indicated time points shows four and five amino acid changes are sufficient for knockdown of viral particle formation. **c.** Genome scheme of YF Nano and YF4 Nano, showing positions of capsid mutations (red) and the amino acids that correspond to the 5' CS (blue). **d.** Replication kinetics of YF17D WT, YF Nano, and YF4 Nano on Vero cells (MOI 0.01, n=3). 2-way repeated measures ANOVA with Tukey's post-hoc test was used to assess significance (*=p<0.05, **=p<.0.01, ***=p<0.001, ****=p<0.0001). **e.** Luciferase kinetics of YF Nano and YF4 Nano on Vero cells (MOI 0.5, n=4). Significant differences in the data were assessed by 2-way ANOVA with Tukey's post-hoc test. **f.** Passaging results for YF Nano and YF4 Nano. See Fig 2d for passaging scheme. The RT-PCR band from intact reporter virus is 2,388 bp, while the non-reporter band (with luciferase gene deleted) is 631 bp. The consistent band size seen in YF4 Nano indicates its stability through 10 passages. **g.** Luciferase assay comparing P0 and P10 luciferase activity between YF Nano and YF4 Nano at different MOIs (n=3). Infection was carried out for 24 h on Vero cells. Significant differences were measured using 2-way ANOVA with Tukey's post-hoc test (*=p<0.05, **=p<.0.01, ***=p<0.001, ****=p<0.0001).

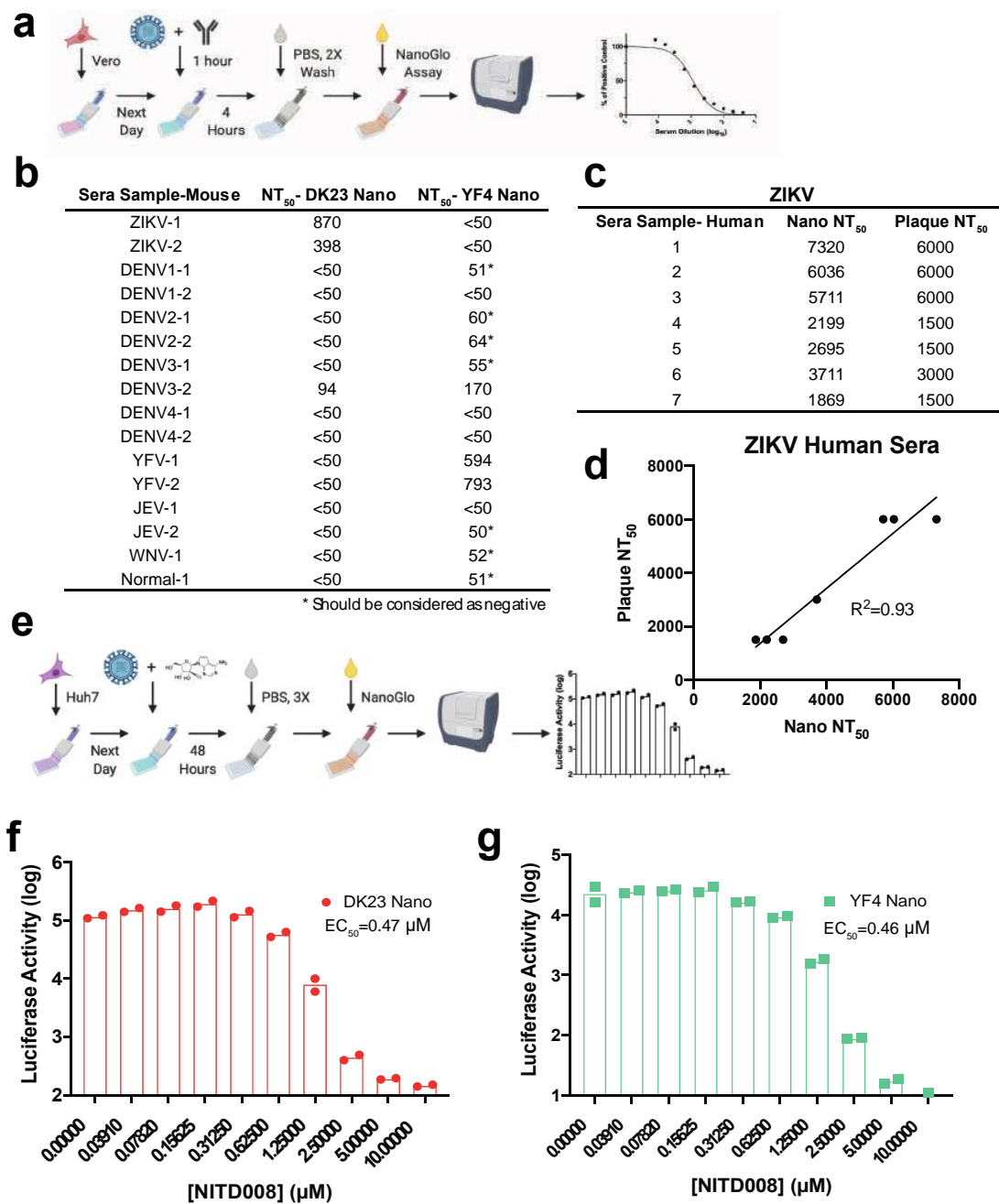


Figure 2.5 Applications of Stable Reporter Viruses.

a. Scheme for four-hour reporter neutralization test. Briefly, Vero cells are plated at 1.5×10^4 cells per well in a 96 well plate. The next day, sera are serially diluted 2-fold (starting at 1:50, $n=2$) and mixed 1:1 with virus and incubated for 1 h at 37°C. The sera:virus mixture is plated on the cells and incubated for 4 h. Following PBS wash, the plates are read by

plate reader after addition of luciferase substrate. **b.** Table with NT₅₀ values of a panel of sera from mice inoculated with the indicated virus. Sera were tested against both DK23 Nano and YF4 Nano viruses. **c.** NT₅₀ values from a panel of Zika-positive human serum samples, tested by both 4-h reporter neutralization test and traditional plaque assay. Data generated by colleague Xuping Xie. **d.** Graphical comparison of reporter and plaque NT₅₀ values. Simple linear regression was used to create a line of best fit. **e.** Antiviral assay scheme. Huh7 cells are seeded at 1.5×10^4 cells per well in a 96 well plate. The following day, reporter virus is mixed with diluted compound and plated on the cells (n=2). Following a 48-h incubation, cells are washed, and luciferase substrate is added. Luciferase levels are read by plate reader. **f-g.** Antiviral activity against DK23 Nano and YF4 Nano, respectively, assessed by luciferase levels.

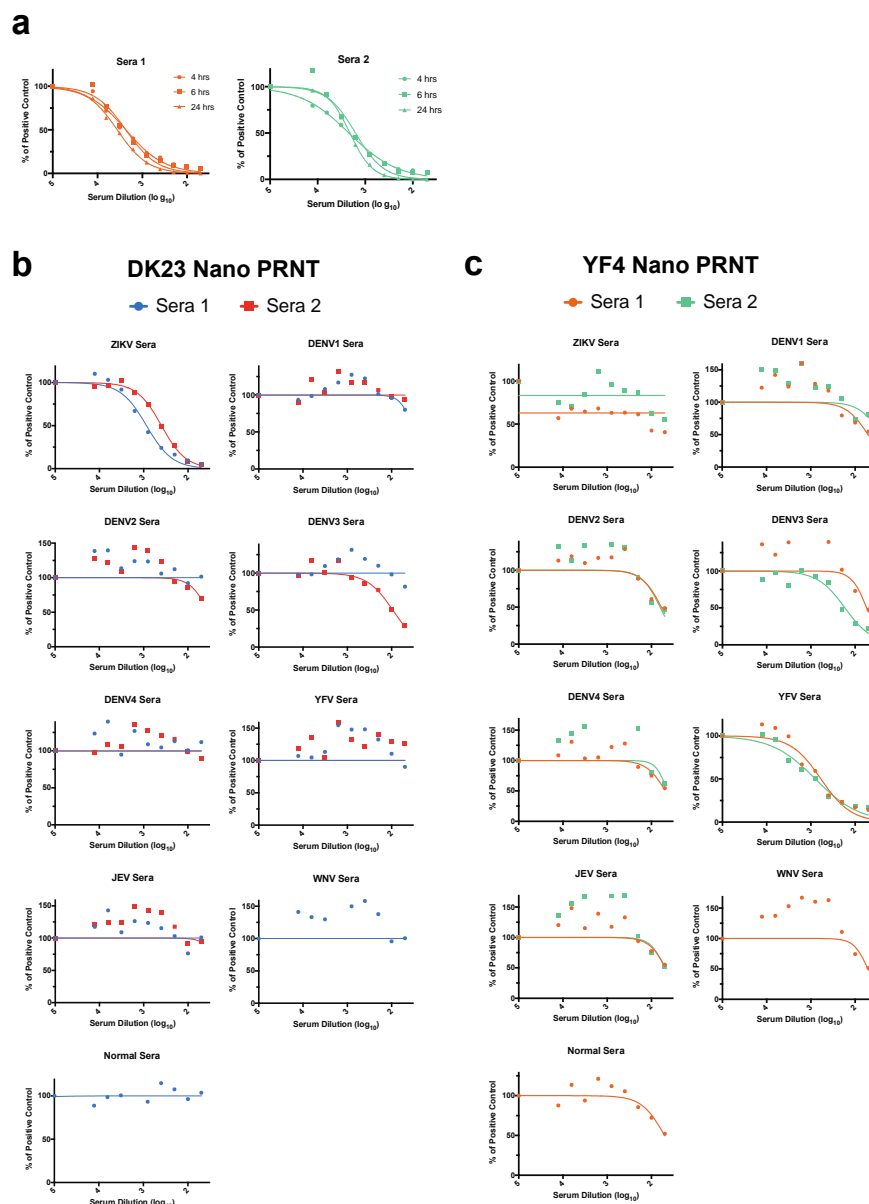


Figure 2.6 Neutralization Curves

a. Neutralization curves obtained from sera neutralizing YF4 Nano read at 4, 6, and 24 hours after addition of sera:virus mixture to Vero cells. **b-c.** Reporter neutralization curves used to determine NT₅₀ values in Fig 4b for DK23 Nano and YF4 Nano, respectively. Luciferase values from negative control wells were averaged and subtracted out as background. Positive controls were set at 100% and other values plotted as a percent of the positive control.

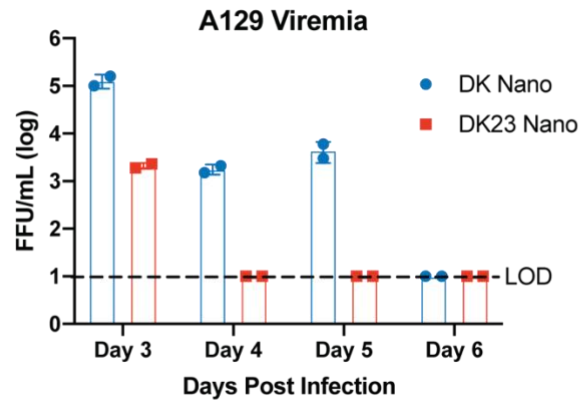
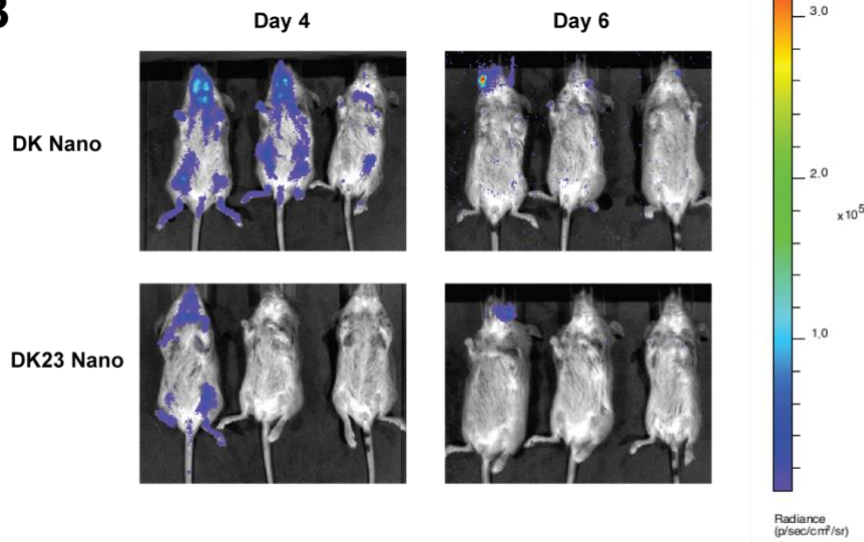
A**B**

Figure 2.7 DK Nano and DK23 Nano in A129 Mice

Three-week old A129 mice were inoculated subcutaneously inoculated with 1×10^6 FFU/mL. **A.** Two mice from each group were bled by retro-orbital route on days 3-6. Each sample was titrated by focus-forming assay. **B.** Viral luciferase signals were assessed by IVIS imaging. Mice were given 100 μ L of NanoGlo substrate in PBS and anesthetized by isofluorane. They were then placed in the machine and then imaged. The mouse on the right of each picture is a non-infected control.

MIAF-WRCEVA, UTMB	
Virus	Strain
ZIKV	FSS 13025
DENV1	Hawaii
DENV2	NGC
DENV3	H 87
DENV4	Unknown
YFV	Asibi
JEV	Unknown
WNV	Ib An 23601

Table 2.1 Virus strains used to raise MIAF

Chapter 3: Reporter Stabilization by Optimization of Capsid

Duplication Length³

INTRODUCTION

Viruses from the arthropod-borne genus *Flavivirus* afflict people across the globe causing febrile, neurologic, and hemorrhagic disease [123]. Notable among the flaviviruses are the four serotypes of dengue virus (DENV), which cause an estimated 96 million symptomatic infections yearly [7], Japanese encephalitis virus (JEV) which causes the annual loss of 709,000 disability-adjusted life years [124], the recently emerged Zika virus (ZIKV), which has become associated with congenital malformations [125], encephalitic West Nile virus (WNV), and yellow fever virus (YFV), which periodically emerges from its sylvatic transmission cycle to start an urban transmission cycle [126]. Concerted efforts by scientists and clinicians have brought about vaccines for YFV, JEV, and DENV [8,127] though effective antiviral drugs have yet to be approved. Reporter flaviviruses, first published in 2003 [74], have been critical for high-throughput antiviral compound screens [87,100], host and virus pathogenesis studies [128], and serological diagnosis [102,103]. Despite these advances, reporter flaviviruses suffer from genetic instability during longer periods of growth or passaging, thought to be primarily mediated by recombination [75,86].

Our previous work showed that we could overcome the genetic instability problem by the use of recombination-dependent lethal mutations, though that technique had only been applied ZIKV and YFV [101]. We next sought to apply this technique to other flaviviruses in order to expand the serological and pharmaceutical tools available. First, we used the DK23 Nano backbone and made a panel of prME chimeric flaviviruses using

³ Content of this chapter has been previously published: Baker, C.; Liu, Y.; Zou, J.; Muruato, A.; Xie, X.; Shi, P.-Y. Identifying optimal capsid duplication length for the stability of reporter flaviviruses. *Emerg Microbes Infect* 2020, 1–32, doi:10.1080/22221751.2020.1829994.

DENV1-4, JEV, YFV, and WNV as prME donors. This technique is well described for the generation of vaccines using both the YF17D and JEV 14-14-2 vaccine strains [57,129–131], as well as in diagnostic applications [104,105,107,132]. After questions arose about these viruses' ability to be neutralized in the same way authentic viruses were, the decision was made to pursue a panel of authentic, stable reporter viruses instead of continuing testing of the chimeric viruses.

Reporter genes are routinely engineered at the beginning of the single open reading frame of the viral polyprotein, between the 5' UTR and the capsid gene, as first described using YFV [84]. RNA signals that aid in genome cyclization, which is essential for viral replication, and facilitate translation are continuous from the 5' UTR into the beginning of the capsid. These signals must function together, therefore it is necessary to duplicate a portion of the capsid gene and place it upstream of the inserted reporter gene. Until recently, efforts to stabilize these constructs centered on reducing homology between the duplicated capsid sequences by codon scrambling in an effort to reduce homologous recombination [84,88]. This also had the benefit of expunging the *cis*-acting elements in the full capsid sequence, leaving only the upstream elements. Two additional methods for stabilizing reporter flaviviruses have been newly developed, both focusing on blocking recombined reporter viruses from continued infection. Volkova and colleagues report a single-nucleotide insertion to the duplicated capsid portion of a reporter ZIKV that minimally perturbs critical RNA elements but causes a +1 frameshift [82]. If recombination occurs between the duplicated capsid sequences that flank the reporter gene, this frameshift mutation is incorporated into the viral polyprotein and causes mistranslation, effectively taking out recombined viruses from the population. We developed a related method for reporter ZIKV and YFV using recombination-dependent lethal mutations in the duplicated capsid [101]. These lethal mutations stop viral particle formation if recombination brings them into the viral polyprotein.

The length of capsid duplications in different flavivirus reporter constructs that have been reported varies from 25, to 33 or 34, 38, 50, or even the full capsid [82,84,85,87–91,93]. Shorter lengths are tolerated by some viruses and not by others. At the onset of this investigation, there was no published comparison of the effect of capsid duplication length and its effect on stability. It was believed that shorter capsid repeats were preferred because the shorter homologous sequence minimizes homologous recombination. We hypothesize that an optimal length of capsid duplication is required for efficient viral replication; a shortened capsid duplication imposes a selection pressure on viral replication, leading to undesired recombination and deletion of the engineered reporter gene. The goal of this study was to test this hypothesis by engineering different lengths of capsid duplication and investigating the length effect on the stability of the reporter gene in various flaviviruses. Indeed, we found an optimal length of capsid duplication of 34 or 38 amino acids that can increase the reporter gene stability for at least ten rounds of cell culture passages. Taking this new approach, we have developed a panel of long-term stable NanoLuc-tagged flaviviruses, including the four serotypes of DENV, JEV, YFV, WNV, and ZIKV. In addition, we demonstrated the use of the reporter flaviviruses for rapid antibody neutralization testing and antiviral drug discovery. Taken together, our results have established a previously unrecognized approach to generate stable reporter flaviviruses that are useful for research and countermeasure development.

MATERIALS AND METHODS

Viruses and cells

Zika virus strain Dakar 41525, yellow fever strain 17D YFS11, dengue virus 1 strain Western Pacific, dengue virus 2 strain New Guinea C, Japanese encephalitis virus strain 14-14-2 1454, and West Nile virus strain NY99 with NS5 E218A [133,134] were cloned into full-length plasmids using the low copy pCC1 vector as has been previously

described [116]. NEBuilder HiFi DNA Assembly mix (NEB E2621) was used to assemble all plasmids. Full length dengue virus 3 strain VN32 and dengue virus 4 strain MY01 transcripts were assembled from four and three fragments, respectively, by *in vitro* ligation. Viruses were recovered after electroporation (Biorad GenePulser Xcell) of *in vitro* transcribed RNAs in Vero (ATCC Cat# CCL-81) or BHK21 (ATCC Cat# CCL-10) cells as previously described [89]. Vero and BHK21 cells were grown in DMEM (Gibco 11965) with 10% fetal bovine serum (FBS, Hyclone SH30071) and 1% penicillin/streptomycin (Gibco 15140). Huh7 cells were grown in DMEM with Glutamax (Gibco 10566) supplemented with 10% FBS, 1% penicillin/streptomycin, and 1% non-essential amino acids (Gibco 11140). C6/36 mosquito cells were grown in DMEM supplemented with 10% FBS and 1% penicillin/streptomycin. Infections were carried out in the same media excepting supplementation with 2% fetal bovine serum instead of 10%. Vero, BHK21, and Huh7 cells were grown at 37°C in a humidified incubator with 5% CO₂. C6/36 cells were grown at 30°C in a humidified incubator with 5% CO₂.

Immunofluorescence assay

Vero cells were seeded into chamber slides immediately post-electroporation. At the indicated time points, cells were washed with PBS and fixed with cold methanol at -30°C for >30 minutes. Slides were washed with PBS and blocked with PBS+1% FBS overnight at 4°C. The flavivirus envelope reactive antibody 4G2 (ATCC Cat# HB-112), diluted in blocking buffer, was used as a primary antibody incubated for 1 hour at room temperature. A secondary goat anti-mouse IgG antibody conjugated with Alexa Fluor 488 (Thermo Fisher Scientific Cat# A-11001) was then used to probe for 4G2 for 1 hour. Slides were then washed 3X with PBS and stained with DAPI (Vector Laboratories, H-1200) and then imaged on a Nikon Eclipse Ti2 microscope. ImageJ (NIH) was used to process the images.

Focus forming assay

All viruses were titered by focus-forming assay. Viruses were serially diluted ten-fold in DMEM supplemented with 2% FBS and used to infect Vero cells that had been seeded the day previously at 2×10^5 cells per well in a 24-well plate. After a 1-h infection with rocking every 15 minutes, the virus was removed and methylcellulose (Sigma C5013) /DMEM overlay was added. After four days of infection, the overlay was removed, and cells were fixed with a 1:1 solution of methanol/acetone for >15 minutes. Plates were then washed 3X with PBS, blocked with PBS+3% FBS for 30 minutes, and then incubated with virus-specific mouse immune ascites fluid (MIAF, World Reference Center for Emerging Viruses and Arboviruses, UTMB, see Table 2.1). After >1-h incubation with MIAF, plates were washed with PBS and incubated with a horseradish peroxidase-conjugated anti-mouse IgG antibody (SeraCare KPL Cat# 474-1806). After a 3X PBS wash, foci were developed in the dark using an AEC peroxidase substrate kit (Enzo 43825) according to the manufacturer's protocol and imaged using a BioRad ChemiDoc Imaging System.

Reporter virus passaging and stability

Virus recovered from electroporation was termed P0. 500 μ L of this was added to a T75 flask with a confluent layer of Vero cells. Once cell death was observed the supernatant was collected and clarified by centrifugation. 500 μ L of the new passage was then used to infect a new T75 flask for the next passage. This was carried out in two parallel series for each virus. Stability was assessed by isolating viral RNA (Qiagen 52904 or TriZOL, Invitrogen 15596026) from each passage and using this as a template for an RT-PCR (Invitrogen 12574) with primers that spanned the 5' UTR to the end of the capsid. The products were then run on a 0.6% agarose gel and imaged with a BioRad GelDoc EZ Imager.

Growth kinetics by focus forming assay

Six well plates were seeded at 8×10^5 cells per well with Vero cells the day before infection. Cells were infected at a MOI of 0.01 in triplicate for 1 h with shaking every 15 minutes, followed by a 3X PBS wash and addition of media supplemented with 2% FBS. Supernatant samples were taken at 24, 48, 72, 96, and 120 h and titered by focus-forming assay.

Reporter neutralization assays

Reporter neutralization tests were done by two-fold serially diluting sera, starting at 1:50 in DMEM with 2% FBS. Sera samples positive for ZIKV and DENV1-4 were pooled from mice infected with the respective virus. YFV and JEV serum samples were from vaccinated mice. Sera dilutions were mixed 1:1 by volume with the respective reporter virus and incubated at 37°C for 1 h. The virus/sera mixture was then plated on Vero cells in a white, opaque 96 well plate that was seeded at 1.5×10^4 cells per well. After a 4-h incubation at 37°C, the wells were washed 2X with PBS and 50 μ L of NanoGlo substrate diluted 1:50 in NanoGlo Assay Buffer was added to the cells. Plates were read in a BioTek Cytation 5 plate reader after 3 minutes with a gain of 150. Positive controls consisted of virus infection with no sera. Negative controls comprised virus plated in wells with no cells. This negative control allows for subtraction of background luciferase signals from the virus media. After subtraction of negative controls, values were converted to a percent of the positive control. The data were then analyzed by four parameter nonlinear regression, with the top and bottom constrained to 100 and zero, respectively, and the NT₅₀ reported.

Antiviral assays

The panflavivirus inhibitor NITD008 was diluted in 90% DMSO to 10 μ M and then two-fold serially diluted 8 times. These dilutions were mixed with virus (MOI 0.1-DENV1,

DENV2, DENV3; MOI 0.01-ZIKV; MOI 0.001-DENV4, YFV, JEV) and plated on Huh7 cells that were seeded at 1.5×10^4 cells per well the previous day in media with 2% FBS. Cells were washed 48 h post infection three times with PBS followed by addition of NanoGlo substrate diluted 1:100 in NanoGlo Assay Buffer. Plates were read by a BioTek Cytation 5 plate reader after 3 minutes.

Luciferase Expression

Luciferase expression was assayed on C6/36 cells. The day prior to infection, 2×10^4 cells per well were seeded into a white, opaque 96 well plate. Infections were done at MOI 0.1. Inoculum was removed at the assay time point, followed by 2X wash with 150 μ L of PBS. 50 μ L of NanoGlo substrate diluted 1:50 in Nano Assay Buffer was added to each well, followed by a three-minute incubation. Plates were read by a BioTek Cytation 5 instrument at a gain of 100.

Mosquito infections

For the micro-injection study, Rockefeller strain *Aedes aegypti* mosquitoes were injected (100 nL) intrathoracically with virus diluted in PBS so that each mosquito received 50 FFU. Mosquitoes were cultured at 28°C for 8, 12, and 18 days. For blood feeding study, sheep's blood was centrifuged at 1000g, 4°C for 20 minutes to separate plasma and cells. The plasma was heat-inactivated at 56°C for 1 hour and the cells were washed twice with PBS after which they were combined again. The blood was spiked with virus to a concentration of 2×10^6 FFU/mL. Engorged mosquitoes were further reared and harvested at 8, 12, and 18 days. At the time points indicated mosquito samples from both experiments were thoroughly homogenized (Qiagen TissueLyser II) in 200 μ L PBS and centrifuged to pellet the tissue. 50 μ L of supernatant was used for both RT-qPCR and luciferase assay. RNA was harvested using Qiagen RNeasy minikit and used in a Taqman RT-qPCR reaction targeting a region in NS5. *Aedes aegypti* actin served as a control. For luciferase

assay, 50 μ L of supernatant from homogenized mosquito was added to a 96 well opaque white plate, followed by addition of NanoGlo substrate, diluted 1:50 in NanoGlo Assay Buffer. Samples were read in a BioTek Cytation 5 plate reader. Background luciferase levels (no mosquitoes) and clean, uninfected mosquitoes were used as negative controls.

Statistical analysis

Graphpad Prism 8 was used for graphing and statistical analysis. Statistical tests used, as well as significance levels, are noted in the figure legends. All replicated values are shown on each graph.

Illustrations

Figures were created using Biorender and Abode Illustrator.

RESULTS

Panel of reporter flaviviruses

Reporter flaviviruses were constructed as first described by [84] using capsid duplication lengths as found in the literature [84,87,89,91,93] (Fig. 3.1A-B). All viruses except DENV3 and DENV4, which were assembled by *in vitro* ligation (Fig. 3.2), were constructed using traditional, plasmid-based reverse genetics approaches [73]. DENV3 and DENV4 full genomes are difficult to clone in bacteria, due to putative toxic elements present [135,136]. The NanoLuc gene followed by the 2A sequence from thossea asigna virus (T2A) were inserted between a duplicated portion of the capsid and the full-length capsid. To help prevent homologous recombination, the codons in the capsid sequence corresponding to the duplicated portion were scrambled to reduce homology. All full-length DNAs were used as a template in an *in vitro* transcription reaction to generate full-length RNAs, which were subsequently electroporated into Vero cells (for ZIKV, YFV, and WNV) or baby hamster kidney (BHK) cells (for DENV1-4 and JEV).

Immunofluorescence assay (IFA) was used to indicate viral spread, post electroporation (Figs. 3.1B and 3.3A). Focus-forming assay shows all reporter viruses form distinct foci (Fig. 3.1C), but no plaques when stained with crystal violet (data not shown). The IFA and focus-forming results corroborate the viral replication kinetics among different versions of reporter viruses (see later replication kinetic results in Fig. 3.3). To assess stability, viruses were passaged ten times on Vero cells according to the scheme in Fig. 3.4A. RT-PCR products corresponding to each passage show consistent band size for all viruses out to P10, including West Nile virus (WNV) which results were obtained after the initial review of this manuscript (Fig. 3.3B). The exception to this positive outcome is ZIKV and YFV, which have the shortest capsid duplication, 25 amino acids (Fig. 3.1D). These two viruses showed a decrease in band size during passaging. These results suggested that the length of the capsid duplication may have an impact on virus stability.

Extended capsid duplication

The results from passaging these different flaviviruses indicated that a longer capsid duplication could positively impact its stability. This hypothesis was tested by creation of ZIKV and YFV C38 NanoLuc viruses. C38 was chosen based on the robust results from DENV1-4 using this length. During this time, Volkova, et al., published a report on reporter ZIKV and the effect of capsid duplication size on replication. Their conclusion was that C50 is the optimal length for viral growth, with this being the shortest length that was not statistically attenuated compared to WT virus [82]. Based on this report, we also constructed a C50 ZIKV. IFA results post-electroporation suggested that ZIKV C38 virus replicated more robustly than the C25 and C50 virus, while YFV C38 showed little difference compared to YFV C25 (Fig. 3.5A, compare to Fig. 3.1B). Focus size (Fig. 3.5B) comparison between ZIKV C25 and ZIKV C50 showed little difference but, ZIKV C38 formed clear, larger plaques similar to non-reporter wild-type ZIKV (Fig. 3.4B). YFV C38 focus size was only slightly larger than YFV C25. The C38 ZIKV and YFV and C50 ZIKV

were continuously passaged and analyzed for reporter gene stability by RT-PCR (Fig 3.5C). Unexpectedly, ZIKV C50 showed early instability, so only passaging results from P0-P2 are shown. In contrast, ZIKV and YFV C38 were stable after ten rounds of continuous cell culture. These results suggest that an optimal length of duplicated capsid sequence (e.g., C38) is required for reporter virus stability. Under such condition, the frameshift or other mutations in the duplicated capsid region is not required for the stability of reporter virus.

Effect of extended capsid duplication on viral growth

The effect of capsid duplication length on viral growth was assessed on Vero cells. Cells were infected with ZIKV C25, C38, and C50 at a MOI of 0.01 and assessed at 24, 48, 72, 96, and 120 h post infection by focus forming assay (Fig. 3.6A). ZIKV C38 replicated to significantly higher titers than ZIKV C25 and ZIKV C50, reaching 10^7 FFU/mL, at 24, 48, and 72 h post infection. ZIKV C25 and ZIKV C50 growth are similar across the same time period, though ZIKV C25 titers did continue to increase until 96 h. Conversely, growth comparison of YFV C25 and YFV C38 showed no significant difference at any time point, despite YFV C38's increased stability (Fig. 3.6B). DENV1-4 and JEV growth kinetics on Vero cells (MOI 0.01) show that DENV1 replicated significantly higher at times 24-96 h post infection (Fig. 3.6C). Together these data show that among C25, C38, and C50, C38 is the most optimal capsid duplication length for ZIKV replication. In contrast to these results, there seems to be no replication advantage for YFV C38 over YFV C25.

To directly examine the effect of reporter gene insertion on viral replication, we compared the replication kinetics between the parental wild-type ZIKV and the reporter ZIKV C38 on Vero cells (Fig. 3.7A). The results showed that replication between the two is similar at all time points but 72 h, where WT virus is 10-fold lower, possibly due to death of the host cells.

Rapid neutralization tests and antiviral discovery

One of the aims of this study was to develop stable reporter flaviviruses for neutralization tests and antiviral compound assays. As we have previously done, the stable reporter viruses were used to test a panel of flavivirus-immune mouse sera (Fig. 3.8A) in a four-hour neutralization test. NT₅₀ results are indicative of the previous infection with the homologous virus yielding the highest NT₅₀, though some cross-neutralization by heterologous viruses was observed (Fig. 3.8B). Using the flavivirus inhibitor NITD008 [119,120], each virus was used in an antiviral compound assay (Fig. 3.8C). Increasing concentrations of NITD008 decreased luciferase expression compared to control (Fig. 3.4D) resulting in potent EC₅₀ values, comparable to previously published data demonstrating sub-micromolar efficacy [119] (Fig. 3.8E). These results support our previous data showing that NanoLuc-tagged flaviviruses can be valuable tools in rapid sero-diagnostic assays and antiviral compound screens.

ZIKV C38 in mosquitoes

Reporter virus use in mosquito experiments is highly advantageous, where RNA extraction from individual mosquitoes is time-consuming. Intrathoracic injection of mosquitoes with ZIKV C25 showed no viral replication and no luciferase expression (data not shown), possibly due to reporter gene induced replication attenuation. Because ZIKV C38 had more robust luciferase expression compared to C25 in C6/36 cells (Fig 3.9A) we characterized ZIKV C38 replication in whole *Aedes aegypti* mosquitoes by both micro-injection, which surpasses the midgut barrier, and membrane blood feeding. Mosquitoes were micro-injected in the thorax with 50 FFU ZIKV C38 and at days 8, 12, and 18, whole mosquitoes were homogenized in PBS and assayed by both qPCR (Fig. 3.10A, left panel) and luciferase assay (right panel). Although viral RNA did not increase from day 8 to day 12, the luciferase assay shows a statistically significant peak at day 12. In a separate experiment, mosquitoes were allowed to feed on blood spiked with 2×10^6 FFU/mL ZIKV

C38. These mosquitoes were also homogenized on days 8, 12, and 18 and evaluated by both qPCR and luciferase assay (Fig. 3.10B, right and left panel, respectively). By blood feeding, ZIKV C38 titers increased at each time point by qPCR, though the increase was not statistically significant. Corroboratively, the luciferase activities significantly increased from day 8 to 18. Uninfected mosquitoes were also assayed (Fig. 3.10B, right panel) as a negative control. These data show that ZIKV C38 replicates in *Aedes aegypti* mosquitoes and luciferase output can be used to assay viral replication.

DISCUSSION

Flavivirus reporter constructs have been notoriously unstable since they were first reported [75,76]. Improvements in design [84] have increased the stability, but previous efforts have fallen short of the high standard of ten passages. Here we report a panel of NanoLuc-tagged flaviviruses with stability to at least ten passages in cell culture, which is double the passages routinely reported. It was found that C38 ZIKV and YFV reporter viruses were more stable than their C25 counterparts, and in the case of ZIKV, C38 had a distinct replication advantage. Previous hypotheses for constructing reporter flaviviruses assumes that shorter capsid duplication lengths would be more stable, due to a shorter stretch of homologous sequence. These results challenge that assumption, suggesting that C38 is optimal. The establishment of a stable reporter virus system will greatly facilitate the production of reporter virus in cell culture through viral infection and amplification rather than transfection of viral RNA transcribed from its infectious cDNA plasmid. The ease of stable reporter virus production enables potential high-throughput flavivirus neutralization testing and antiviral screening, as recently demonstrated for reporter SARS-CoV-2 [137,138].

Many different *cis*-acting elements present in the flavivirus capsid coding region have been mapped, including the 5'CS [34], the cHP [36], the 5' DAR [122], and the DCS-

PK [40] (see Fig 1.1B). These elements work together to regulate RNA translation, genome cyclization, and viral replication. C25 includes all of those elements except the full DCS-PK, a pseudoknot that has been modeled in various flavivirus genomes, including ZIKV [139], and experimentally been found to aid viral replication in DENV2 [140] and DENV4 [40]. Extending C25 to C38 includes the full DCS-PK (see Fig 1.1B), which may explain the increased replication capacity of ZIKV C38 compared to ZIKV C25. We hypothesize that the lack of the DCS-PK in ZIKV C25 caused increased selective pressure and helped drive recombination. Inclusion of DCS-PK in ZIKV C38 lessened this selective pressure, expanding its stability. In contrast, YFV C38 replicated very similarly to YFV C25, supporting a model that YFV lacks, or has a shortened, DCS-PK [40]. Despite this, the lengthened capsid duplication still had a positive effect on YFV stability. It remains to be determined what RNA element in the C38 coding sequence facilitates YFV replication.

Previous work with reporter ZIKV identified C50 as an optimal length for capsid duplication in relation to replication but its effect on stability was not independently tested [82]. In our hands, C38 performed remarkably better in both stability and viral replication when compared to C50. The discrepancy could be due to different ZIKV strains, different sequences flanking the reporter gene, and the absence of a frameshift mutation which was included to help block recombination. ZIKV C50 includes the DCS-PK, along with the other required replication elements and as such would be expected to replicate similar to ZIKV C38. The extra capsid amino acids C39-C50, which contain residues shown to be important in capsid dimerization [12], could allow the C50 capsid fragment to interfere with full-length capsid, thus explaining the attenuation of C50 compared to C38. This selective pressure, along with a larger region for possible recombination, could also be driving the poor stability seen during passaging.

We used sera from known virus-infected mice to demonstrate the utility of the reporter virus for neutralization testing. The reporter virus neutralization assay has been optimized in a 96-well format for high-throughput testing. For clinical use of the reporter neutralization testing, the assay must be first validated using patient sera with well-defined viral infections. The validation could be achieved by comparing the antibody neutralizing titers derived from the conventional plaque reduction neutralization test (PRNT) with those derived from the reporter virus assay. Efforts are ongoing to obtain the well-defined patient sera to perform the clinical validation of reporter virus neutralization assay.

CONCLUSION

Together, these results demonstrate that extending the portion of capsid duplicated to make ZIKV and YFV reporter viruses can increase their stability and in the case of ZIKV enhance its replication capabilities in mammalian cells and whole mosquitoes. These data help inform a new generation of stable flavivirus reporter constructs to be used for high-throughput drug screens, serological diagnosis, pathogenesis studies, and transgene delivery.

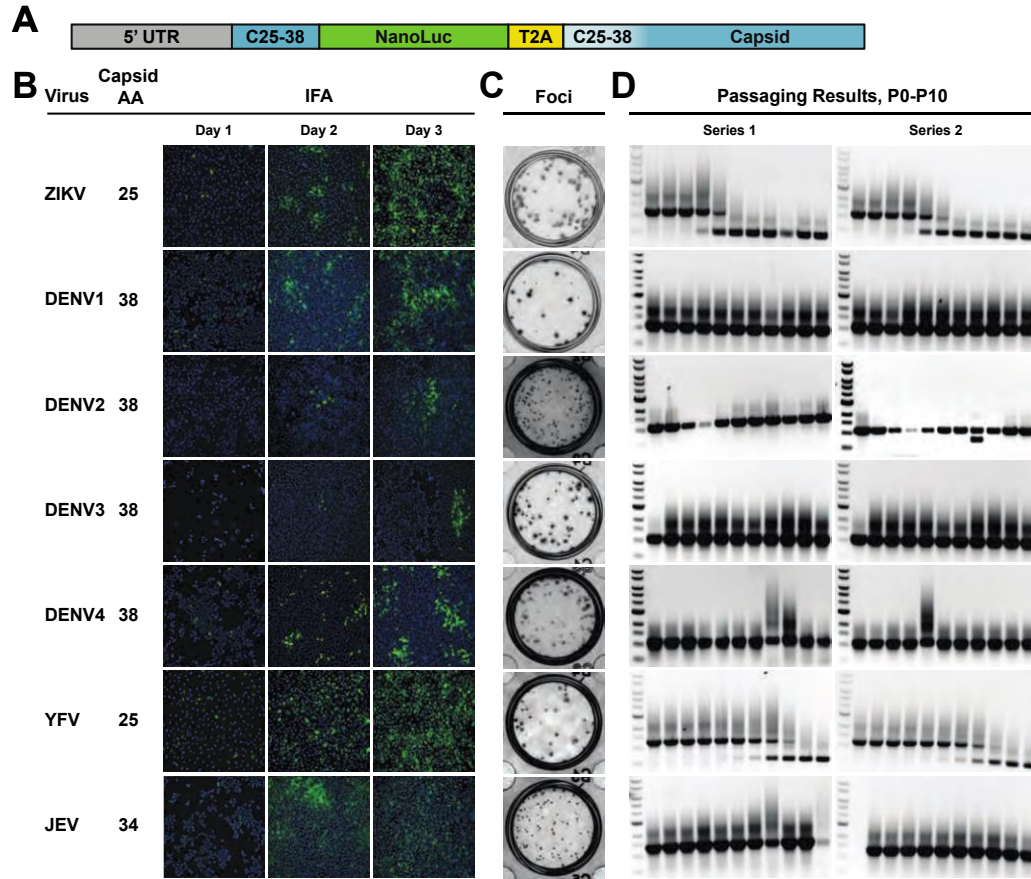


Figure 3.1 Panel of Reporter Flaviviruses.

A. Scheme of NanoLuc insertion in the flavivirus genome. The duplicated capsid portion varies from 25 to 38 amino acids, depending on the virus. The white beginning of the capsid gene indicates the codon scrambling to reduce homology with the duplicated portion. **B.** Virus, corresponding number of capsid amino acids duplicated, and representative IFA images from Day 1 to 3 post electroporation. The pan-flavivirus envelope antibody 4G2 was used to probe for virus and cells were counterstained with DAPI. **C.** Focus-forming assay after 4-day infection on Vero cells. **D.** Genetic stability results after two independent series of ten passages in Vero cells. Viral RNAs from each passage were used as templates in an RT-PCR reaction with primers that spanned the 5' UTR to the capsid. Full-length band sizes are as follows ZIKV: 1,162 bp; DENV1: 1,086 bp; DENV2: 1,128 bp; DENV3: 1,126 bp; DENV4: 1,131 bp; YFV: 1,282 bp; JEV: 1,360 bp.

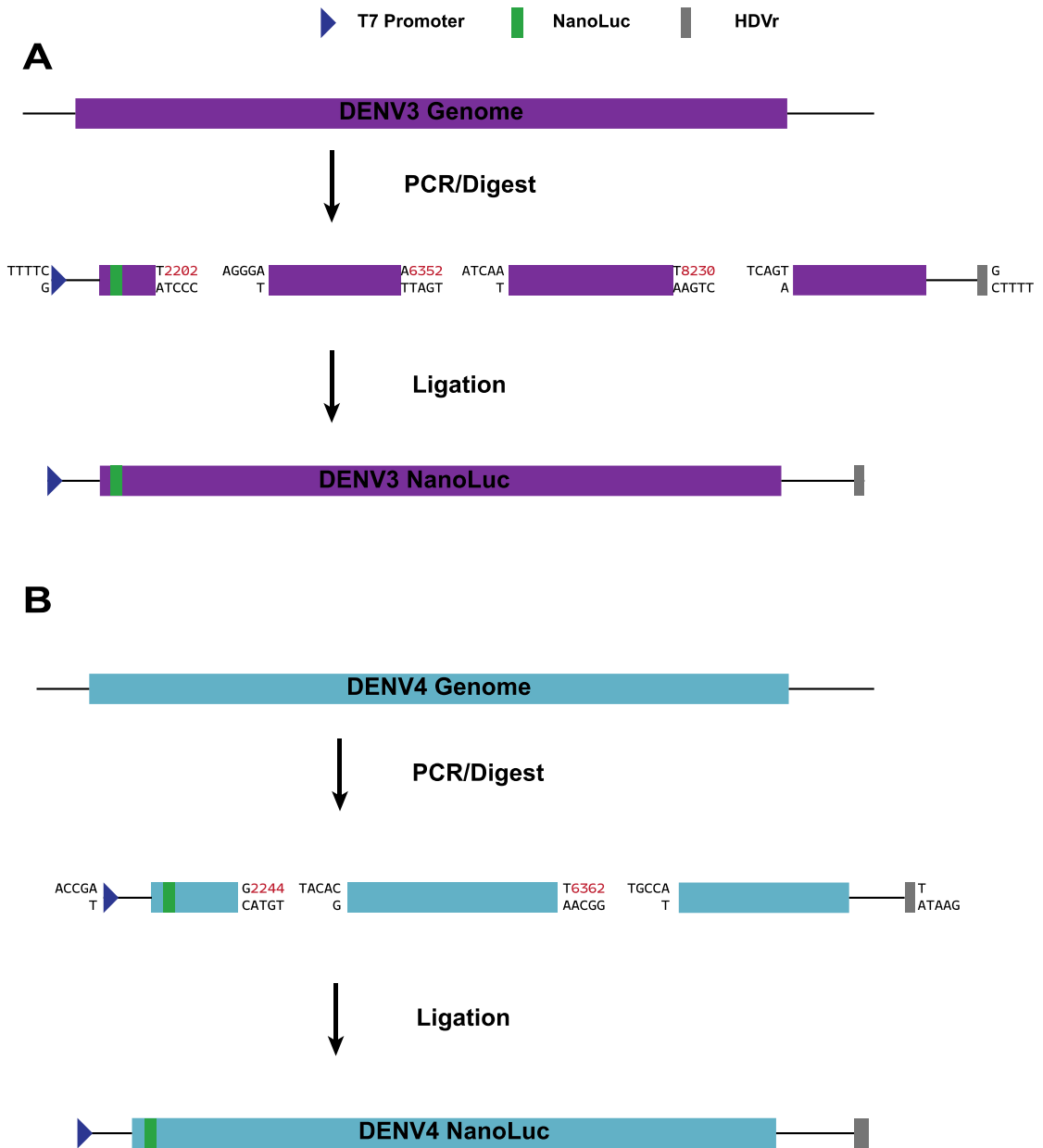


Figure 3.2 DENV3 and DENV4 In vitro ligation cloning scheme

In vitro ligation scheme for DENV3 (**A**) and DENV4 (**B**). The nucleotide positions of each fragment junction are indicated in red according to GenBank accession numbers EU482459 and FN429920, respectively.

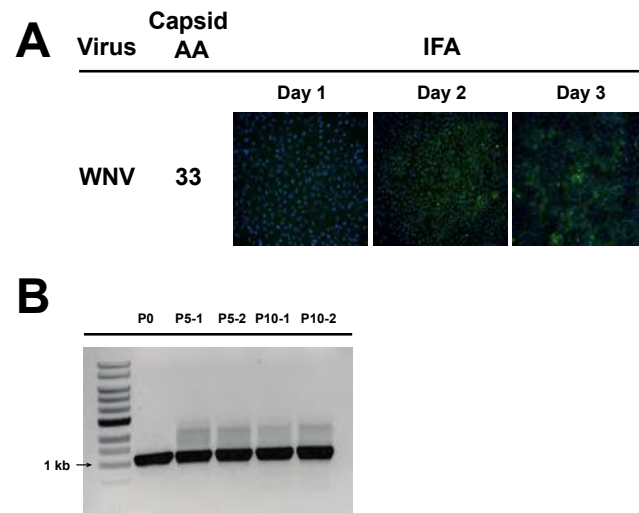


Figure 3.3 WNV IFA and Genetic Stability

A. Capsid duplication length of WNV along with IFA images stained with 4G2 and DAPI.

B. Stability results of passaged WNV-Nano, full length size 1,140 bp. Passaging done by colleague Antonio Muruato.

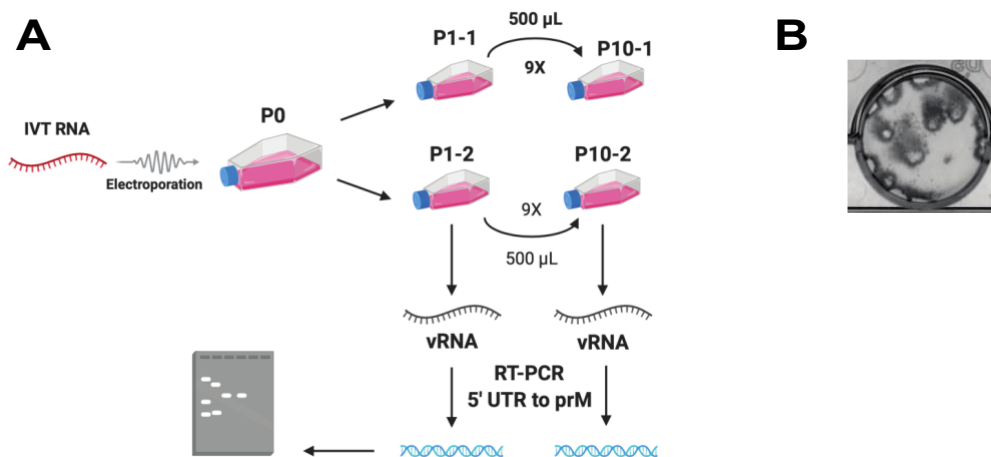


Figure 3.4 Passing Scheme

A. Scheme for passaging reporter viruses. P0 is used to denote viral stock recovered after electroporation. 500 μ L of P0 was used to inoculate a T75 flask of confluent Vero cells. Infection was allowed to proceed until cell death was observed. This was repeated until P10 virus was obtained. Viral RNA was obtained from each passage and used in an RT-PCR reaction that bridged the reporter gene. These products were run on an agarose gel to observe band size. **B.** Focus-forming assay using WT ZIKV on Vero cells after a 4-day infection.

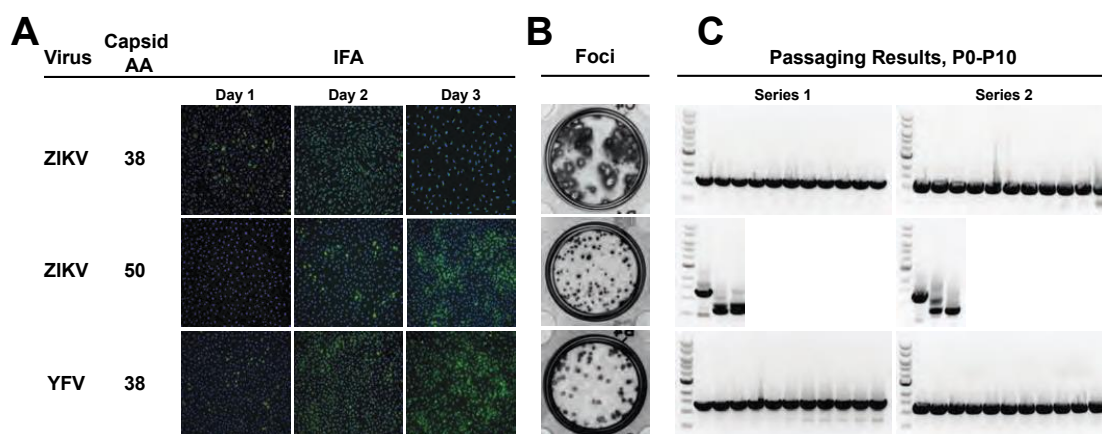


Figure 3.5 Extended Capsid Duplication.

A. Virus, corresponding number of duplicated capsid amino acids, and representative Day 1 to Day 3 IFA images. The anti-flavivirus envelope antibody 4G2 was used. **B.** Focus-forming assay on Vero cells after four-day infection. **C.** Reporter gene retention after ten passages on Vero cells. RT-PCR products covering the reporter gene are shown for the two independent passaging series. ZIKV C50 passaging was discontinued after P2 due to loss of reporter gene. Band sizes corresponding to the full-length reporter gene are as follows ZIKV C38: 1,201 bp; ZIKV C50: 1,237 bp; YFV C38: 1,321 bp.

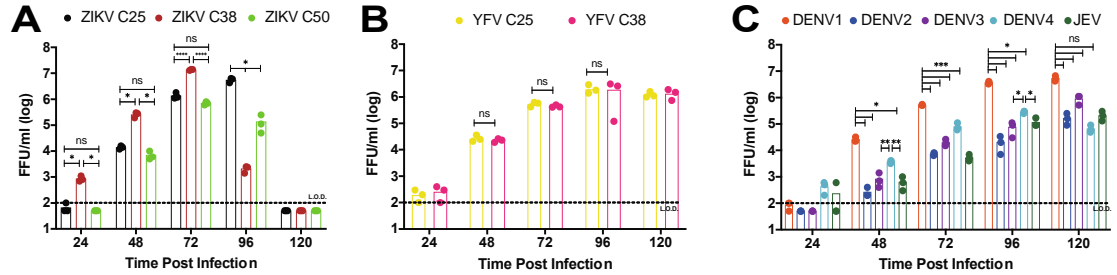


Figure 3.6 Effect of Capsid Duplication Length on Viral Growth.

Multi-step growth kinetics (MOI 0.01, n=3) on Vero cells, using focus-forming assay to quantify growth for **A.** ZIKV C25, C38, and C50; **B.** YFV C25 and C38; **C.** DENV1-4 and JEV. 2-way repeated measures ANOVA with Tukey's multiple comparisons test was used to assess significance for **A** and **C**. 2-way repeated measures ANOVA with Sidak's multiple comparisons test was used for **B** ($p > 0.5 = \text{ns}$, $p < 0.5 = *$, $p < 0.1 = **$, $p < 0.01 = ***$, $p < 0.001 = ****$).

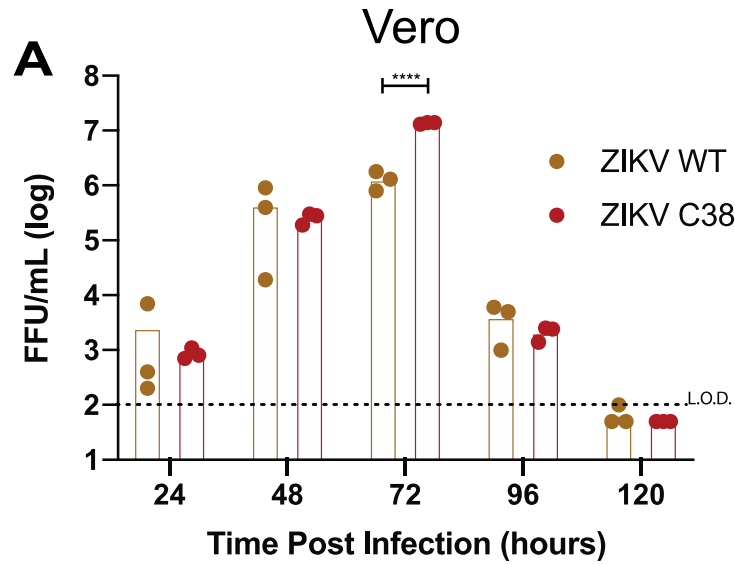


Figure 3.7 ZIKV and ZIKV WT Growth Comparison

A. Growth kinetics comparison of ZIKV C38 and WT ZIKV on Vero cells (MOI 0.01, n=3). Significant differences were assessed with 2-way repeated measures ANOVA with Sidak's multiple comparisons test ($p > 0.5 = \text{ns}$, $p < 0.5 = *$, $p < 0.1 = **$, $p < 0.01 = ***$, $p < 0.001 = ****$). Data for ZIKV C38 is the same as shown in Fig 3A.

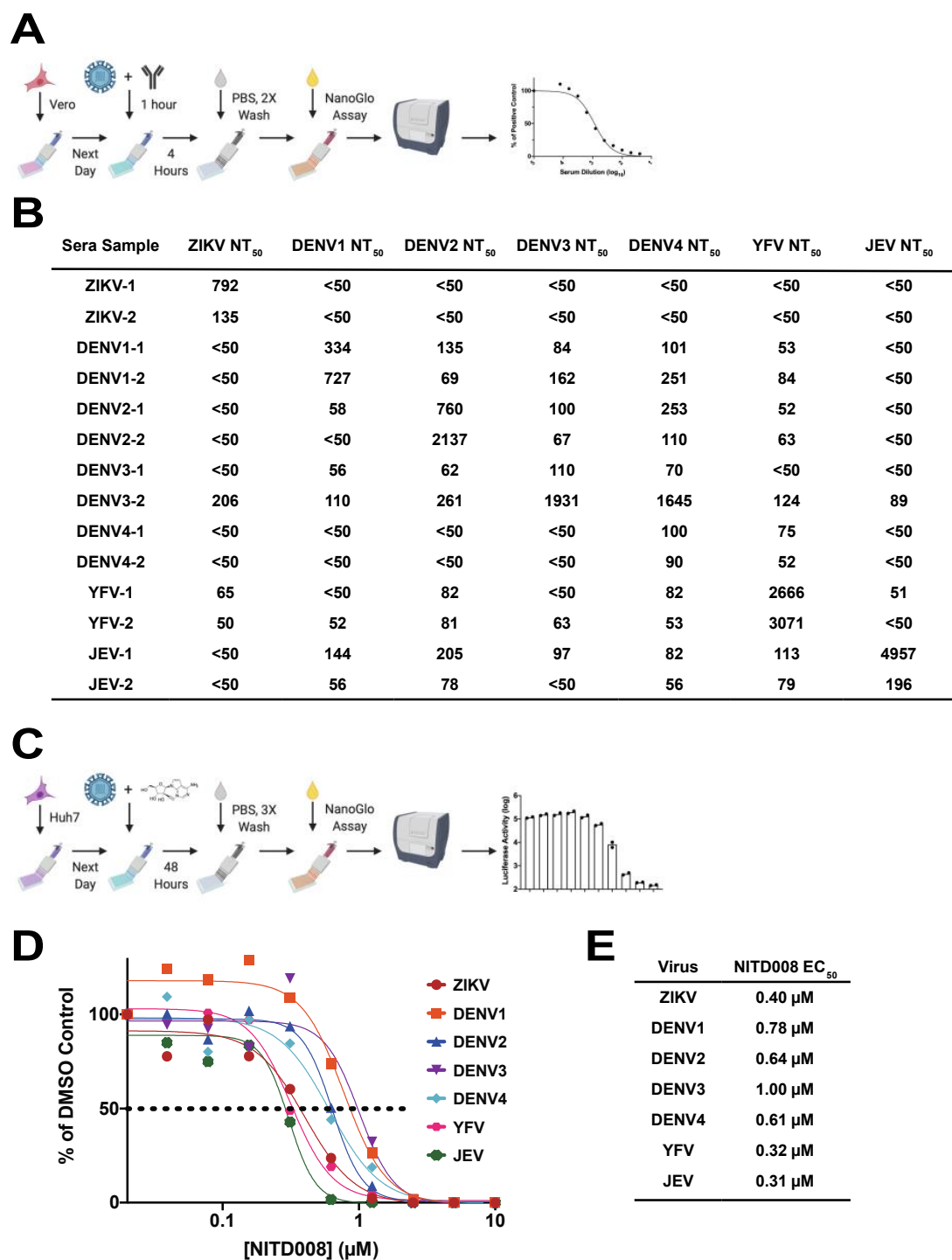


Figure 3.8 Neutralization and Antiviral Assays.

A. Reporter virus neutralization scheme. Vero cells were seeded in an opaque, white 96 well plate at 1.5×10^4 cells per well the day before. Sera samples were two-fold serially

diluted, starting at 1:50 and then mixed with equal volume of virus and incubated for 1 h at 37°C. The sera:virus mixture was then used to inoculate Vero cells in a 96 well plate. After 4 h incubation at 37°C, plates were washed twice with PBS and then NanoGlo substrate was added and luciferase levels read by plate reader. **B.** NT₅₀ values of a panel of mouse sera tested with the stable reporter viruses. For ZIKV and YFV NT₅₀ tests, the C38 virus was used in both instances. **C.** Antiviral assay scheme. Huh7 cells (1.5x10⁴ cells per well) were seeded the previous day. NITD008 was two-fold serially diluted starting at 10 µM. The dilutions were mixed with virus and plated on the Huh7 cells in a white, opaque 96 well plate and incubated at 37°C for 48 h. Following a 3X PBS wash, results were read by plate reader after addition of NanoGlo substrate. **D-E.** EC₅₀ results from testing NITD008 against the panel of stable reporter viruses in both graphical and table formats, respectively.

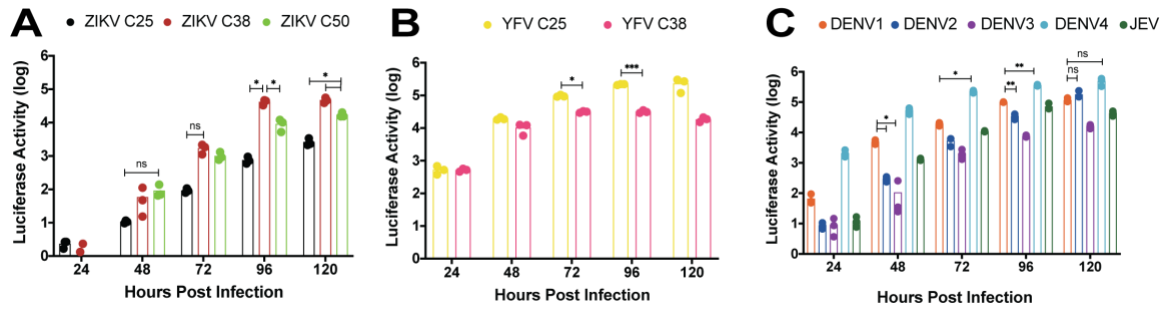


Figure 3.9 Kinetics of luciferase expression on C6/36 cells.

C6/36 cells were infected at MOI 0.1, $n=3$ and assayed for luciferase activity at 24, 48, 72, 96, and 120 hours for ZIKV (A), YFV (B), and DENV or JEV (C). 2-way repeated measures ANOVA with Tukey's post-hoc test was used to assess significance (*= $p<0.05$, **= $p<0.01$, ***= $p<0.001$, ****= $p<0.0001$).

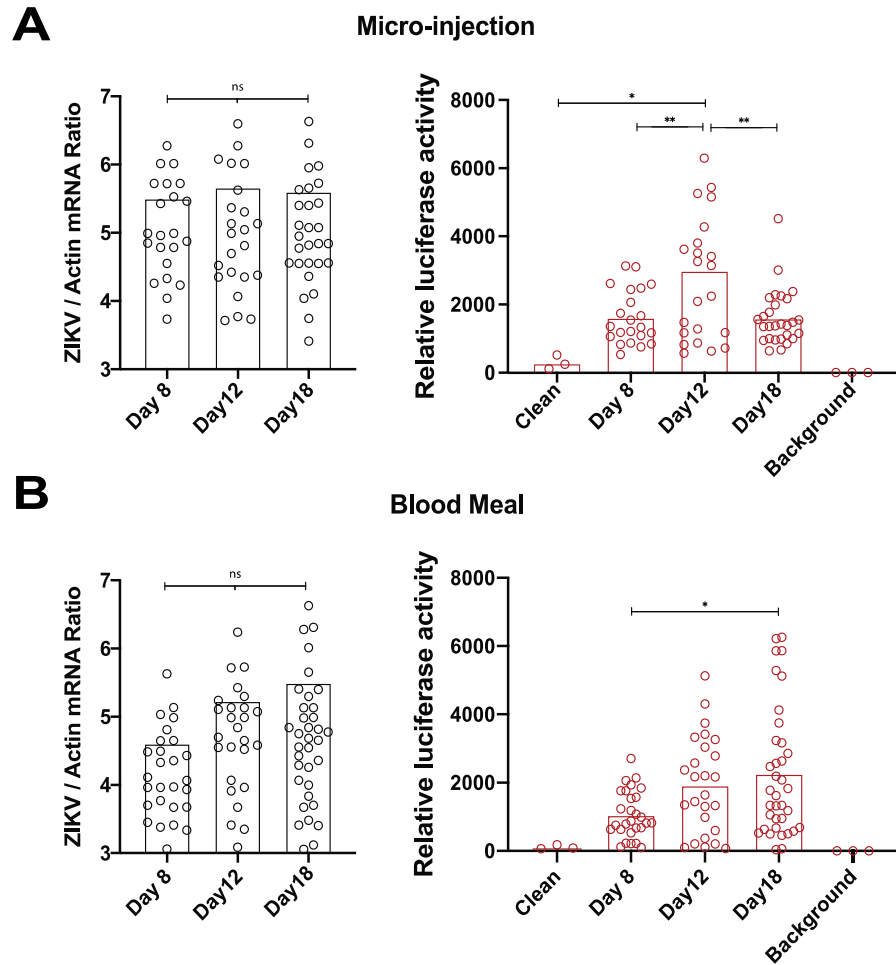


Figure 3.10 ZIKV C38 Nano in Mosquitoes.

A. *Aedes aegypti* mosquitoes were micro-injected with 50 FFU ZIKV C38 Nano (n=30 per day). On days 8, 12, and 18, whole mosquitoes were collected and individually homogenized in PBS. Samples were analyzed by both qPCR (left panel) or luciferase assay (right panel). **B.** *Aedes aegypti* mosquitoes (n=50 per group) were inoculated by membrane blood-feeding on sheep's blood spiked with 2×10^6 FFU/mL ZIKV C38 Nano. Mosquitoes were then analyzed as in panel A. For the luciferase assay, clean (uninfected) mosquitoes were used as a control. Values for luciferase activity are reported relative to background (no mosquito) levels. ANOVA with Tukey's post-hoc test was used to assess significant differences in all panels ($p > 0.5 = \text{ns}$, $p < 0.5 = *$, $p < 0.1 = **$, $p < 0.01 = ***$, $p < 0.001 = ****$). Data generated by colleague Yang Liu.

DISCUSSION

Chapter 4: Development of Stable Transgene-bearing Flaviviruses

INTRODUCTION

As detailed in the introduction, progress had already been made in increasing the stability of flavivirus reporter constructs [79,84,87,91] over what was initially published [75,100]. This work builds further on that, describing two different methods, recombination-dependent lethal mutations and extended capsid duplication, that can further increase the stability of reporter flaviviruses, focusing initially on ZIKV as a model, but also expanding to a panel of the most medically relevant viruses including all four DENV serotypes, JEV, YFV, and WNV [101,141].

RECOMBINATION-DEPENDENT LETHAL MUTATIONS IN OTHER FLAVIVIRUSES

After showing that recombination-dependent lethal mutations successfully stabilize reporter ZIKV and YFV, we sought to apply this method to DENV1-4 and JEV to have a panel of stable viruses. Thus each virus was cloned first without any mutations and then also initially with four or five capsid mutations in similar locations as was done with ZIKV and YFV. To our surprise, these viruses were substantially less tolerant of these mutations than ZIKV and YFV. This was most explored with JEV, in which WT reporter virus grew to greater than 10^8 FFU/mL while virus with 5 mutations was unrecoverable, 4 mutations grew to 10^4 FFU/mL, 3 mutations grew to 10^5 FFU/mL, and 2 mutations grew to 10^7 FFU/mL. This observation is exemplified in comparison of IFA data from the different JEV reporter viruses (Fig 4.1)

It is expected that a greater number of mutations would exacerbate attenuation, but this was a more marked case than was seen with ZIKV or YFV. It is still unknown exactly

how these mutations attenuated the virus, though it is expected that these mutations are disrupting RNA elements and structures that enable efficient genome replication. It highlights the differences between flaviviruses in this region and hints that what is applicable in one virus does not always translate to its close relative. It seems that JEV is more sensitive to changes in the RNA sequence and structure around the *cis*-acting RNA elements than ZIKV or YFV. Whether that difference in sensitivity is from differences in RNA structure or NS5 recognition, or a combination of both, remains to be seen.

COMBINATION OF METHODS

Multiple methods have recently been published to enhance stability of reporter flaviviruses, two of which are described here. The question arises if they are compatible to be used in conjunction with each other to further stabilize the reporter virus. When Volkova, et al. described the frame-shift mutation to stabilize reporter ZIKV [82], they first tested capsid duplication lengths, surmising that C50 is the optimal length, and then added the frame shift mutation. Neither were tested independently of each other for stability. Our own results suggest that C50 is not stable by itself, though C38 is. With the idea that a frameshift mutation was less attenuating than capsid mutations, we have made trans-gene bearing ZIKVs that combine both C38 and the frameshift mutation in an effort to further increase stability. Though still early, preliminary results suggest that the effect of these are not additive, as addition of a frameshift mutation had little, if any effect, on transgene stability. The frameshift mutation is not detrimental to the virus if the recombination happens at a point that is beyond the return of the normal reading frame (thus downstream viral proteins are in-frame). Alternatively, recombination can occur in such a way that will restore the original reading frame (i.e. in the middle of a codon instead of between them). It may also be that the frameshift mutation is more beneficial for stability in the context of the extra 12 amino acids found in C50 than in C38.

Recombination-dependent lethal mutations are also susceptible to some of these faults, as they do not stop recombination from occurring within a long transgene, only from C25 to the full capsid. Indeed, longer reporter genes, such as mScarlet (696 bp) [142] or iRFP670 (933 bp) [143], are not as stable as NanoLuc (513 bp) in this system (Fig 4.2). Despite this, recombination-dependent lethal mutations may be a more robust method for stabilization of reporter flaviviruses. In virus with C38 and a frameshift mutation (C38a), recombination events from the end of C38a into the beginning of the capsid gene were observed (see Fig 4.3). In this scenario, C38 is out of frame but the greater balance of the capsid protein is in-frame and this virus is viable, in part we believe, due to the presence of positively charged amino acids still present in the frameshifted C38. If, instead, this C38 virus was further stabilized by recombination-dependent lethal mutations, the charge change brought by capsid mutations would render this particular recombined virus deficient in viral particle formation. Thus, an immediate future direction is the creation and characterization of recombination-dependent lethal mutation-bearing C38 ZIKV and YFV for testing of this hypothesis. It is believed that these methods would be synergistic and further stabilize the transgene.

FURTHER OPTIMIZATION

Further optimization, beyond combination of methods, of the stable reporter viruses reported here is possible, as has been shown with reporter JEV and the optimization it underwent [98,99]. Though many different factors could be contributing to the attenuation that occurs when engineering foreign genes into the flavivirus genome, including differing codon usage, added genome length and possible packaging constraints, and changes in polyprotein structure, the proximity of 5' gene insertions to cyclization signals lends itself to the possibility that perturbation of these elements is the greatest source of attenuation. The conclusion that C38 is more stable and robust than C25 because it contains a more complete set of these signals also supports this hypothesis [141].

Understanding of the regions important for cyclization and replication has expanded immensely over the past two decades [42,117,118]. The original methods utilizing *in silico* modeling, biochemical probing, and reverse genetic approaches have also been supplemented with newer methods such as next generation sequencing techniques [139] and RNA crystallography. These methods have been instructive for determining WT conformations, but how transgenes interact with these signals on an RNA level is still unknown. Probing of the RNA structure of reporter flaviviruses could identify sequence and structural motifs that inhibit normal interactions and allow improvement of the reporter gene sequence, resulting in a virus superior in replication and stability.

FUTURE DIRECTIONS

Beyond combining ours and other's methods to test if they can work in tandem and determining the RNA structure of the reporter insertion, there remain a number of other future directions and further applications of the platforms discussed above.

Flavivirus Diagnostics

Infections with different flaviviruses are often difficult to distinguish from one another, as they are often endemic in overlapping areas and are accompanied in many cases with non-specific symptoms, such as fever, rash, malaise, and arthralgia [144]. The surest way to diagnose infection is by RT-PCR, but the window of viremia is often fleeting, and so serological tests are used [123]. Despite having a much longer timeframe for effective diagnosis, differentiating different flavivirus infections by is serological also complicated due to the high cross-reactivity of immune sera. To date, the most specific tests for serodiagnosis remains the plaque-reduction neutralization test (PRNT) [103,145] though the test requires skilled technicians, biocontainment, and long incubation times [123].

Recent work in our lab, including that described here, has employed reporter viruses to dramatically limit the incubation down to 24 or even 4 hours [101,103,141].

While the incubation time has been decreased, the 4-hour rapid neutralization tests have not yet been compared head-to-head with traditional PRNTs. This comparison is needed to ensure the rapid test performs similarly to the traditional assay and this remains an outstanding research aim. We are optimistic that this comparison will show the rapid neutralization tests are a good substitute based off of positive results from the small amount of human patient ZIKV-immune serum samples tested [101] as well as previous head-to-head comparisons made using a similar assay [146]. A large panel of human immune sera against our panel of reporter flaviviruses, tested both against analogous and heterologous sera, will enable these viruses to be validated for clinical diagnosis.

Glioblastoma

Glioblastoma, a particularly recalcitrant type of brain tumor, effects over 12,000 people in the United States every year and has a bleak survival rate of 5% at five years [147]. Current therapies are limited, namely resection followed by radiotherapy and the chemotherapy drug temozolomide, which altogether increase the two-year survival rate from 10% to 27% [148]. The most recent advance was the addition of tumor-treating fields (TTF) to therapeutic options. These electrical fields target dividing cells and were shown to increase progression-free survival by 2.7 months in conjunction with temozolomide compared to temozolomide alone [149]. Despite these advances, prognosis is still bleak and new therapeutics, like immunotherapies, oncolytic viruses, and targeted therapies, are slow to come [147].

One of the prevailing hypotheses explaining, among other hurdles, the difficulty in treating glioblastoma is that of the cancer stem cell theory. In this theory, a subset of stem

cell-like cancer cells retains the ability to differentiate into the different malignant cell populations. These cells can initiate new tumors, are responsible for metastasis, and are also resistant to chemotherapy [150]. Stem-like cells have been identified in glioblastoma [151,152], and have been experimentally shown, in at least some cases, to arise from neural stem cells (NSCs) which accumulate low level mutations [153]. Additionally, these glioblastoma stem-like cells (GSCs) have been directly implicated in chemotherapy resistance and tumor recurrence [154]. Taken together, the evidence is accumulating for targeting GSCs as a novel and effective cancer therapy.

The neurotropic ZIKV has been shown to preferentially infect NSCs and neural progenitor cells (NPC) over neurons or glial cells [155,156]. Immune activation causes shrinkage of this cell population and cell death [157,158]. Other work shows infection inhibits neurogenesis and induces autophagy [29]. Given ZIKV's ability to preferentially infect NSCs over other neural cell types, it was tested in several models of glioblastoma both as WT virus [159] and attenuated vaccine strain [160] in an effort to see if it would target the difficult to treat GSCs. These studies showed that ZIKV targets the stem-like cell populations in glioblastoma just as it does in benign tissue, and that intracranial inoculation in tumor bearing mice significantly improved survival. Experiments with other CNS tumors showed similar stem-cell like targeting and increased survival in the treatment group [161]. These show that treatment of glioblastoma using ZIKV may be a viable new therapeutic.

Given ZIKV's status as a potential new cancer therapy, we hypothesized that its oncolytic activity could be enhanced by stable engineering of a transgene. This increased cell killing could be achieved by applying a number of different approaches, including gene therapy, immune activation, and checkpoint blockade [162,163]. In typical gene therapy treatments, foreign genetic material is introduced into cancer cells by either adenovirus or

retrovirus vector. These genes include known drug targets, such as herpes virus thymidine kinase or bacterial/fungal cytosine deaminase. These enzymes, once introduced to the cell, can then convert prodrug, given locally or systemically, into a cytotoxic active drug, killing the host cell [163]. Immune activation works by stimulating the body's natural, anti-cancer immune response to help control aberrant proliferation. The CNS is typically thought of as an immune-privileged site, though this dogma is changing [164], and cytokines such as IL-2, interferon, or GM-CSF, may help stimulate the desired anti-cancer response. Lastly, immune checkpoint blockade uses antibodies to target the tumor-initiated downregulation of the immune system by PD-1/PD-L1 (programmed cell death protein 1/programmed cell death protein 1 ligand) and CTLA4 (cytotoxic T-lymphocyte-associated protein 4) [162,165].

ZIKVs bearing transgenes covering these different methods of increasing its effectiveness as an anti-glioblastoma therapy are currently being designed and tested. This represents a novel and exciting application of the stable reporter virus technology and demonstrates its ability to be translated to other areas of medicine.

Bioluminescent Imaging

Luciferase expression can be monitored in real-time through the skin of live animals using highly sensitive charge-coupled device cameras in bioluminescent imaging (BLI). Used in gene expression studies [166–168] and frequently in oncology to monitor tumors [159,160], this technology was first applied to an infection model using bacteria transformed with bacterial luciferase [169] and then later in viral infections with herpes simplex virus, Sindbis virus, and vaccinia virus [170–172]. In all of the above examples, light output correlated with pathogen levels and was localized to specific body areas or tissues. The power of this type of model comes in the continual monitoring of infection in the same animals, instead of the serial sacrifice of infected animals that is required for

monitoring any tissue besides blood. The effect of antibiotic, antiviral, or interferon treatments can also be monitored by this method.

BLI has been used to study both DENV2 [90] and JEV [93]. In DENV2 infection of AG129 mice by intravenous route, luciferase expression was detected at the site of infection and spread to associated lymph nodes and other areas of the gut. To further tease apart locations of DENV infection in this model, organs were also imaged *ex vivo*, with the surprising finding that gut-associated lymphoid tissue was infected as well as the spleen. Luciferase levels dropped or were completely eliminated with treatment of antibodies or antivirals. In JEV infection, BLI was used to image infection in the brain, as well as visceral organs. Treatment with ribavirin and NITD008 were evaluated with this model as well as immunization with the vaccine virus JEV 14-14-2. Similar work has also been recently published using ZIKV [173]. The work with ZIKV shows similar dissemination and results after treatment with immune sera as JEV but adds a new dimension by imaging pregnant mice and the fetuses, enabling *in vivo* imaging of congenital infection.

Work with the alphavirus Chikungunya virus shows that infected mosquitoes can also be imaged using BLI [174]. This potential opens up many future directions for flaviviruses, most notably being the ability to image the complete infection cycle between mammalian and insect hosts. These studies would start with the infection in mosquitoes, which would be allowed to feed on and infect mice. Once the mice were viremic, fresh mosquitoes would take a blood meal and the infection could be monitored at each stage. This kind of long-term experiment could be highly useful in getting a full view of the effect of mutations or medical interventions on the transmission cycle of flaviviruses; however, this type of setup would also require a reporter virus with ensured stability. This remains an outstanding goal of this project, one we have moved a step closer to showing that ZIKV C38 NanoLuc replicates, and produces luciferase, in mosquitoes [141].

Vaccine Platform

As has already been discussed, the 17D vaccine strain of YFV has been used as a platform to vaccinate against other diseases, most successfully DENV and JEV. This has been accomplished using prME chimeric technology first developed for DENV [57,175]. YFV17D has also served as an experimental vaccine against diverse conditions with the insertion of short T and B cell epitopes, as well as longer gene insertions at junctions in the polyprotein [176]. A recently released preprint shows the full S protein of SARS CoV2 engineered in the E/NS1 junction and indicates that this method can be used to successfully vaccinate mice and hamsters against emerging pathogenic threats [177]. Though a promising strategy, details on how the S protein was engineered and how stable it is were not available.

The platform described here for stable reporter viruses could be easily adapted to express foreign antigens in the backbone of vaccine strain flaviviruses like YF17D or JE 14-14-2. Possible protective antigens against important or emerging viruses include SARS CoV2 S receptor binding domain [178,179], influenza stem fragments for universal flu vaccination [180,181], GP38 from Crimean-Congo hemorrhagic fever virus [182], or the head of Ebola virus glycoprotein [183]. Coupled with plasmid -launched DNA vaccination technology [116,184], this platform could be used to rapidly develop, distribute, and vaccinate against rapidly emerging diseases.

CONCLUSION

This work describes two methods that can be used to stabilize NanoLuc tagged reporter flaviviruses, overcoming a long-standing hurdle in the use of these virological tools. Recombination-dependent lethal mutations block virion formation if recombination occurs and optimized capsid duplications relax replication constraints by providing complete RNA replication signals. These stable viruses can be used in antiviral drug testing

and rapid, 4-hour neutralization tests, as well as assaying pathogenesis in mosquitoes. They have many potential future applications including flavivirus serodiagnosis, glioblastoma treatment, live animal imaging and transmission studies, as well as rapid vaccine development.

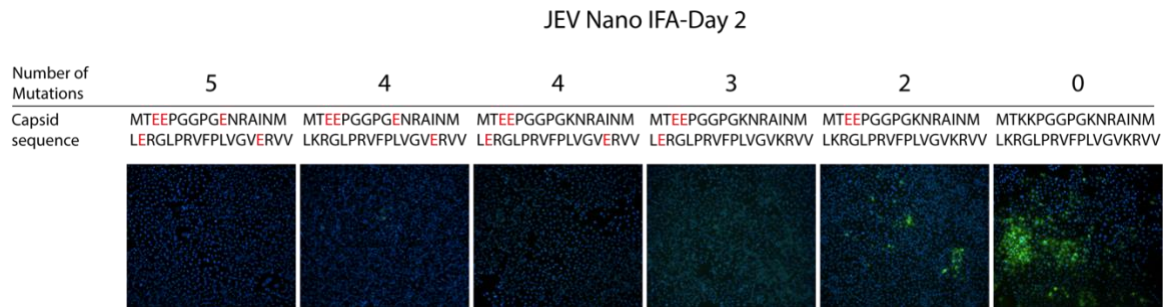


Figure 4.1 Increasing number of capsid mutations in JEV Nano.

IFA pictures from JEV Nano two days post electroporation. The number of mutations in the capsid duplication are presented above each picture, as well as the sequence, with the charge reversing mutations in red.

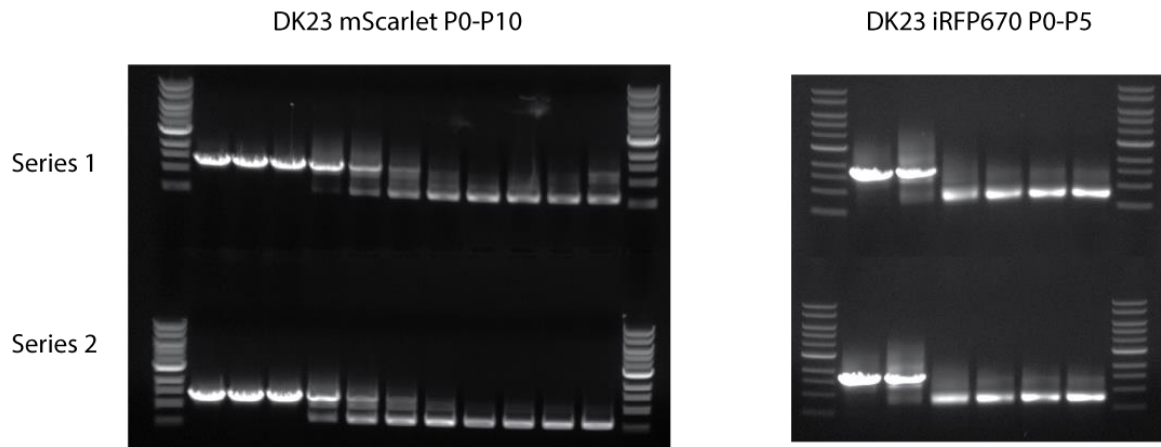


Figure 4.2 Stability of DK23 mScarlet and DK23 iRFP670

Reporter ZIKVs with the mScarlet and iRFP670 genes were passaged on Vero cells in two independent series 10 (mScarlet) or 5 (iRFP670) times. Stability was assayed by RT-PCR on viral RNA from each passage covering the reporter gene region. A shift in band size indicates instability.

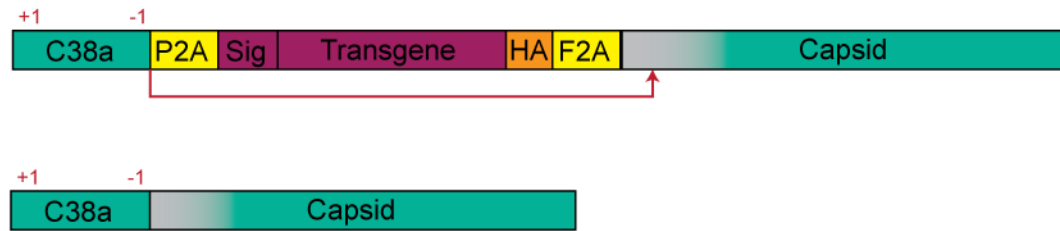


Figure 4.3 C38a Recombination.

Scheme indicates observed recombination events during passaging of C38 viruses with a frameshift mutation (indicated by red +1 and -1).

References

1. Pierson, T.C.; Diamond, M.S. The continued threat of emerging flaviviruses. *Nat Microbiol* **2020**, 1–17, doi:10.1038/s41564-020-0714-0.
2. Wit, E. de; Doremalen, N. van; Falzarano, D.; Munster, V.J. SARS and MERS: recent insights into emerging coronaviruses. *Nat Rev Microbiol* **2016**, 14, 523–34, doi:10.1038/nrmicro.2016.81.
3. Dawood, F.S.; Iuliano, A.D.; Reed, C.; Meltzer, M.I.; Shay, D.K.; Cheng, P.-Y.; Bandaranayake, D.; Breiman, R.F.; Brooks, W.A.; Buchy, P.; et al. Estimated global mortality associated with the first 12 months of 2009 pandemic influenza A H1N1 virus circulation: a modelling study. *Lancet Infect Dis* **2012**, 12, 687–95, doi:10.1016/s1473-3099(12)70121-4.
4. Malvy, D.; McElroy, A.K.; Clerck, H. de; Günther, S.; Griensven, J. van Ebola virus disease. *Lancet Lond Engl* **2019**, 393, 936–948, doi:10.1016/s0140-6736(18)33132-5.
5. Baud, D.; Gubler, D.J.; Schaub, B.; Lanteri, M.C.; Musso, D. An update on Zika virus infection. *Lancet* **2017**, 390, 2099–2109, doi:10.1016/s0140-6736(17)31450-2.
6. Dong, E.; Du, H.; Gardner, L. An interactive web-based dashboard to track COVID-19 in real time. *Lancet Infect Dis* **2020**, 20, 533–534, doi:10.1016/s1473-3099(20)30120-1.
7. Bhatt, S.; Gething, P.W.; Brady, O.J.; Messina, J.P.; Farlow, A.W.; Moyes, C.L.; Drake, J.M.; Brownstein, J.S.; Hoen, A.G.; Sankoh, O.; et al. The global distribution and burden of dengue. *Nature* **2013**, 496, 504, doi:10.1038/nature12060.
8. Ishikawa, T.; Yamanaka, A.; Konishi, E. A review of successful flavivirus vaccines and the problems with those flaviviruses for which vaccines are not yet available. *Vaccine* **2014**, 32, 1326–1337, doi:10.1016/j.vaccine.2014.01.040.
9. Mukhopadhyay, S.; Kuhn, R.J.; Rossmann, M.G. A structural perspective of the flavivirus life cycle. *Nat Rev Microbiol* **2005**, 3, 13–22, doi:10.1038/nrmicro1067.
10. Xia, H.; Xie, X.; Zou, J.; Noble, C.G.; Russell, W.K.; Holthauzen, L.M.F.; Choi, K.H.; White, M.A.; Shi, P.-Y. A cocrystal structure of dengue capsid protein in complex of inhibitor. *Proc National Acad Sci* **2020**, 117, 17992–18001, doi:10.1073/pnas.2003056117.
11. Dokland, T.; Walsh, M.; Mackenzie, J.M.; Khromykh, A.A.; Ee, K.-H.; Wang, S. West Nile Virus Core Protein Tetramer Structure and Ribbon Formation. *Structure* **2004**, 12, 1157–1163, doi:10.1016/j.str.2004.04.024.
12. Shang, Z.; Song, H.; Shi, Y.; Qi, J.; Gao, G.F. Crystal Structure of the Capsid Protein from Zika Virus. *J Mol Biol* **2018**, 430, 948–962, doi:10.1016/j.jmb.2018.02.006.

13. Ma, L.; Jones, C.T.; Groesch, T.D.; Kuhn, R.J.; Post, C.B. Solution structure of dengue virus capsid protein reveals another fold. *P Natl Acad Sci Usa* **2004**, *101*, 3414–3419, doi:10.1073/pnas.0305892101.
14. Tan, T.Y.; Fibriansah, G.; Kostyuchenko, V.A.; Ng, T.-S.; Lim, X.-X.; Zhang, S.; Lim, X.-N.; Wang, J.; Shi, J.; Morais, M.C.; et al. Capsid protein structure in Zika virus reveals the flavivirus assembly process. *Nat Commun* **2020**, *11*, 895, doi:10.1038/s41467-020-14647-9.
15. Hasan, S.S.; Sevvana, M.; Kuhn, R.J.; Rossmann, M.G. Structural biology of Zika virus and other flaviviruses. *Nat Struct Mol Biol* **2018**, *25*, 13–20, doi:10.1038/s41594-017-0010-8.
16. Wang, S.; Zhang, Q.; Tiwari, S.K.; Lichinchi, G.; Yau, E.H.; Hui, H.; Li, W.; Furnari, F.; Rana, T.M. Integrin $\alpha\beta 5$ Internalizes Zika Virus during Neural Stem Cells Infection and Provides a Promising Target for Antiviral Therapy. *Cell Reports* **2020**, *30*, 969-983.e4, doi:10.1016/j.celrep.2019.11.020.
17. Zhu, Z.; Mesci, P.; Bernatchez, J.A.; Gimple, R.C.; Wang, X.; Schafer, S.T.; Wettersten, H.I.; Beck, S.; Clark, A.E.; Wu, Q.; et al. Zika Virus Targets Glioblastoma Stem Cells through a SOX2-Integrin $\alpha\beta 5$ Axis. *Cell Stem Cell* **2020**, *26*, 187-204.e10, doi:10.1016/j.stem.2019.11.016.
18. Laureti, M.; Narayanan, D.; Rodriguez-Andres, J.; Fazakerley, J.K.; Kedzierski, L. Flavivirus Receptors: Diversity, Identity, and Cell Entry. *Front Immunol* **2018**, *9*, 2180, doi:10.3389/fimmu.2018.02180.
19. Campos, J.L.S.; Mongkolsapaya, J.; Screaton, G.R. The immune response against flaviviruses. *Nat Immunol* **2018**, *19*, 1189–1198, doi:10.1038/s41590-018-0210-3.
20. Rastogi, M.; Sharma, N.; Singh, S.K. Flavivirus NS1: a multifaceted enigmatic viral protein. *Virol J* **2016**, *13*, 131, doi:10.1186/s12985-016-0590-7.
21. Puerta-Guardo, H.; Glasner, D.R.; Espinosa, D.A.; Biering, S.B.; Patana, M.; Ratnasiri, K.; Wang, C.; Beatty, P.R.; Harris, E. Flavivirus NS1 Triggers Tissue-Specific Vascular Endothelial Dysfunction Reflecting Disease Tropism. *Cell Reports* **2019**, *26*, 1598-1613.e8, doi:10.1016/j.celrep.2019.01.036.
22. Muller, D.A.; Young, P.R. The flavivirus NS1 protein: Molecular and structural biology, immunology, role in pathogenesis and application as a diagnostic biomarker. *Antivir Res* **2013**, *98*, 192–208, doi:10.1016/j.antiviral.2013.03.008.
23. Zhang, X.; Xie, X.; Xia, H.; Zou, J.; Huang, L.; Popov, V.L.; Chen, X.; Shi, P.-Y. Zika Virus NS2A-Mediated Virion Assembly. *Mbio* **2019**, *10*, e02375-19, doi:10.1128/mbio.02375-19.
24. Xie, X.; Zou, J.; Zhang, X.; Zhou, Y.; Routh, A.L.; Kang, C.; Popov, V.L.; Chen, X.; Wang, Q.-Y.; Dong, H.; et al. Dengue NS2A Protein Orchestrates Virus Assembly. *Cell Host & Microbe* **2019**, doi:10.1016/j.chom.2019.09.015.
25. Li, K.; Phoo, W.W.; Luo, D. Functional interplay among the flavivirus NS3 protease, helicase, and cofactors. *Virol Sin* **2014**, *29*, 74–85, doi:10.1007/s12250-014-3438-6.

26. Nitsche, C. Dengue and Zika: Control and Antiviral Treatment Strategies. *Adv Exp Med Biol* **2018**, *1062*, 175–186, doi:10.1007/978-981-10-8727-1_13.
27. Plaszczyca, A.; Scaturro, P.; Neufeldt, C.J.; Cortese, M.; Cerikan, B.; Ferla, S.; Brancale, A.; Pichlmair, A.; Bartenschlager, R. A novel interaction between dengue virus nonstructural protein 1 and the NS4A-2K-4B precursor is required for viral RNA replication but not for formation of the membranous replication organelle. *Plos Pathog* **2019**, *15*, e1007736, doi:10.1371/journal.ppat.1007736.
28. Zou, J.; Xie, X.; Wang, Q.-Y.; Dong, H.; Lee, M.Y.; Kang, C.; Yuan, Z.; Shi, P.-Y. Characterization of Dengue Virus NS4A and NS4B Protein Interaction. *J Virol* **2015**, *89*, 3455–3470, doi:10.1128/jvi.03453-14.
29. Liang, Q.; Luo, Z.; Zeng, J.; Chen, W.; Foo, S.-S.; Lee, S.-A.; Ge, J.; Wang, S.; Goldman, S.A.; Zlokovic, B.V.; et al. Zika Virus NS4A and NS4B Proteins Deregulate Akt-mTOR Signaling in Human Fetal Neural Stem Cells to Inhibit Neurogenesis and Induce Autophagy. *Cell Stem Cell* **2016**, *19*, 663–671, doi:10.1016/j.stem.2016.07.019.
30. Xia, H.; Luo, H.; Shan, C.; Muruato, A.E.; Nunes, B.T.D.; Medeiros, D.B.A.; Zou, J.; Xie, X.; Giraldo, M.I.; Vasconcelos, P.F.C.; et al. An evolutionary NS1 mutation enhances Zika virus evasion of host interferon induction. *Nat Commun* **2018**, *9*, 414, doi:10.1038/s41467-017-02816-2.
31. Lu, G.; Gong, P. A structural view of the RNA-dependent RNA polymerases from the Flavivirus genus. *Virus Res* **2017**, *234*, 34–43, doi:10.1016/j.virusres.2017.01.020.
32. Klema, V.J.; Padmanabhan, R.; Choi, K.H. Flaviviral Replication Complex: Coordination between RNA Synthesis and 5'-RNA Capping. *Viruses* **2015**, *7*, 4640–4656, doi:10.3390/v7082837.
33. Thurmond, S.; Wang, B.; Song, J.; Hai, R. Suppression of Type I Interferon Signaling by Flavivirus NS5. *Viruses* **2018**, *10*, 712, doi:10.3390/v10120712.
34. Filomatori, C.V.; Lodeiro, M.F.; Alvarez, D.E.; Samsa, M.M.; Pietrasanta, L.; Gamarnik, A.V. A 5' RNA element promotes dengue virus RNA synthesis on a circular genome. *Gene Dev* **2006**, *20*, 2238–2249, doi:10.1101/gad.1444206.
35. Zhang, B.; Dong, H.; Stein, D.A.; Iversen, P.L.; Shi, P.-Y. West Nile virus genome cyclization and RNA replication require two pairs of long-distance RNA interactions. *Virology* **2008**, *373*, 1–13, doi:10.1016/j.virol.2008.01.016.
36. Clyde, K.; Harris, E. RNA Secondary Structure in the Coding Region of Dengue Virus Type 2 Directs Translation Start Codon Selection and Is Required for Viral Replication. *J Virol* **2006**, *80*, 2170–2182, doi:10.1128/jvi.80.5.2170-2182.2006.
37. Clyde, K.; Barrera, J.; Harris, E. The capsid-coding region hairpin element (cHP) is a critical determinant of dengue virus and West Nile virus RNA synthesis. *Virology* **2008**, *379*, 314–323, doi:10.1016/j.virol.2008.06.034.
38. Hahn, C.S.; Hahn, Y.S.; Rice, C.M.; Lee, E.; Dalgarno, L.; Strauss, E.G.; Strauss, J.H. Conserved elements in the 3' untranslated region of flavivirus RNAs and potential

- cyclization sequences. *J Mol Biol* **1987**, *198*, 33–41, doi:10.1016/0022-2836(87)90455-4.
39. Friebe, P.; Peña, J.; Pohl, M.O.F.; Harris, E. Composition of the sequence downstream of the dengue virus 5' cyclization sequence (dCS) affects viral RNA replication. *Virology* **2012**, *422*, 346–356, doi:10.1016/j.virol.2011.10.025.
 40. Liu, Z.-Y.; Li, X.-F.; Jiang, T.; Deng, Y.-Q.; Zhao, H.; Wang, H.-J.; Ye, Q.; Zhu, S.-Y.; Qiu, Y.; Zhou, X.; et al. Novel cis-acting element within the capsid-coding region enhances flavivirus viral-RNA replication by regulating genome cyclization. *J Virol* **2013**, *87*, 6804–18, doi:10.1128/jvi.00243-13.
 41. Groat-Carmona, A.M.; Orozco, S.; Friebe, P.; Payne, A.; Kramer, L.; Harris, E. A novel coding-region RNA element modulates infectious dengue virus particle production in both mammalian and mosquito cells and regulates viral replication in *Aedes aegypti* mosquitoes. *Virology* **2012**, *432*, 511–526, doi:10.1016/j.virol.2012.06.028.
 42. Ng, W.C.; Soto-Acosta, R.; Bradrick, S.S.; Garcia-Blanco, M.A.; Ooi, E.E. The 5' and 3' Untranslated Regions of the Flaviviral Genome. *Viruses* **2017**, *9*, 137, doi:10.3390/v9060137.
 43. Silva, P.A.G.C.; Pereira, C.F.; Dalebout, T.J.; Spaan, W.J.M.; Bredenbeek, P.J. An RNA Pseudoknot Is Required for Production of Yellow Fever Virus Subgenomic RNA by the Host Nuclease XRN1 ∇ . *J Virol* **2010**, *84*, 11395–11406, doi:10.1128/jvi.01047-10.
 44. Funk, A.; Truong, K.; Nagasaki, T.; Torres, S.; Floden, N.; Melian, E.B.; Edmonds, J.; Dong, H.; Shi, P.-Y.; Khromykh, A.A. RNA Structures Required for Production of Subgenomic Flavivirus RNA ∇ . *J Virol* **2010**, *84*, 11407–11417, doi:10.1128/jvi.01159-10.
 45. Pijlman, G.P.; Funk, A.; Kondratieva, N.; Leung, J.; Torres, S.; Aa, L. van der; Liu, W.J.; Palmenberg, A.C.; Shi, P.-Y.; Hall, R.A.; et al. A Highly Structured, Nuclease-Resistant, Noncoding RNA Produced by Flaviviruses Is Required for Pathogenicity. *Cell Host Microbe* **2008**, *4*, 579–591, doi:10.1016/j.chom.2008.10.007.
 46. Manokaran, G.; Finol, E.; Wang, C.; Gunaratne, J.; Bahl, J.; Ong, E.Z.; Tan, H.C.; Sessions, O.M.; Ward, A.M.; Gubler, D.J.; et al. Dengue subgenomic RNA binds TRIM25 to inhibit interferon expression for epidemiological fitness. *Science* **2015**, *350*, 217–221, doi:10.1126/science.aab3369.
 47. Schuessler, A.; Funk, A.; Lazear, H.M.; Cooper, D.A.; Torres, S.; Daffis, S.; Jha, B.K.; Kumagai, Y.; Takeuchi, O.; Hertzog, P.; et al. West Nile Virus Noncoding Subgenomic RNA Contributes to Viral Evasion of the Type I Interferon-Mediated Antiviral Response. *J Virol* **2012**, *86*, 5708–5718, doi:10.1128/jvi.00207-12.
 48. Schnettler, E.; Sterken, M.G.; Leung, J.Y.; Metz, S.W.; Geertsema, C.; Goldbach, R.W.; Vlak, J.M.; Kohl, A.; Khromykh, A.A.; Pijlman, G.P. Noncoding Flavivirus RNA Displays RNA Interference Suppressor Activity in Insect and Mammalian Cells. *J Virol* **2012**, *86*, 13486–13500, doi:10.1128/jvi.01104-12.

49. Arakawa, M.; Morita, E. Flavivirus Replication Organelle Biogenesis in the Endoplasmic Reticulum: Comparison with Other Single-Stranded Positive-Sense RNA Viruses. *Int J Mol Sci* **2019**, *20*, 2336, doi:10.3390/ijms20092336.
50. Mondotte, J.A.; Lozach, P.-Y.; Amara, A.; Gamarnik, A.V. Essential Role of Dengue Virus Envelope Protein N Glycosylation at Asparagine-67 during Viral Propagation. *J Virol* **2007**, *81*, 7136–7148, doi:10.1128/jvi.00116-07.
51. Fontes-Garfias, C.R.; Shan, C.; Luo, H.; Muruato, A.E.; Medeiros, D.B.A.; Mays, E.; Xie, X.; Zou, J.; Roundy, C.M.; Wakamiya, M.; et al. Functional Analysis of Glycosylation of Zika Virus Envelope Protein. *Cell Reports* **2017**, *21*, 1180–1190, doi:10.1016/j.celrep.2017.10.016.
52. Peters, R.; Stevenson, M. Zika Virus Diagnosis: Challenges and Solutions. *Clin Microbiol Infect* **2018**, *25*, 142–146, doi:10.1016/j.cmi.2018.12.002.
53. Musso, D.; Ko, A.I.; Baud, D. Zika Virus Infection — After the Pandemic. *New Engl J Med* **2019**, *381*, 1444–1457, doi:10.1056/nejmra1808246.
54. Sharp, T.M.; Fischer, M.; Muñoz-Jordán, J.L.; Paz-Bailey, G.; Staples, J.E.; Gregory, C.J.; Waterman, S.H. Dengue and Zika Virus Diagnostic Testing for Patients with a Clinically Compatible Illness and Risk for Infection with Both Viruses. *Mmwr Recomm Rep* **2019**, *68*, 1–10, doi:10.15585/mmwr.rr6801a1.
55. Adebajo, T.; Godfred-Cato, S.; Viens, L.; Fischer, M.; Staples, J.E.; Kuhnert-Tallman, W.; Walke, H.; Oduyebo, T.; Polen, K.; Peacock, G.; et al. Update: Interim Guidance for the Diagnosis, Evaluation, and Management of Infants with Possible Congenital Zika Virus Infection — United States, October 2017. *Mmwr Morbidity Mortal Wkly Rep* **2017**, *66*, 1089–1099, doi:10.15585/mmwr.mm6641a1.
56. Aubry, F.; Nougairède, A.; Gould, E.A.; Lamballerie, X. de Flavivirus reverse genetic systems, construction techniques and applications: A historical perspective. *Antivir Res* **2015**, *114*, 67–85, doi:10.1016/j.antiviral.2014.12.007.
57. Guy, B.; Guirakhoo, F.; Barban, V.; Higgs, S.; Monath, T.P.; Lang, J. Preclinical and clinical development of YFV 17D-based chimeric vaccines against dengue, West Nile and Japanese encephalitis viruses. *Vaccine* **2010**, *28*, 632–649, doi:10.1016/j.vaccine.2009.09.098.
58. Fontes-Garfias, C.R.; Baker, C.K.; Shi, P.-Y. Reserve genetic approaches for the development of Zika vaccines and therapeutics. *Curr Opin Virol* **2020**, *44*, 7–15, doi:10.1016/j.coviro.2020.05.002.
59. Kümmerer, B.M. Establishment and Application of Flavivirus Replicons. *Adv Exp Med Biol* **2018**, *1062*, 165–173, doi:10.1007/978-981-10-8727-1_12.
60. Khromykh, A.A.; Westaway, E.G. Subgenomic replicons of the flavivirus Kunjin: construction and applications. *J Virol* **1997**, *71*, 1497–505.
61. Varnavski, A.N.; Khromykh, A.A. Noncytopathic Flavivirus Replicon RNA-Based System for Expression and Delivery of Heterologous Genes. *Virology* **1999**, *255*, 366–375, doi:10.1006/viro.1998.9564.

62. Shi, P.-Y.; Tilgner, M.; Lo, M.K. Construction and Characterization of Subgenomic Replicons of New York Strain of West Nile Virus. *Virology* **2002**, *296*, 219–233, doi:10.1006/viro.2002.1453.
63. Blight, K.J.; Kolykhalov, A.A.; Rice, C.M. Efficient Initiation of HCV RNA Replication in Cell Culture. *Science* **2000**, *290*, 1972–1974, doi:10.1126/science.290.5498.1972.
64. Lohmann, V.; Körner, F.; Koch, J.-O.; Herian, U.; Theilmann, L.; Bartenschlager, R. Replication of Subgenomic Hepatitis C Virus RNAs in a Hepatoma Cell Line. *Science* **1999**, *285*, 110–113, doi:10.1126/science.285.5424.110.
65. Rice, C.M.; Grakoui, A.; Galler, R.; Chambers, T.J. Transcription of infectious yellow fever RNA from full-length cDNA templates produced by in vitro ligation. *New Biologist* **1989**, *1*, 285–96.
66. Sumiyoshi, H.; Hoke, C.H.; Trent, D.W. Infectious Japanese encephalitis virus RNA can be synthesized from in vitro-ligated cDNA templates. *J Virol* **1992**, *66*, 5425–31.
67. Kapoor, M.; Zhang, L.; Mohan, P.M.; Padmanabhan, R. Synthesis and characterization of an infectious dengue virus type-2 RNA genome (New Guinea C strain). *Gene* **1995**, *162*, 175–180, doi:10.1016/0378-1119(95)00332-z.
68. Mandl, C.W.; Heinz, F.X.; Holzmann, H.; Kunz, C.; Ecker, M. Infectious cDNA clones of tick-borne encephalitis virus European subtype prototypic strain Neudoerfl and high virulence strain Hypr. *J Gen Virol* **1997**, *78*, 1049–1057, doi:10.1099/0022-1317-78-5-1049.
69. Lai, C.J.; Zhao, B.T.; Hori, H.; Bray, M. Infectious RNA transcribed from stably cloned full-length cDNA of dengue type 4 virus. *Proc National Acad Sci* **1991**, *88*, 5139–5143, doi:10.1073/pnas.88.12.5139.
70. Khromykh, A.A.; Westaway, E.G. Completion of Kunjin virus RNA sequence and recovery of an infectious RNA transcribed from stably cloned full-length cDNA. *J Virol* **1994**, *68*, 4580–8.
71. Hurrelbrink, R.J.; Nestorowicz, A.; McMinn, P.C. Characterization of infectious Murray Valley encephalitis virus derived from a stably cloned genome-length cDNA The GenBank accession number of the sequence reported in this paper is AF161266. *J Gen Virol* **1999**, *80*, 3115–3125, doi:10.1099/0022-1317-80-12-3115.
72. Campbell, M.S.; Pletnev, A.G. Infectious cDNA Clones of Langat Tick-Borne Flavivirus That Differ from Their Parent in Peripheral Neurovirulence. *Virology* **2000**, *269*, 225–237, doi:10.1006/viro.2000.0220.
73. Shi, P.-Y.; Tilgner, M.; Lo, M.K.; Kent, K.A.; Bernard, K.A. Infectious cDNA Clone of the Epidemic West Nile Virus from New York City. *J Virol* **2002**, *76*, 5847–5856, doi:10.1128/jvi.76.12.5847-5856.2002.
74. Yun, S.-I.; Kim, S.-Y.; Rice, C.M.; Lee, Y.-M. Development and Application of a Reverse Genetics System for Japanese Encephalitis Virus. *J Virol* **2003**, *77*, 6450–6465, doi:10.1128/jvi.77.11.6450-6465.2003.

75. Pierson, T.C.; Diamond, M.S.; Ahmed, A.A.; Valentine, L.E.; Davis, C.W.; Samuel, M.A.; Hanna, S.L.; Puffer, B.A.; Doms, R.W. An infectious West Nile Virus that expresses a GFP reporter gene. *Virology* **2005**, *334*, 28–40, doi:10.1016/j.virol.2005.01.021.
76. Deas, T.S.; Binduga-Gajewska, I.; Tilgner, M.; Ren, P.; Stein, D.A.; Moulton, H.M.; Iversen, P.L.; Kauffman, E.B.; Kramer, L.D.; Shi, P.-Y. Inhibition of Flavivirus Infections by Antisense Oligomers Specifically Suppressing Viral Translation and RNA Replication. *J Virol* **2005**, *79*, 4599–4609, doi:10.1128/jvi.79.8.4599-4609.2005.
77. Kaptein, S.J.F.; Burghgraeve, T.D.; Froeyen, M.; Pastorino, B.; Alen, M.M.F.; Mondotte, J.A.; Herdewijn, P.; Jacobs, M.; Lamballerie, X. de; Schols, D.; et al. A derivate of the antibiotic doxorubicin is a selective inhibitor of dengue and yellow fever virus replication in vitro. *Antimicrob Agents Ch* **2010**, *54*, 5269–80, doi:10.1128/aac.00686-10.
78. Yun, S.-I.; Song, B.-H.; Woolley, M.E.; Frank, J.C.; Julander, J.G.; Lee, Y.-M. Development, Characterization, and Application of Two Reporter-Expressing Recombinant Zika Viruses. *Viruses* **2020**, *12*, 572, doi:10.3390/v12050572.
79. Bonaldo, M.C.; Mello, S.M.; Trindade, G.F.; Rangel, A.A.; Duarte, A.S.; Oliveira, P.J.; Freire, M.S.; Kubelka, C.F.; Galler, R. Construction and characterization of recombinant flaviviruses bearing insertions between E and NS1 genes. *Virol J* **2007**, *4*, 115, doi:10.1186/1743-422x-4-115.
80. Simon-Loriere, E.; Holmes, E.C. Why do RNA viruses recombine? *Nat Rev Microbiol* **2011**, *9*, 617–26, doi:10.1038/nrmicro2614.
81. Grabowski, J.M.; Tsetsarkin, K.A.; Long, D.; Scott, D.P.; Rosenke, R.; Schwan, T.G.; Mlera, L.; Offerdahl, D.K.; Pletnev, A.G.; Bloom, M.E. Flavivirus Infection of *Ixodes scapularis* (Black-Legged Tick) Ex Vivo Organotypic Cultures and Applications for Disease Control. *Mbio* **2017**, *8*, e01255-17, doi:10.1128/mbio.01255-17.
82. Volkova, E.; Tsetsarkin, K.A.; Sippert, E.; Assis, F.; Liu, G.; Rios, M.; Pletnev, A.G. Novel Approach for Insertion of Heterologous Sequences into Full-Length ZIKV Genome Results in Superior Level of Gene Expression and Insert Stability. *Viruses* **2020**, *12*, 61, doi:10.3390/v12010061.
83. Santana, M.G.V. de; Neves, P.C.C.; Santos, J.R. dos; Lima, N.S.; Santos, A.A.C. dos; Watkins, D.I.; Galler, R.; Bonaldo, M.C. Improved genetic stability of recombinant yellow fever 17D virus expressing a lentiviral Gag gene fragment. *Virology* **2014**, *452–453*, 202–211, doi:10.1016/j.virol.2014.01.017.
84. Shustov, A.V.; Mason, P.W.; Frolov, I. Production of Pseudoinfectious Yellow Fever Virus with a Two-Component Genome ∇ . *J Virol* **2007**, *81*, 11737–11748, doi:10.1128/jvi.01112-07.
85. Samsa, M.M.; Mondotte, J.A.; Iglesias, N.G.; Assunção-Miranda, I.; Barbosa-Lima, G.; Poian, A.T.D.; Bozza, P.T.; Gamarnik, A.V. Dengue virus capsid protein usurps

- lipid droplets for viral particle formation. *Plos Pathog* **2009**, *5*, e1000632, doi:10.1371/journal.ppat.1000632.
86. Samsa, M.M.; Mondotte, J.A.; Caramelo, J.J.; Gamarnik, A.V. Uncoupling cis-Acting RNA Elements from Coding Sequences Revealed a Requirement of the N-Terminal Region of Dengue Virus Capsid Protein in Virus Particle Formation. *J Virol* **2012**, *86*, 1046–1058, doi:10.1128/jvi.05431-11.
 87. Zou, G.; Xu, H.Y.; Qing, M.; Wang, Q.-Y.; Shi, P.-Y. Development and characterization of a stable luciferase dengue virus for high-throughput screening. *Antivir Res* **2011**, *91*, 11–19, doi:10.1016/j.antiviral.2011.05.001.
 88. Mutso, M.; Saul, S.; Rausalu, K.; Susova, O.; Žusinaite, E.; Mahalingam, S.; Merits, A. Reverse genetic system, genetically stable reporter viruses and packaged subgenomic replicon based on a Brazilian Zika virus isolate. *J Gen Virol* **2017**, *98*, 2712–2724, doi:10.1099/jgv.0.000938.
 89. Shan, C.; Xie, X.; Muruato, A.E.; Rossi, S.L.; Roundy, C.M.; Azar, S.R.; Yang, Y.; Tesh, R.B.; Bourne, N.; Barrett, A.D.; et al. An Infectious cDNA Clone of Zika Virus to Study Viral Virulence, Mosquito Transmission, and Antiviral Inhibitors. *Cell Host Microbe* **2016**, *19*, 891–900, doi:10.1016/j.chom.2016.05.004.
 90. Schoggins, J.W.; Dorner, M.; Feulner, M.; Imanaka, N.; Murphy, M.Y.; Ploss, A.; Rice, C.M. Dengue reporter viruses reveal viral dynamics in interferon receptor-deficient mice and sensitivity to interferon effectors in vitro. *P Natl Acad Sci Usa* **2012**, *109*, 14610–5, doi:10.1073/pnas.1212379109.
 91. Zhang, P.-T.; Shan, C.; Li, X.-D.; Liu, S.-Q.; Deng, C.-L.; Ye, H.-Q.; Shang, B.-D.; Shi, P.-Y.; Lv, M.; Shen, B.-F.; et al. Generation of a recombinant West Nile virus stably expressing the Gaussia luciferase for neutralization assay. *Virus Res* **2016**, *211*, 17–24, doi:10.1016/j.virusres.2015.09.015.
 92. He, Y.; Liu, P.; Wang, T.; Wu, Y.; Lin, X.; Wang, M.; Jia, R.; Zhu, D.; Liu, M.; Zhao, X.; et al. Genetically stable reporter virus, subgenomic replicon and packaging system of duck Tembusu virus based on a reverse genetics system. *Virology* **2019**, *533*, 86–92, doi:10.1016/j.virol.2019.05.003.
 93. Li, X.-F.; Li, X.-D.; Deng, C.-L.; Dong, H.-L.; Zhang, Q.-Y.; Ye, Q.; Ye, H.-Q.; Huang, X.-Y.; Deng, Y.-Q.; Zhang, B.; et al. Visualization of a neurotropic flavivirus infection in mouse reveals unique viscerotropism controlled by host type I interferon signaling. *Theranostics* **2017**, *7*, 912–925, doi:10.7150/thno.16615.
 94. Suphatrakul, A.; Duangchinda, T.; Jupatanakul, N.; Prasittisa, K.; Onnome, S.; Pengon, J.; Siridechadilok, B. Multi-color fluorescent reporter dengue viruses with improved stability for analysis of a multi-virus infection. *Plos One* **2018**, *13*, e0194399, doi:10.1371/journal.pone.0194399.
 95. Gadea, G.; Bos, S.; Krejbich-Trotot, P.; Clain, E.; Viranaicken, W.; El-Kalamouni, C.; Mavingui, P.; Desprès, P. A robust method for the rapid generation of recombinant Zika virus expressing the GFP reporter gene. *Virology* **2016**, *497*, 157–162, doi:10.1016/j.virol.2016.07.015.

96. Kamiyama, D.; Sekine, S.; Barsi-Rhyne, B.; Hu, J.; Chen, B.; Gilbert, L.A.; Ishikawa, H.; Leonetti, M.D.; Marshall, W.F.; Weissman, J.S.; et al. Versatile protein tagging in cells with split fluorescent protein. *Nat Commun* **2016**, *7*, 11046, doi:10.1038/ncomms11046.
97. Dixon, A.S.; Schwinn, M.K.; Hall, M.P.; Zimmerman, K.; Otto, P.; Lubben, T.H.; Butler, B.L.; Binkowski, B.F.; Machleidt, T.; Kirkland, T.A.; et al. NanoLuc Complementation Reporter Optimized for Accurate Measurement of Protein Interactions in Cells. *Acs Chem Biol* **2015**, *11*, 400–408, doi:10.1021/acschembio.5b00753.
98. Tamura, T.; Fukuhara, T.; Uchida, T.; Ono, C.; Mori, H.; Sato, A.; Fauzyah, Y.; Okamoto, T.; Kurosu, T.; Setoh, Y.X.; et al. Characterization of Recombinant Flaviviridae Viruses Possessing a Small Reporter Tag. *J Virol* **2017**, *92*, e01582-17, doi:10.1128/jvi.01582-17.
99. Tamura, T.; Igarashi, M.; Enkhbold, B.; Suzuki, T.; Okamatsu, M.; Ono, C.; Mori, H.; Izumi, T.; Sato, A.; Fauzyah, Y.; et al. In Vivo Dynamics of Reporter Flaviviridae Viruses. *J Virol* **2019**, *93*, doi:10.1128/jvi.01191-19.
100. Puig-Basagoiti, F.; Deas, T.S.; Ren, P.; Tilgner, M.; Ferguson, D.M.; Shi, P.-Y. High-Throughput Assays Using a Luciferase-Expressing Replicon, Virus-Like Particles, and Full-Length Virus for West Nile Virus Drug Discovery. *Antimicrob Agents Ch* **2005**, *49*, 4980–4988, doi:10.1128/aac.49.12.4980-4988.2005.
101. Baker, C.; Xie, X.; Zou, J.; Muruato, A.; Fink, K.; Shi, P.-Y. Using recombination-dependent lethal mutations to stabilize reporter flaviviruses for rapid serodiagnosis and drug discovery. *Ebiomedicine* **2020**, *57*, 102838, doi:10.1016/j.ebiom.2020.102838.
102. Pierson, T.C.; Sánchez, M.D.; Puffer, B.A.; Ahmed, A.A.; Geiss, B.J.; Valentine, L.E.; Altamura, L.A.; Diamond, M.S.; Doms, R.W. A rapid and quantitative assay for measuring antibody-mediated neutralization of West Nile virus infection. *Virology* **2006**, *346*, 53–65, doi:10.1016/j.virol.2005.10.030.
103. Shan, C.; Xie, X.; Ren, P.; Loeffelholz, M.J.; Yang, Y.; Furuya, A.; Dupuis, A.P.; Kramer, L.D.; Wong, S.J.; Shi, P.-Y. A Rapid Zika Diagnostic Assay to Measure Neutralizing Antibodies in Patients. *Ebiomedicine* **2017**, *17*, 157–162, doi:10.1016/j.ebiom.2017.03.006.
104. Frumence, E.; Viranaicken, W.; Gadea, G.; Desprès, P. A GFP Reporter MR766-Based Flow Cytometry Neutralization Test for Rapid Detection of Zika Virus-Neutralizing Antibodies in Serum Specimens. *Nato Adv Sci Inst Se* **2019**, *7*, 66, doi:10.3390/vaccines7030066.
105. Matsuda, M.; Yamanaka, A.; Yato, K.; Yoshii, K.; Watashi, K.; Aizaki, H.; Konishi, E.; Takasaki, T.; Kato, T.; Muramatsu, M.; et al. High-throughput neutralization assay for multiple flaviviruses based on single-round infectious particles using dengue virus type 1 reporter replicon. *Sci Rep-uk* **2018**, *8*, 16624, doi:10.1038/s41598-018-34865-y.

106. Yamanaka, A.; Moi, M.L.; Takasaki, T.; Kurane, I.; Matsuda, M.; Suzuki, R.; Konishi, E. Utility of Japanese encephalitis virus subgenomic replicon-based single-round infectious particles as antigens in neutralization tests for Zika virus and three other flaviviruses. *J Virol Methods* **2017**, *243*, 164–171, doi:10.1016/j.jviromet.2017.02.011.
107. Yamanaka, A.; Suzuki, R.; Konishi, E. Evaluation of single-round infectious, chimeric dengue type 1 virus as an antigen for dengue functional antibody assays. *Vaccine* **2014**, *32*, 4289–4295, doi:10.1016/j.vaccine.2014.06.017.
108. Bonaldo, M.C.; Garratt, R.C.; Caufour, P.S.; Freire, M.S.; Rodrigues, M.M.; Nussenzweig, R.S.; Galler, R. Surface expression of an immunodominant malaria protein B cell epitope by yellow fever virus 17D. Edited by J. Karn. *J Mol Biol* **2002**, *315*, 873–885, doi:10.1006/jmbi.2001.5258.
109. Bonaldo, M.C.; Garratt, R.C.; Marchevsky, R.S.; Coutinho, E.S.F.; Jabor, A.V.; Almeida, L.F.C.; Yamamura, A.M.Y.; Duarte, A.S.; Oliveira, P.J.; Lizeu, J.O.P.; et al. Attenuation of Recombinant Yellow Fever 17D Viruses Expressing Foreign Protein Epitopes at the Surface. *J Virol* **2005**, *79*, 8602–8613, doi:10.1128/jvi.79.13.8602-8613.2005.
110. Barba-Spaeth, G.; Longman, R.S.; Albert, M.L.; Rice, C.M. Live attenuated yellow fever 17D infects human DCs and allows for presentation of endogenous and recombinant T cell epitopes. *J Exp Medicine* **2005**, *202*, 1179–1184, doi:10.1084/jem.20051352.
111. Tao, D.; Barba-Spaeth, G.; Rai, U.; Nussenzweig, V.; Rice, C.M.; Nussenzweig, R.S. Yellow fever 17D as a vaccine vector for microbial CTL epitopes. *J Exp Medicine* **2005**, *201*, 201–209, doi:10.1084/jem.20041526.
112. McAllister, A.; Arbetman, A.E.; Mandl, S.; Peña-Rossi, C.; Andino, R. Recombinant Yellow Fever Viruses Are Effective Therapeutic Vaccines for Treatment of Murine Experimental Solid Tumors and Pulmonary Metastases. *J Virol* **2000**, *74*, 9197–9205, doi:10.1128/jvi.74.19.9197-9205.2000.
113. Martins, M.A.; Wilson, N.A.; Piaskowski, S.M.; Weisgrau, K.L.; Furlott, J.R.; Bonaldo, M.C.; Santana, M.G.V. de; Rudersdorf, R.A.; Rakasz, E.G.; Keating, K.D.; et al. Vaccination with Gag, Vif, and Nef gene fragments affords partial control of viral replication after mucosal challenge with SIVmac239. *J Virol* **2014**, *88*, 7493–516, doi:10.1128/jvi.00601-14.
114. Münster, M.; Płaszczyc, A.; Cortese, M.; Neufeldt, C.J.; Goellner, S.; Long, G.; Bartenschlager, R. A Reverse Genetics System for Zika Virus Based on a Simple Molecular Cloning Strategy. *Viruses* **2018**, *10*, 368, doi:10.3390/v10070368.
115. Hanson, G.; Collier, J. Codon optimality, bias and usage in translation and mRNA decay. *Nat Rev Mol Cell Bio* **2018**, *19*, 20–30, doi:10.1038/nrm.2017.91.
116. Zou, J.; Xie, X.; Luo, H.; Shan, C.; Muruato, A.E.; Weaver, S.C.; Wang, T.; Shi, P.-Y. A single-dose plasmid-launched live-attenuated Zika vaccine induces protective immunity. *Ebiomedicine* **2018**, *36*, 92–102, doi:10.1016/j.ebiom.2018.08.056.

117. Brinton, M.A.; Basu, M. Functions of the 3' and 5' genome RNA regions of members of the genus Flavivirus. *Virus Res* **2015**, *206*, 108–19, doi:10.1016/j.virusres.2015.02.006.
118. Liu, Z.-Y.; Qin, C.-F. Structure and function of cis-acting RNA elements of flavivirus. *Rev Med Virol* **2019**, e2092, doi:10.1002/rmv.2092.
119. Yin, Z.; Chen, Y.-L.; Schul, W.; Wang, Q.-Y.; Gu, F.; Duraiswamy, J.; Kondreddi, R.R.; Niyomrattanakit, P.; Lakshminarayana, S.B.; Goh, A.; et al. An adenosine nucleoside inhibitor of dengue virus. *P Natl Acad Sci Usa* **2009**, *106*, 20435–9, doi:10.1073/pnas.0907010106.
120. Deng, Y.-Q.; Zhang, N.-N.; Li, C.-F.; Tian, M.; Hao, J.-N.; Xie, X.-P.; Shi, P.-Y.; Qin, C.-F. Adenosine Analog NITD008 Is a Potent Inhibitor of Zika Virus. *Open Forum Infect Dis* **2016**, *3*, ofw175, doi:10.1093/ofid/ofw175.
121. Li, T.; Zhao, Q.; Yang, X.; Chen, C.; Yang, K.; Wu, C.; Zhang, T.; Duan, Y.; Xue, X.; Mi, K.; et al. Structural insight into the Zika virus capsid encapsulating the viral genome. *Cell Res* **2018**, *28*, 497–499, doi:10.1038/s41422-018-0007-9.
122. Friebe, P.; Harris, E. Interplay of RNA Elements in the Dengue Virus 5' and 3' Ends Required for Viral RNA Replication ▽. *J Virol* **2010**, *84*, 6103–6118, doi:10.1128/jvi.02042-09.
123. Chong, H.Y.; Leow, C.Y.; Majeed, A.B.A.; Leow, C.H. Flavivirus infection-A review of immunopathogenesis, immunological response, and immunodiagnosis. *Virus Res* **2019**, *274*, 197770, doi:10.1016/j.virusres.2019.197770.
124. Mathers, C.D.; Ezzati, M.; Lopez, A.D. Measuring the Burden of Neglected Tropical Diseases: The Global Burden of Disease Framework. *Plos Neglect Trop D* **2007**, *1*, e114, doi:10.1371/journal.pntd.0000114.
125. Schuler-Faccini, L.; Ribeiro, E.M.; Feitosa, I.M.L.; Horovitz, D.D.G.; Cavalcanti, D.P.; Pessoa, A.; Doriqui, M.J.R.; Neri, J.I.; Neto, J.M. de P.; Wanderley, H.Y.C.; et al. Possible Association Between Zika Virus Infection and Microcephaly - Brazil, 2015. *Mmwr Morbidity Mortal Wkly Rep* **2016**, *65*, 59–62, doi:10.15585/mmwr.mm6503e2.
126. Barrett, A.D.T.; Higgs, S. Yellow Fever: A Disease that Has Yet to be Conquered. *Annu Rev Entomol* **2007**, *52*, 209–229, doi:10.1146/annurev.ento.52.110405.091454.
127. Guy, B.; Noriega, F.; Ochiai, R.L.; L'azou, M.; Delore, V.; Skipetrova, A.; Verdier, F.; Coudeville, L.; Savarino, S.; Jackson, N. A recombinant live attenuated tetravalent vaccine for the prevention of dengue. *Expert Rev Vaccines* **2017**, *16*, 1–13, doi:10.1080/14760584.2017.1335201.
128. Schoggins, J.W.; Wilson, S.J.; Panis, M.; Murphy, M.Y.; Jones, C.T.; Bieniasz, P.; Rice, C.M. A diverse range of gene products are effectors of the type I interferon antiviral response. *Nature* **2011**, *472*, 481–485, doi:10.1038/nature09907.
129. Giel-Moloney, M.; Goncalvez, A.P.; Catalan, J.; Lecouturier, V.; Girerd-Chambaz, Y.; Diaz, F.; Maldonado-Arocho, F.; Gomila, R.C.; Bernard, M.-C.; Oomen, R.; et

- al. Chimeric yellow fever 17D-Zika virus (ChimeriVax-Zika) as a live-attenuated Zika virus vaccine. *Sci Rep-uk* **2018**, 8, 13206, doi:10.1038/s41598-018-31375-9.
130. Arroyo, J.; Miller, C.; Catalan, J.; Myers, G.A.; Ratterree, M.S.; Trent, D.W.; Monath, T.P. ChimeriVax-West Nile Virus Live-Attenuated Vaccine: Preclinical Evaluation of Safety, Immunogenicity, and Efficacy. *J Virol* **2004**, 78, 12497–12507, doi:10.1128/jvi.78.22.12497-12507.2004.
 131. Li, X.-F.; Dong, H.-L.; Wang, H.-J.; Huang, X.-Y.; Qiu, Y.-F.; Ji, X.; Ye, Q.; Li, C.; Liu, Y.; Deng, Y.-Q.; et al. Development of a chimeric Zika vaccine using a licensed live-attenuated flavivirus vaccine as backbone. *Nat Commun* **2018**, 9, 673, doi:10.1038/s41467-018-02975-w.
 132. Hobson-Peters, J.; Harrison, J.J.; Watterson, D.; Hazlewood, J.E.; Vet, L.J.; Newton, N.D.; Warrilow, D.; Colmant, A.M.G.; Taylor, C.; Huang, B.; et al. A recombinant platform for flavivirus vaccines and diagnostics using chimeras of a new insect-specific virus. *Sci Transl Med* **2019**, 11, eaax7888, doi:10.1126/scitranslmed.aax7888.
 133. Daffis, S.; Szretter, K.J.; Schriewer, J.; Li, J.; Youn, S.; Errett, J.; Lin, T.-Y.; Schneller, S.; Zust, R.; Dong, H.; et al. 2'-O methylation of the viral mRNA cap evades host restriction by IFIT family members. *Nature* **2010**, 468, 452–6, doi:10.1038/nature09489.
 134. Kaiser, J.A.; Luo, H.; Widen, S.G.; Wood, T.G.; Huang, C.Y.-H.; Wang, T.; Barrett, A.D.T. Genotypic and phenotypic characterization of West Nile virus NS5 methyltransferase mutants. *Vaccine* **2019**, 37, 7155–7164, doi:10.1016/j.vaccine.2019.09.045.
 135. Gallichotte, E.N.; Widman, D.G.; Yount, B.L.; Wahala, W.M.; Durbin, A.; Whitehead, S.; Sariol, C.A.; Crowe, J.E.; Silva, A.M. de; Baric, R.S. A new quaternary structure epitope on dengue virus serotype 2 is the target of durable type-specific neutralizing antibodies. *Mbio* **2015**, 6, e01461-15, doi:10.1128/mbio.01461-15.
 136. Messer, W.B.; Yount, B.; Hacker, K.E.; Donaldson, E.F.; Huynh, J.P.; Silva, A.M. de; Baric, R.S. Development and characterization of a reverse genetic system for studying dengue virus serotype 3 strain variation and neutralization. *Plos Neglect Trop D* **2012**, 6, e1486, doi:10.1371/journal.pntd.0001486.
 137. Xie, X.; Muruato, A.E.; Zhang, X.; Lokugamage, K.G.; Fontes-Garfias, C.R.; Zou, J.; Liu, J.; Ren, P.; Balakrishnan, M.; Cihlar, T.; et al. A nanoluciferase SARS-CoV-2 for rapid neutralization testing and screening of anti-infective drugs for COVID-19. *Nat. Commun.* **2020**, Submitted.
 138. Muruato, A.E.; Fontes-Garfias, C.R.; Ren, P.; Garcia-Blanco, M.A.; Menachery, V.D.; Xie, X.; Shi, P.-Y. A high-throughput neutralizing antibody assay for COVID-19 diagnosis and vaccine evaluation. *Nat. Commun.* **2020**, In press.
 139. Li, P.; Wei, Y.; Mei, M.; Tang, L.; Sun, L.; Huang, W.; Zhou, J.; Zou, C.; Zhang, S.; Qin, C.-F.; et al. Integrative Analysis of Zika Virus Genome RNA Structure

- Reveals Critical Determinants of Viral Infectivity. *Cell Host Microbe* **2018**, *24*, 875–886.e5, doi:10.1016/j.chom.2018.10.011.
140. Borba, L. de; Villordo, S.M.; Iglesias, N.G.; Filomatori, C.V.; Gebhard, L.G.; Gamarnik, A.V. Overlapping Local and Long-Range RNA-RNA Interactions Modulate Dengue Virus Genome Cyclization and Replication. *J Virol* **2015**, *89*, 3430–3437, doi:10.1128/jvi.02677-14.
 141. Baker, C.; Liu, Y.; Zou, J.; Muruato, A.; Xie, X.; Shi, P.-Y. Identifying optimal capsid duplication length for the stability of reporter flaviviruses. *Emerg Microbes Infect* **2020**, 1–32, doi:10.1080/22221751.2020.1829994.
 142. Bindels, D.S.; Haarbosch, L.; Weeren, L. van; Postma, M.; Wiese, K.E.; Mastop, M.; Aumonier, S.; Gotthard, G.; Royant, A.; Hink, M.A.; et al. mScarlet: a bright monomeric red fluorescent protein for cellular imaging. *Nat Methods* **2016**, *14*, nmeth.4074, doi:10.1038/nmeth.4074.
 143. Filonov, G.S.; Piatkevich, K.D.; Ting, L.-M.; Zhang, J.; Kim, K.; Verkhusha, V.V. Bright and stable near-infrared fluorescent protein for in vivo imaging. *Nat Biotechnol* **2011**, *29*, 757, doi:10.1038/nbt.1918.
 144. Lee, H.; Halverson, S.; Ezinwa, N. Mosquito-Borne Diseases. *Prim Care Clin Office Pract* **2018**, *45*, 393–407, doi:10.1016/j.pop.2018.05.001.
 145. Katzelnick, L.C.; Coloma, J.; Harris, E. Dengue: knowledge gaps, unmet needs, and research priorities. *Lancet Infect Dis* **2017**, *17*, e88–e100, doi:10.1016/s1473-3099(16)30473-x.
 146. Shan, C.; Ortiz, D.A.; Yang, Y.; Wong, S.J.; Kramer, L.D.; Shi, P.-Y.; Loeffelholz, M.J.; Ren, P. Evaluation of a Novel Reporter Virus Neutralization Test for Serological Diagnosis of Zika and Dengue Virus Infection. *J Clin Microbiol* **2017**, *55*, 3028–3036, doi:10.1128/jcm.00975-17.
 147. Alexander, B.M.; Cloughesy, T.F. Adult Glioblastoma. *J Clin Oncol Official J Am Soc Clin Oncol* **2017**, *35*, 2402–2409, doi:10.1200/jco.2017.73.0119.
 148. Omuro, A.; DeAngelis, L.M. Glioblastoma and Other Malignant Gliomas. *Jama* **2013**, *310*, 1842, doi:10.1001/jama.2013.280319.
 149. Stupp, R.; Taillibert, S.; Kanner, A.; Read, W.; Steinberg, D.M.; Lhermitte, B.; Toms, S.; Idhah, A.; Ahluwalia, M.S.; Fink, K.; et al. Effect of Tumor-Treating Fields Plus Maintenance Temozolomide vs Maintenance Temozolomide Alone on Survival in Patients With Glioblastoma: A Randomized Clinical Trial. *Jama* **2017**, *318*, 2306–2316, doi:10.1001/jama.2017.18718.
 150. Clara, J.A.; Monge, C.; Yang, Y.; Takebe, N. Targeting signalling pathways and the immune microenvironment of cancer stem cells — a clinical update. *Nat Rev Clin Oncol* **2020**, *17*, 204–232, doi:10.1038/s41571-019-0293-2.
 151. Singh, S.K.; Hawkins, C.; Clarke, I.D.; Squire, J.A.; Bayani, J.; Hide, T.; Henkelman, R.M.; Cusimano, M.D.; Dirks, P.B. Identification of human brain tumour initiating cells. *Nature* **2004**, *432*, 396–401, doi:10.1038/nature03128.

152. Galli, R.; Binda, E.; Orfanelli, U.; Cipelletti, B.; Gritti, A.; Vitis, S.D.; Fiocco, R.; Foroni, C.; Dimeco, F.; Vescovi, A. Isolation and Characterization of Tumorigenic, Stem-like Neural Precursors from Human Glioblastoma. *Cancer Res* **2004**, *64*, 7011–7021, doi:10.1158/0008-5472.can-04-1364.
153. Lee, J.H.; Lee, J.E.; Kahng, J.Y.; Kim, S.H.; Park, J.S.; Yoon, S.J.; Um, J.-Y.; Kim, W.K.; Lee, J.-K.; Park, J.; et al. Human glioblastoma arises from subventricular zone cells with low-level driver mutations. *Nature* **2018**, *560*, 243–247, doi:10.1038/s41586-018-0389-3.
154. Chen, J.; Li, Y.; Yu, T.-S.; McKay, R.M.; Burns, D.K.; Kernie, S.G.; Parada, L.F. A restricted cell population propagates glioblastoma growth after chemotherapy. *Nature* **2012**, *488*, 522–526, doi:10.1038/nature11287.
155. Tang, H.; Hammack, C.; Ogden, S.C.; Wen, Z.; Qian, X.; Li, Y.; Yao, B.; Shin, J.; Zhang, F.; Lee, E.M.; et al. Zika Virus Infects Human Cortical Neural Progenitors and Attenuates Their Growth. *Cell Stem Cell* **2016**, *18*, 587–90, doi:10.1016/j.stem.2016.02.016.
156. Li, H.; Saucedo-Cuevas, L.; Regla-Nava, J.A.; Chai, G.; Sheets, N.; Tang, W.; Terskikh, A.V.; Shresta, S.; Gleeson, J.G. Zika Virus Infects Neural Progenitors in the Adult Mouse Brain and Alters Proliferation. *Cell Stem Cell* **2016**, *19*, 593–598, doi:10.1016/j.stem.2016.08.005.
157. Dang, J.; Tiwari, S.K.; Lichinchi, G.; Qin, Y.; Patil, V.S.; Eroshkin, A.M.; Rana, T.M. Zika Virus Depletes Neural Progenitors in Human Cerebral Organoids through Activation of the Innate Immune Receptor TLR3. *Cell Stem Cell* **2016**, *19*, 258–265, doi:10.1016/j.stem.2016.04.014.
158. Bayless, N.L.; Greenberg, R.S.; Swigut, T.; Wysocka, J.; Blish, C.A. Zika Virus Infection Induces Cranial Neural Crest Cells to Produce Cytokines at Levels Detrimental for Neurogenesis. *Cell Host Microbe* **2016**, *20*, 423–428, doi:10.1016/j.chom.2016.09.006.
159. Zhu, Z.; Gorman, M.J.; McKenzie, L.D.; Chai, J.N.; Hubert, C.G.; Prager, B.C.; Fernandez, E.; Richner, J.M.; Zhang, R.; Shan, C.; et al. Zika virus has oncolytic activity against glioblastoma stem cells. *J Exp Med* **2017**, *214*, 2843–2857, doi:10.1084/jem.20171093.
160. Chen, Q.; Wu, J.; Ye, Q.; Ma, F.; Zhu, Q.; Wu, Y.; Shan, C.; Xie, X.; Li, D.; Zhan, X.; et al. Treatment of Human Glioblastoma with a Live Attenuated Zika Virus Vaccine Candidate. *Mbio* **2018**, *9*, e01683-18, doi:10.1128/mbio.01683-18.
161. Kaid, C.; Goulart, E.; Caires-Júnior, L.C.; Araujo, B.H.S.; Soares-Schanoski, A.; Bueno, H.M.S.; Silva, K.A.T.; Astray, R.M.; Assoni, A.F.; Júnior, A.F.R.; et al. Zika virus selectively kills aggressive human embryonal CNS tumor cells in vitro and in vivo. *Cancer Res* **2018**, canres.3201.2017, doi:10.1158/0008-5472.can-17-3201.
162. Preusser, M.; Lim, M.; Hafler, D.A.; Reardon, D.A.; Sampson, J.H. Prospects of immune checkpoint modulators in the treatment of glioblastoma. *Nat Rev Neurology* **2015**, *11*, 504–14, doi:10.1038/nrneurol.2015.139.

163. Kwiatkowska, A.; Nandhu, M.S.; Behera, P.; Chiocca, E.A.; Viapiano, M.S. Strategies in Gene Therapy for Glioblastoma. *Cancers* **2013**, *5*, 1271–1305, doi:10.3390/cancers5041271.
164. Brown, N.F.; Carter, T.J.; Ottaviani, D.; Mulholland, P. Harnessing the immune system in glioblastoma. *Brit J Cancer* **2018**, *119*, 1171–1181, doi:10.1038/s41416-018-0258-8.
165. Reardon, D.A.; Freeman, G.; Wu, C.; Chiocca, E.A.; Wucherpennig, K.W.; Wen, P.Y.; Fritsch, E.F.; Curry, W.T.; Sampson, J.H.; Dranoff, G. Immunotherapy advances for glioblastoma. *Neuro-oncology* **2014**, *16*, 1441–1458, doi:10.1093/neuonc/nou212.
166. Yang, M.; Baranov, E.; Moossa, A.R.; Penman, S.; Hoffman, R.M. Visualizing gene expression by whole-body fluorescence imaging. *Proc National Acad Sci* **2000**, *97*, 12278–12282, doi:10.1073/pnas.97.22.12278.
167. Contag, C.H.; Spilman, S.D.; Contag, P.R.; Oshiro, M.; Eames, B.; Dennery, P.; Stevenson, D.K.; Benaron, D.A. Visualizing Gene Expression in Living Mammals Using a Bioluminescent Reporter. *Photochem Photobiol* **1997**, *66*, 523–531, doi:10.1111/j.1751-1097.1997.tb03184.x.
168. Wu, J.C.; Sundaresan, G.; Iyer, M.; Gambhir, S.S. Noninvasive Optical Imaging of Firefly Luciferase Reporter Gene Expression in Skeletal Muscles of Living Mice. *Mol Ther* **2001**, *4*, 297–306, doi:10.1006/mthe.2001.0460.
169. Contag, C.H.; Contag, P.R.; Mullins, J.I.; Spilman, S.D.; Stevenson, D.K.; Benaron, D.A. Photonic detection of bacterial pathogens in living hosts. *Mol Microbiol* **1995**, *18*, 593–603, doi:10.1111/j.1365-2958.1995.mmi_18040593.x.
170. Luker, G.D.; Bardill, J.P.; Prior, J.L.; Pica, C.M.; Piwnica-Worms, D.; Leib, D.A. Noninvasive Bioluminescence Imaging of Herpes Simplex Virus Type 1 Infection and Therapy in Living Mice. *J Virol* **2002**, *76*, 12149–12161, doi:10.1128/jvi.76.23.12149-12161.2002.
171. Cook, S.H.; Griffin, D.E. Luciferase Imaging of a Neurotropic Viral Infection in Intact Animals. *J Virol* **2003**, *77*, 5333–5338, doi:10.1128/jvi.77.9.5333-5338.2003.
172. Luker, K.E.; Hutchens, M.; Schultz, T.; Pekosz, A.; Luker, G.D. Bioluminescence imaging of vaccinia virus: Effects of interferon on viral replication and spread. *Virology* **2005**, *341*, 284–300, doi:10.1016/j.virol.2005.06.049.
173. Wang, T.; Li, P.; Zhang, Y.; Liu, Y.; Tan, Z.; Sun, J.; Ke, X.; Miao, Y.; Luo, D.; Hu, Q.; et al. In vivo imaging of Zika virus reveals dynamics of viral invasion in immune-sheltered tissues and vertical propagation during pregnancy. *Theranostics* **2020**, *10*, 6430–6447, doi:10.7150/thno.43177.
174. Ziegler, S.A.; Nuckols, J.; McGee, C.E.; Huang, Y.-J.S.; Vanlandingham, D.L.; Tesh, R.B.; Higgs, S. In Vivo Imaging of Chikungunya Virus in Mice and Aedes Mosquitoes Using a Renilla Luciferase Clone. *Vector-borne Zoonot* **2011**, *11*, 1471–1477, doi:10.1089/vbz.2011.0648.

175. Bray, M.; Lai, C.J. Construction of intertypic chimeric dengue viruses by substitution of structural protein genes. *Proc National Acad Sci* **1991**, *88*, 10342–10346, doi:10.1073/pnas.88.22.10342.
176. Bonaldo, M.C.; Sequeira, P.C.; Galler, R. The yellow fever 17D virus as a platform for new live attenuated vaccines. *Hum Vacc Immunother* **2014**, *10*, 1256–1265, doi:10.4161/hv.28117.
177. Felipe, L.S.; Vercruysse, T.; Sharma, S.; Ma, J.; Lemmens, V.; Looveren, D. van; Javarappa, M.P.A.; Boudewijns, R.; Malengier-Devlies, B.; Kaptein, S.F.; et al. A single-dose live-attenuated YF17D-vectored SARS-CoV2 vaccine candidate. *Biorxiv* **2020**, 2020.07.08.193045, doi:10.1101/2020.07.08.193045.
178. Yang, J.; Wang, W.; Chen, Z.; Lu, S.; Yang, F.; Bi, Z.; Bao, L.; Mo, F.; Li, X.; Huang, Y.; et al. A vaccine targeting the RBD of the S protein of SARS-CoV-2 induces protective immunity. *Nature* **2020**, 1–6, doi:10.1038/s41586-020-2599-8.
179. Robbiani, D.F.; Gaebler, C.; Muecksch, F.; Lorenzi, J.C.C.; Wang, Z.; Cho, A.; Agudelo, M.; Barnes, C.O.; Gazumyan, A.; Finkin, S.; et al. Convergent antibody responses to SARS-CoV-2 in convalescent individuals. *Nature* **2020**, *584*, 437–442, doi:10.1038/s41586-020-2456-9.
180. Mallajosyula, V.V.A.; Citron, M.; Ferrara, F.; Lu, X.; Callahan, C.; Heidecker, G.J.; Sarma, S.P.; Flynn, J.A.; Temperton, N.J.; Liang, X.; et al. Influenza hemagglutinin stem-fragment immunogen elicits broadly neutralizing antibodies and confers heterologous protection. *Proc National Acad Sci* **2014**, *111*, E2514–E2523, doi:10.1073/pnas.1402766111.
181. Valkenburg, S.A.; Mallajosyula, V.V.A.; Li, O.T.W.; Chin, A.W.H.; Carnell, G.; Temperton, N.; Varadarajan, R.; Poon, L.L.M. Stalking influenza by vaccination with pre-fusion headless HA mini-stem. *Sci Rep-uk* **2016**, *6*, 22666, doi:10.1038/srep22666.
182. Golden, J.W.; Shoemaker, C.J.; Lindquist, M.E.; Zeng, X.; Daye, S.P.; Williams, J.A.; Liu, J.; Coffin, K.M.; Olschner, S.; Flusin, O.; et al. GP38-targeting monoclonal antibodies protect adult mice against lethal Crimean-Congo hemorrhagic fever virus infection. *Sci Adv* **2019**, *5*, eaaw9535, doi:10.1126/sciadv.aaw9535.
183. Saphire, E.O.; Schendel, S.L.; Fusco, M.L.; Gangavarapu, K.; Gunn, B.M.; Wec, A.Z.; Halfmann, P.J.; Brannan, J.M.; Herbert, A.S.; Qiu, X.; et al. Systematic Analysis of Monoclonal Antibodies against Ebola Virus GP Defines Features that Contribute to Protection. *Cell* **2018**, *174*, 938–952.e13, doi:10.1016/j.cell.2018.07.033.
184. Sharma, S.; Schmid, M.A.; Felipe, L.S.; Grenelle, J.; Kaptein, S.J.F.; Coelmont, L.; Neyts, J.; Dallmeier, K. Small-molecule inhibitors of TBK1 serve as an adjuvant for a plasmid-launched live-attenuated yellow fever vaccine. *Hum Vacc Immunother* **2020**, *16*, 2196–2203, doi:10.1080/21645515.2020.1765621.

Vita

Coleman Kent Baker was born on February 29th, 1992 followed four minutes later by his twin sister Brianne. He was born to Wallace and Amy Baker in Idaho Falls, ID. Though brief stints were spent in Salt Lake City, UT and Casper, WY, Coleman was raised in his birthplace of Idaho Falls. His undergraduate degree in Chemistry, with an emphasis in Life Science and a minor in Biology, was attained from Utah State University in Logan, UT. A two-year leave of absence was taken after his first year to serve as a missionary for the Church of Jesus Christ of Latter-Day Saints in the southern half of Taiwan. Research experience at USU included medicinal and organic synthetic chemistry in the lab of Tom Chang. It was also at USU that he met his wife, Jessica, and they had a daughter before finishing their time in Utah.

After graduating from USU, Coleman attended the University of Texas Medical Branch in Galveston, TX in the Microbiology and Immunology Ph D program. Work with flaviviruses in the lab of Dr. Pei-Yong Shi has, at this time, led to two co-author papers, two first-author papers, two reviews, and one patent application. Coleman was also the recipient of the NIAID Emerging and Tropical Infectious Disease Training Program T32 Fellowship, as well as being named a McLaughlin Scholar and being the beneficiary of a number of scholarships and awards, including the Arthur V. Simmang Scholarship, BENCH Program Mentor of the Year Award, and the Mardelle Susman Scientific Writing Award. The time at UTMB also saw Coleman and Jessica add a son to their family.

After graduating with a PhD, Coleman hopes to enter the industry sector and work in Medical Affairs as a Medical Science Liaison, where he will have the chance to interact

with clinicians and other thought leaders to discuss the latest scientific data and improve outcomes for patients. It is hoped this job will eventually take him and his family back to Idaho or Utah where they can be closer to family.

Publications

Baker C, Liu Y, Zou J, Muruato A, Xie X, Shi PY. Identifying optimal capsid duplication length for the stability of reporter flaviviruses. *Emerg Microbes Infect.* 2020 Dec;9(1):2256-2265. doi: 10.1080/22221751.2020.1829994. PubMed PMID: 32981479.

Baker C, Shi PY. Construction of Stable Reporter Flaviviruses and Their Applications. *Viruses.* 2020 Sep 25;12(10). doi: 10.3390/v12101082. Review. PubMed PMID: 32992987.

Baker C, Xie X, Zou J, Muruato A, Fink K, Shi PY. Using recombination-dependent lethal mutations to stabilize reporter flaviviruses for rapid serodiagnosis and drug discovery. *EBioMedicine.* 2020 Jul;57:102838. doi: 10.1016/j.ebiom.2020.102838. Epub 2020 Jun 20. PubMed PMID: 32574959; PubMed Central PMCID: PMC7317239.

Fontes-Garfias CR, **Baker CK**, Shi PY. Reverse genetic approaches for the development of Zika vaccines and therapeutics. *Curr Opin Virol.* 2020 Jun 18;44:7-15. doi: 10.1016/j.coviro.2020.05.002. [Epub ahead of print] Review. PubMed PMID: 32563700.

Strange DP, Jiyarom B, Pourhabibi Zarandi N, Xie X, **Baker C**, Sadri-Ardekani H, Shi PY, Verma S. Axl Promotes Zika Virus Entry and Modulates the Antiviral State of Human Sertoli Cells. *mBio.* 2019 Jul 16;10(4). doi: 10.1128/mBio.01372-19. PubMed PMID: 31311882; PubMed Central PMCID: PMC6635530.

Soto-Acosta R, Xie X, Shan C, **Baker CK**, Shi PY, Rossi SL, Garcia-Blanco MA, Bradrick S. Fragile X mental retardation protein is a Zika virus restriction factor that is antagonized by subgenomic flaviviral RNA. *Elife*. 2018 Dec 4;7. doi: 10.7554/eLife.39023. PubMed PMID: 30511641; PubMed Central PMCID: PMC6279352.

Shrestha JP, **Baker C**, Kawasaki Y, Subedi YP, Vincent de Paul NN, Takemoto JY, Chang CT. Synthesis and bioactivity investigation of quinone-based dimeric cationic triazolium amphiphiles selective against resistant fungal and bacterial pathogens. *Eur J Med Chem*. 2017 Jan 27;126:696-704. doi: 10.1016/j.ejmech.2016.12.008. Epub 2016 Dec 5. PubMed PMID: 27951483.

Permanent address: 2954 Silver Landing Lane Dickinson, TX 77539

This dissertation was typed by Coleman Baker